Unsteady aerodynamic models for agile flight at low Reynolds number

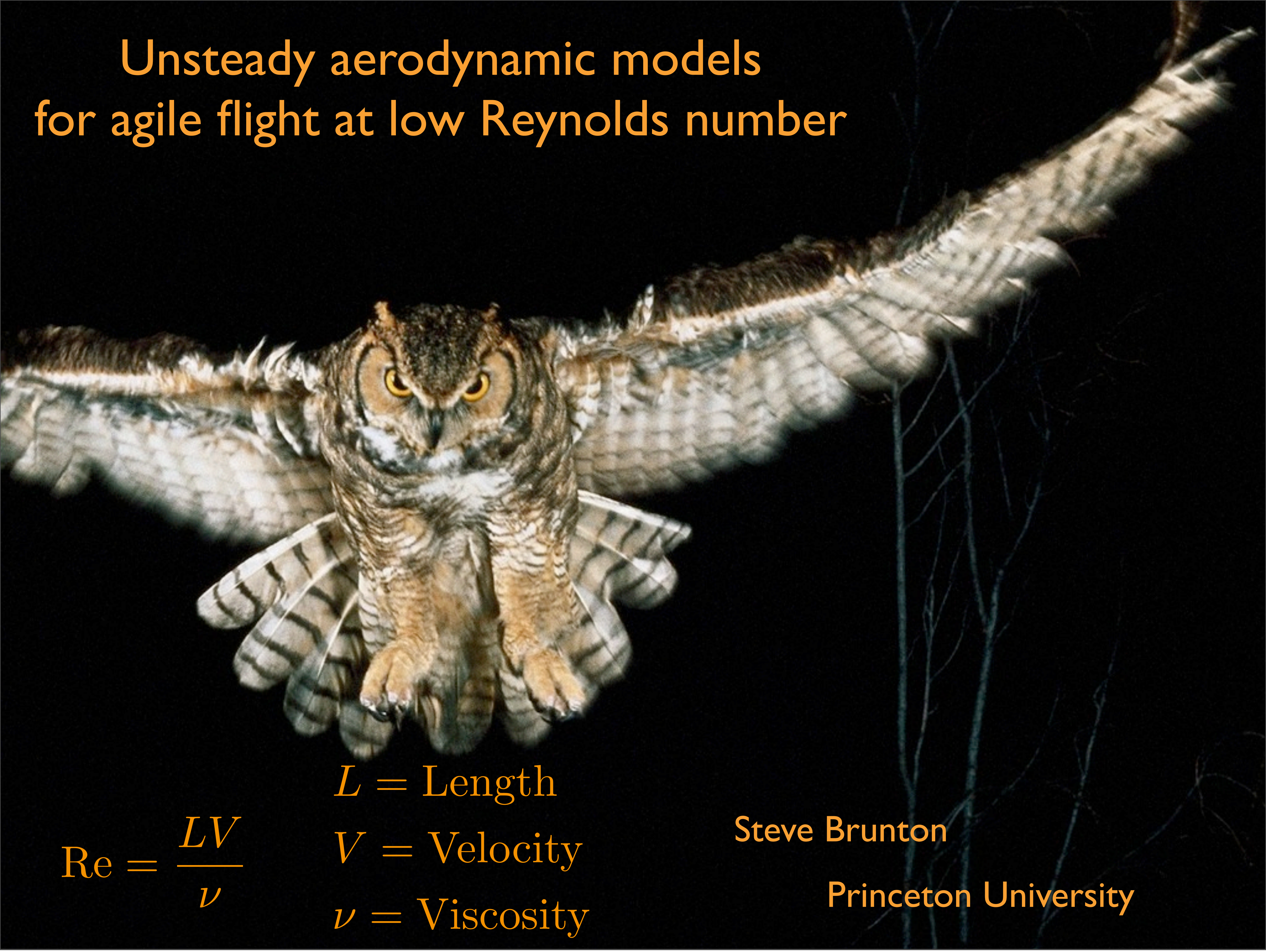

$$\mathrm{Re} = \frac{LV}{\nu}$$

$L = \text{Length}$

$V = \text{Velocity}$

$\nu = \text{Viscosity}$

Steve Brunton

Princeton University

Motivation

Applications of Unsteady Models

- Conventional UAVs (performance/robustness)
- Micro air vehicles (MAVs)
- Flow control, flight dynamic control
- Autopilots / Flight simulators
- Gust disturbance mitigation
- Understand bird/insect flight

Need for State-Space Models

- Need models suitable for control
- Combining with flight models

FLYIT Simulators, Inc.

Predator (General Atomics)

Flexible Wing
(University of Florida)

Bio-locomotion

Flow Control (expert)

Flow Control (expert)

Flight Dynamic Control

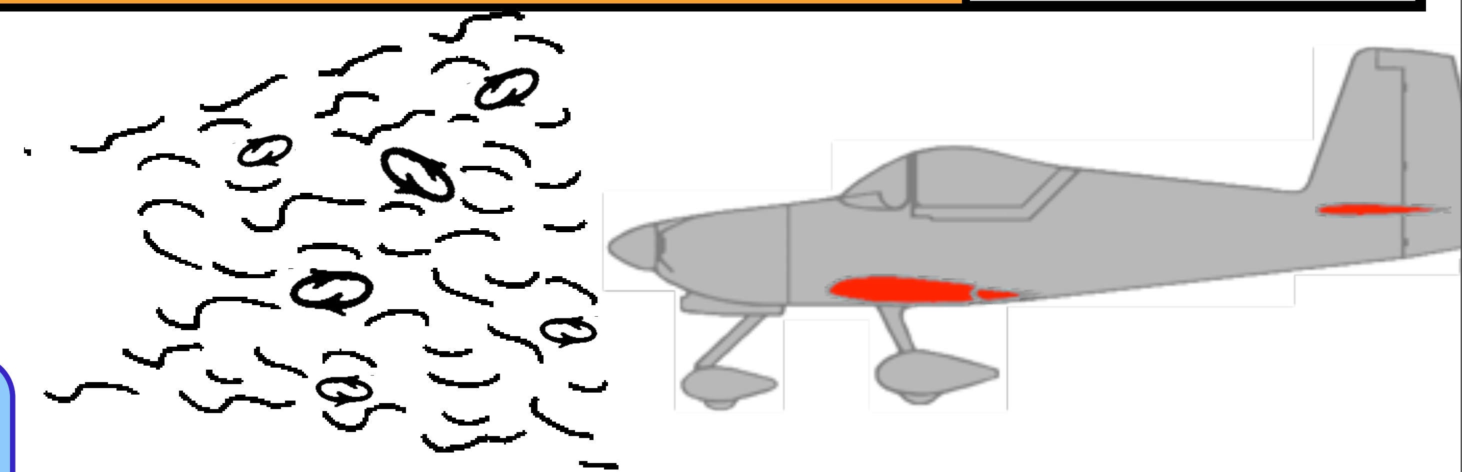

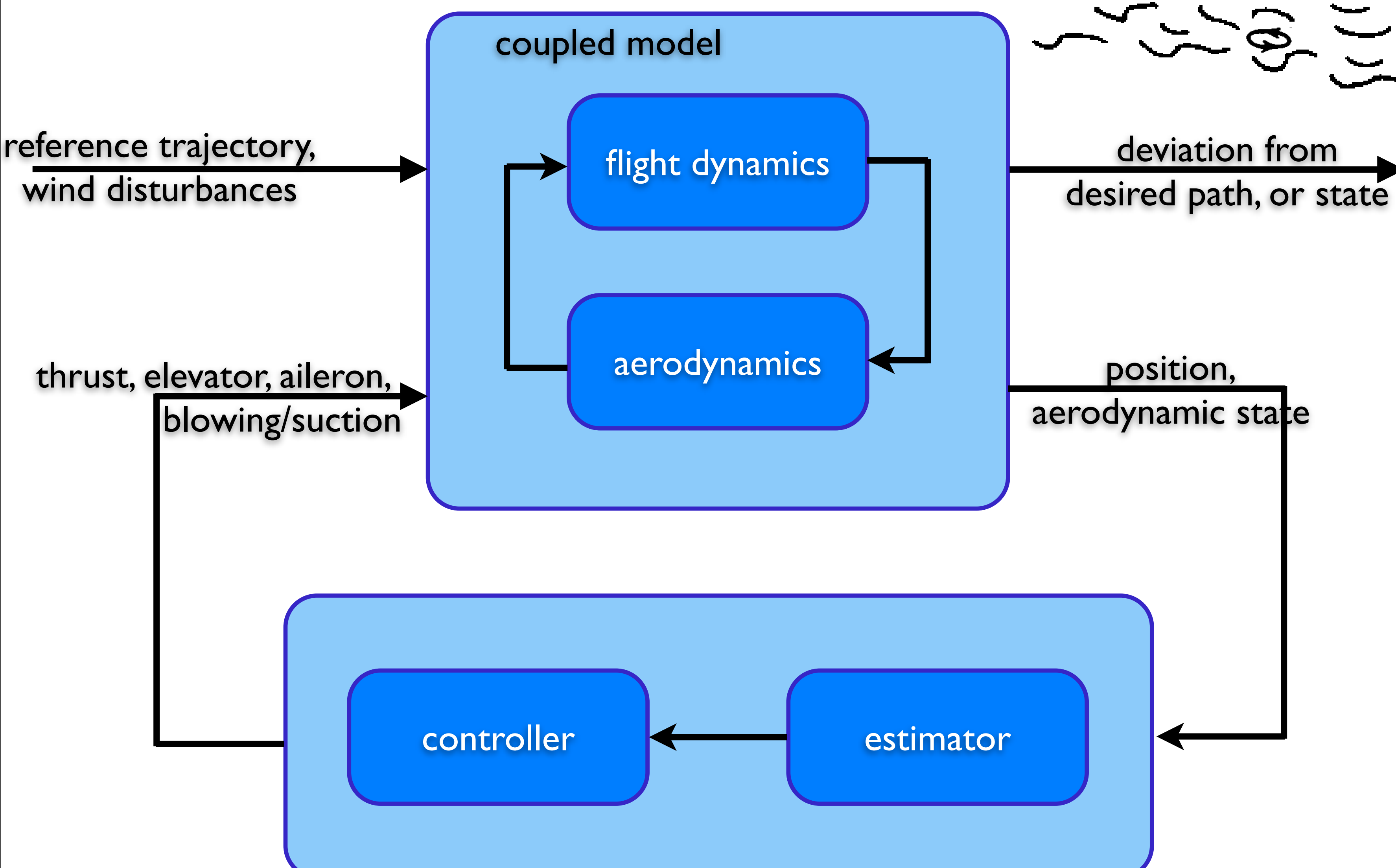

Three Aerodynamic Models

Idealized airfoil, analytical expression

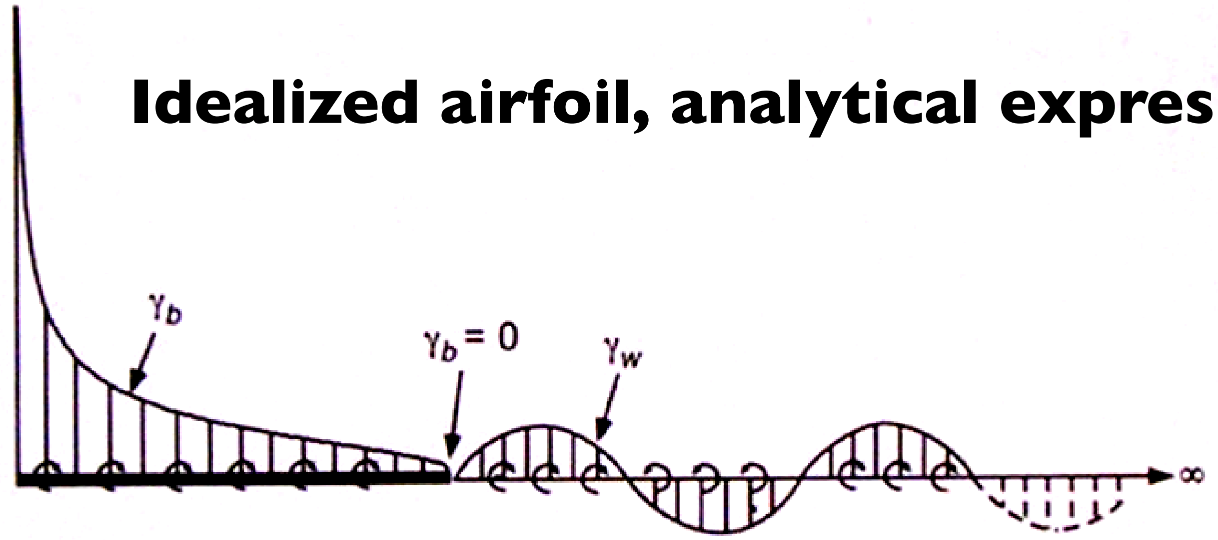

Direct numerical simulations, Re=100

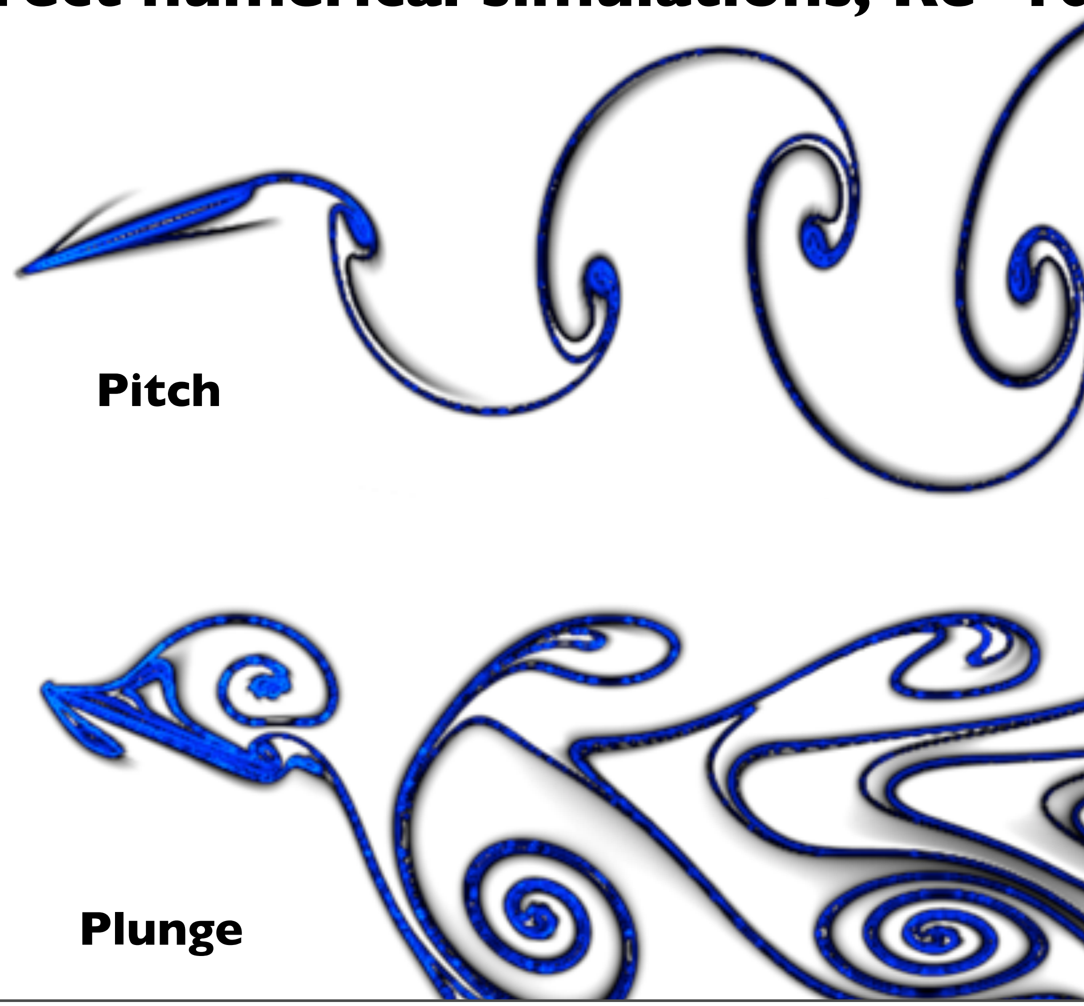

Wind tunnel experiment, Re=65,000

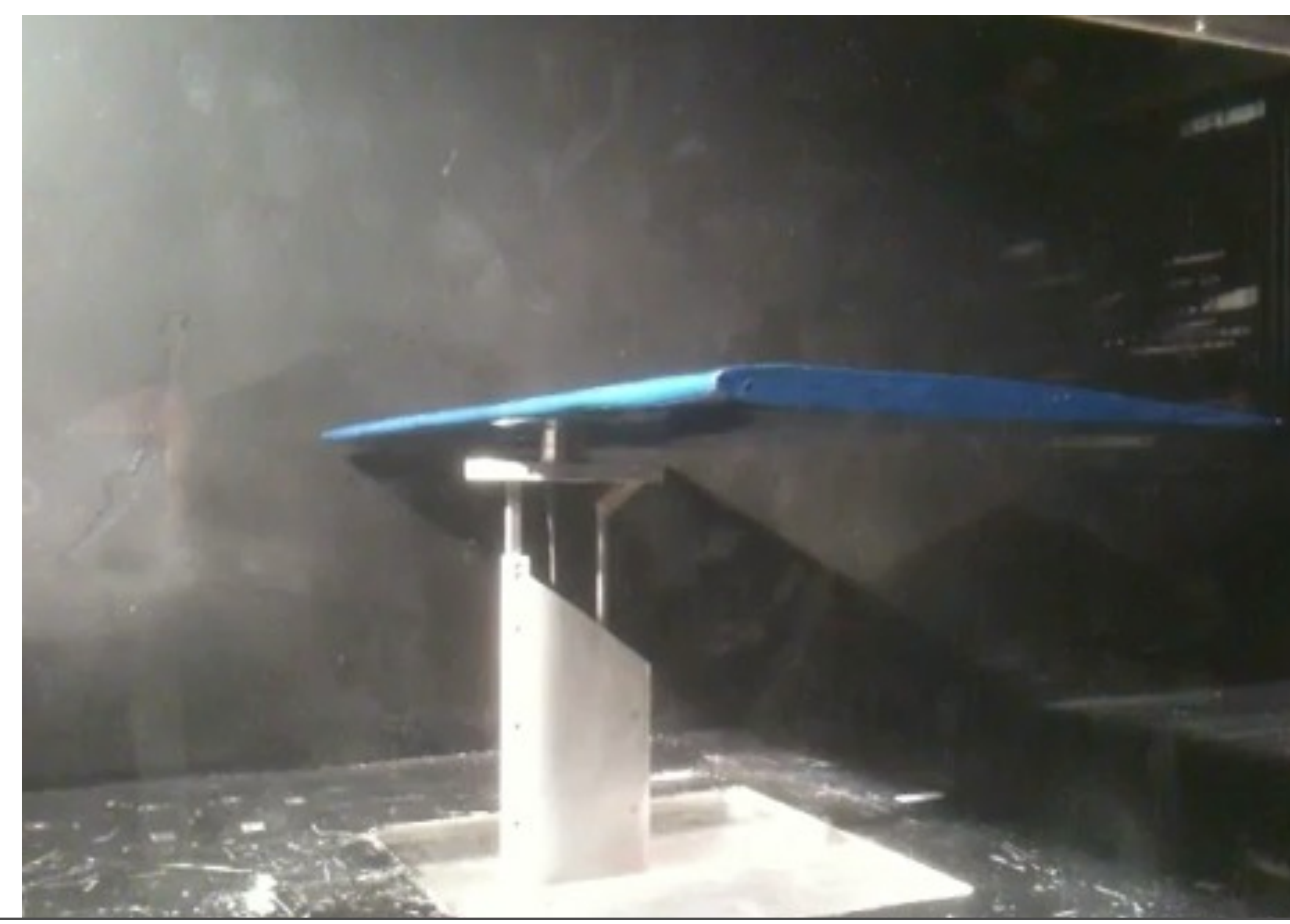

2D Incompressible Flow, (Re=100)

Stationary, AoA = 25

Pitch

Stationary, AoA = 35

Plunge

Immersed boundary method

Multi-domain approach

Boundary forces computed as Lagrange-multipliers to enforce no slip

Colonius & Taira, 2008.

2D Incompressible Navier-Stokes:

$$\frac{\partial \mathbf{u}}{\partial t} + (\mathbf{u} \cdot \nabla)\,\mathbf{u} = -\nabla p + \frac{1}{\mathrm{Re}}\nabla^2 \mathbf{u} + \int_s \mathbf{f}\,(\xi(s,t))\,\delta(\xi - \mathbf{x})ds$$

$$\nabla \cdot \mathbf{u} = 0$$

$$\mathbf{u}\,(\xi(s,t)) = \int_{\mathbf{x}} \mathbf{u}(\mathbf{x})\delta(\mathbf{x} - \xi)d\mathbf{x} = \mathbf{u}_B\,(\xi(s,t))$$

Unsteady Base Flow

Idea: Instead of moving body, move base flow!

Base flow velocity:

$$u(x,y,t) = \|\mathbf{V}\|\cos(\alpha) - \dot{\theta}(y - y_C)$$

$$v(x,y,t) = \|\mathbf{V}\|\sin(\alpha) + \dot{\theta}(x - x_C)$$

Vorticity:

$$\nabla \times (u,v) = v_x - u_y = \dot{\theta} + \dot{\theta} = 2\dot{\theta}$$

where (x_C, y_C) is the center of mass.

Unsteady Base Flow

Faster simulations (Cholesky decomposition)

allows more aggressive maneuvers and gusts

24X faster, more accurate

Immersed Boundary Method

T. Colonius and K. Taira, 2008

A fast immersed boundary method using a nullspace approach and multi-domain far-field boundary conditions.

Finite Time Lyapunov Exponents

Finite Time Lyapunov Exponents (FTLE)

Measure of stretching between neighboring particles

σ **is time-dependent for unsteady flows**

$$\sigma(\Phi_0^T;\mathbf{x_0}) = \frac{1}{|T|}\log\sqrt{\lambda_{\max}(\Delta(\mathbf{x_0}))}$$

where $\Delta = \left(\mathbf{D}\Phi_0^T\right)^* \mathbf{D}\Phi_0^T$

Lagrangian Coherent Structures (LCS)

LCS are hyperbolic ridges in the FTLE field

Generalize invariant manifolds for time varying flows

$\mathbf{\Phi_0^T}$ **- particle flow map**

pLCS - positive-time LCS (repelling)

nLCS - negative-time LCS (attracting)

Haller, 2002;
Shadden *et al.*, 2005

Attracting nLCS

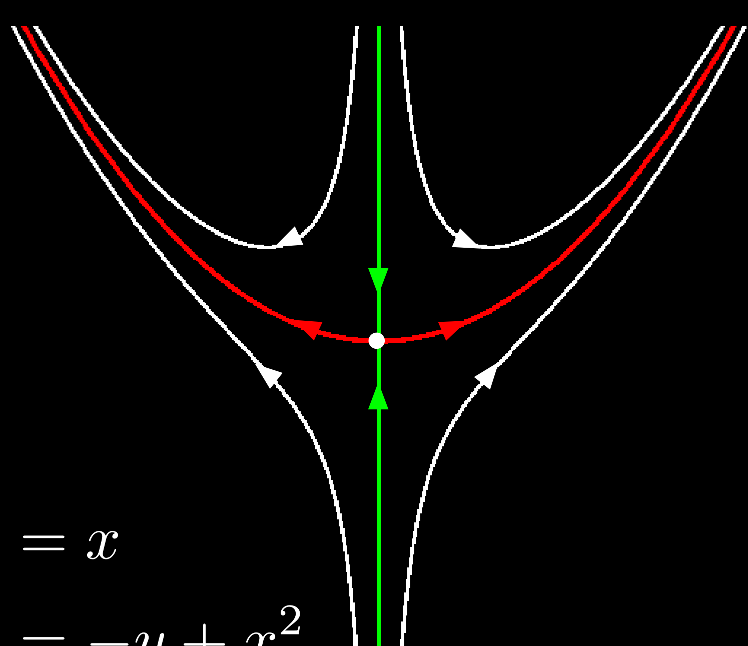

$$\dot{x} = x$$
$$\dot{y} = -y + x^2$$

Finite Time Lyapunov Exponents (FTLE)

Measure of stretching between neighboring particles

σ **is time-dependent for unsteady flows**

$$\sigma(\Phi_0^T;\mathbf{x_0}) = \frac{1}{|T|}\log\sqrt{\lambda_{\max}(\Delta(\mathbf{x_0}))}$$

where $$\Delta = \left(\mathbf{D}\Phi_0^T\right)^*\mathbf{D}\Phi_0^T$$

Lagrangian Coherent Structures (LCS)

LCS are hyperbolic ridges in the FTLE field

Generalize invariant manifolds for time varying flows

$\mathbf{\Phi_0^T}$ **- particle flow map**

pLCS - positive-time LCS (repelling)

nLCS - negative-time LCS (attracting)

Haller, 2002;
Shadden *et al.*, 2005

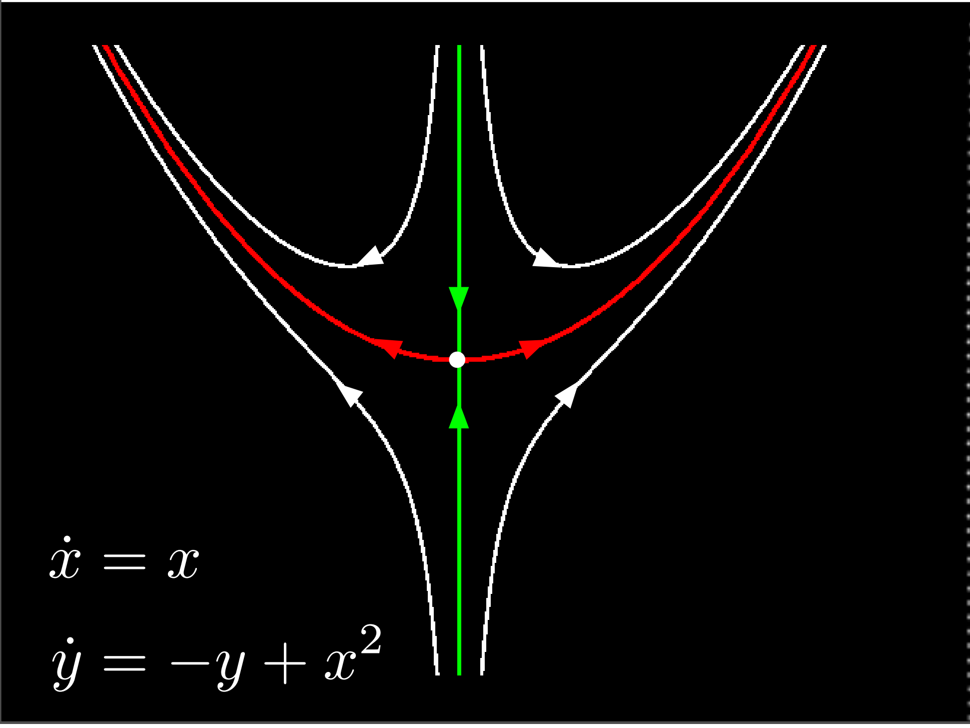

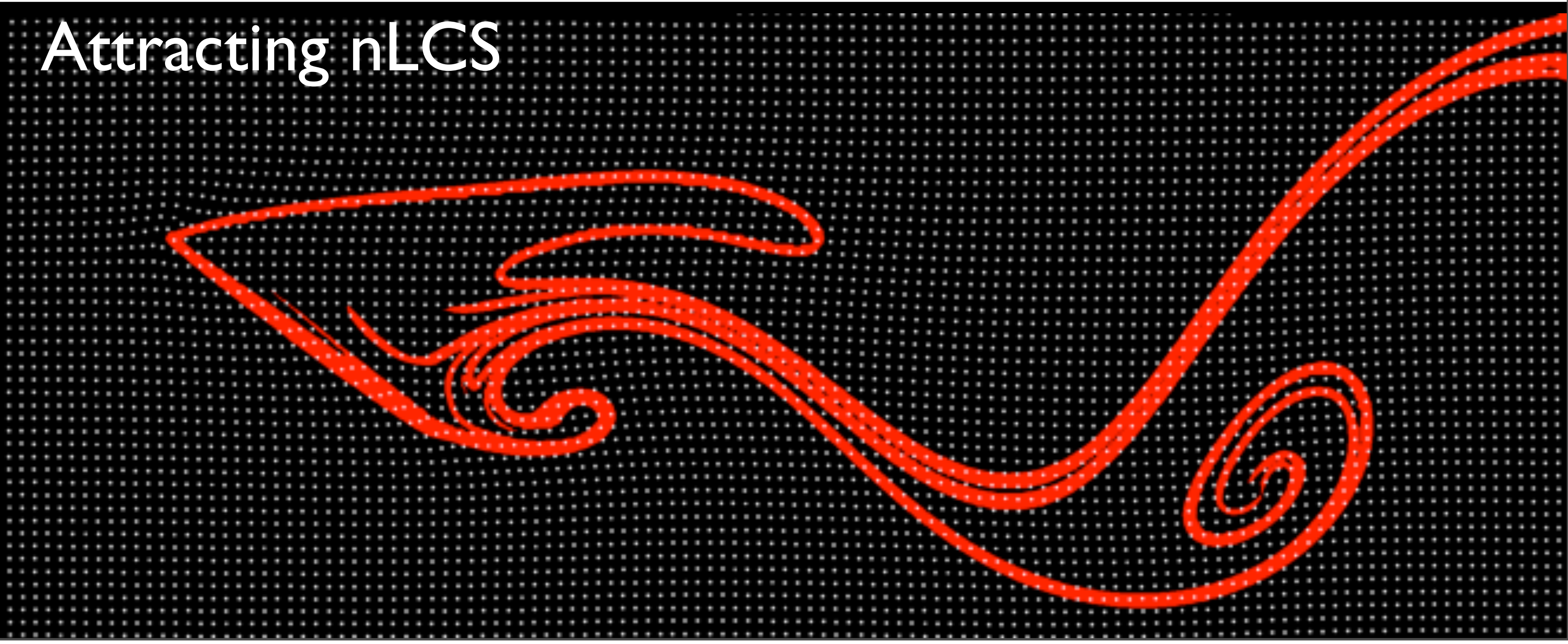

Finite Time Lyapunov Exponents (FTLE)

Measure of stretching between neighboring particles

σ **is time-dependent for unsteady flows**

$$\sigma(\Phi_0^T; \mathbf{x_0}) = \frac{1}{|T|} \log \sqrt{\lambda_{\max}(\Delta(\mathbf{x_0}))}$$

where $$\Delta = \left(\mathbf{D}\Phi_0^T\right)^* \mathbf{D}\Phi_0^T$$

Lagrangian Coherent Structures (LCS)

LCS are hyperbolic ridges in the FTLE field

Generalize invariant manifolds for time varying flows

$\mathbf{\Phi_0^T}$ **- particle flow map**

pLCS - positive-time LCS (repelling)

nLCS - negative-time LCS (attracting)

Haller, 2002;
Shadden *et al.*, 2005

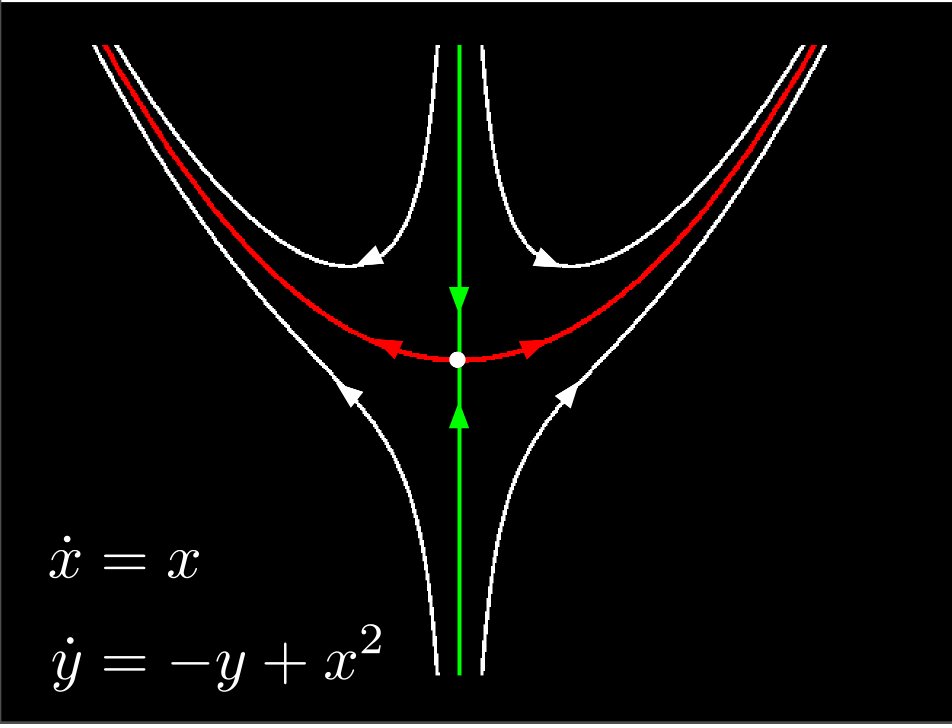

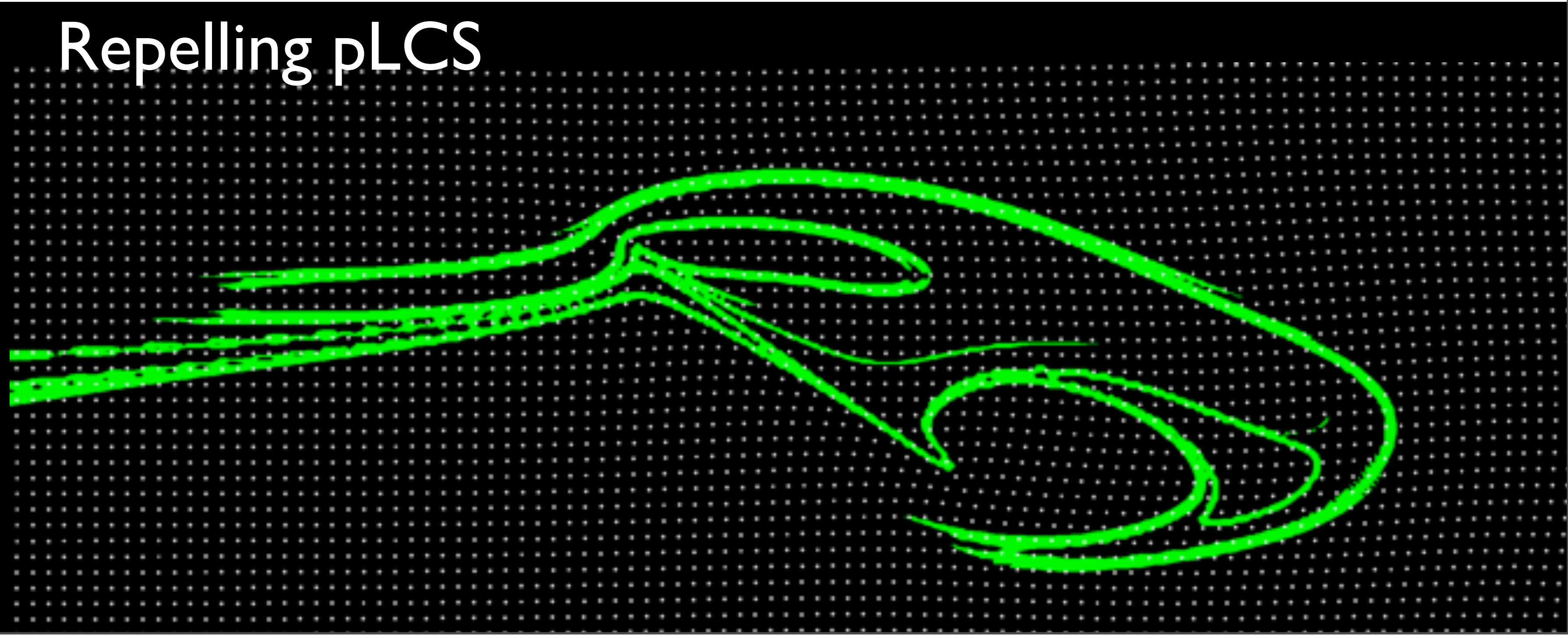

Finite Time Lyapunov Exponents

Finite Time Lyapunov Exponents (FTLE)

Measure of stretching between neighboring particles

σ **is time-dependent for unsteady flows**

$$\sigma(\Phi_0^T; \mathbf{x_0}) = \frac{1}{|T|} \log \sqrt{\lambda_{\max}(\Delta(\mathbf{x_0}))}$$

where $$\Delta = \left(\mathbf{D}\Phi_0^T\right)^* \mathbf{D}\Phi_0^T$$

Lagrangian Coherent Structures (LCS)

LCS are hyperbolic ridges in the FTLE field

Generalize invariant manifolds for time varying flows

$\mathbf{\Phi_0^T}$ **- particle flow map**

pLCS - positive-time LCS (repelling)

nLCS - negative-time LCS (attracting)

Haller, 2002;
Shadden *et al.*, 2005

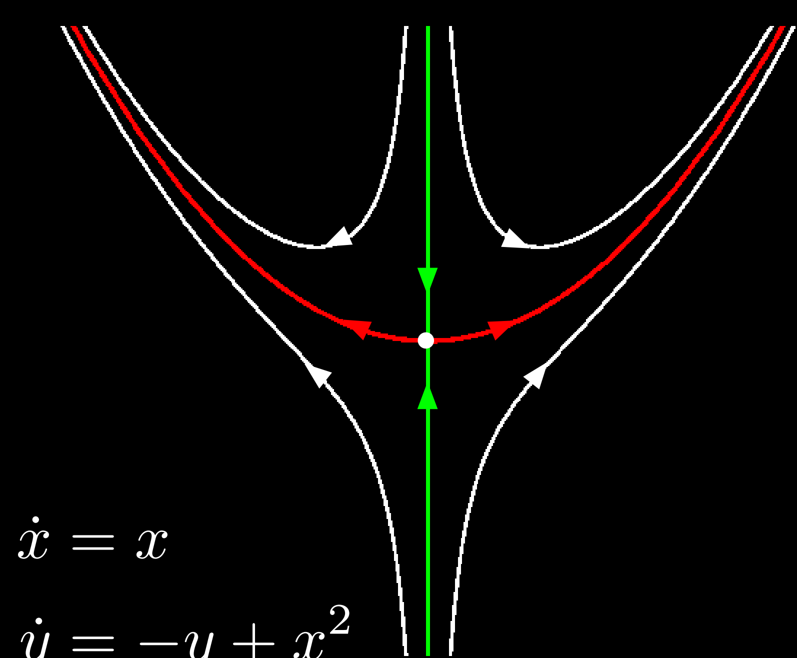

Both nLCS & pLCS

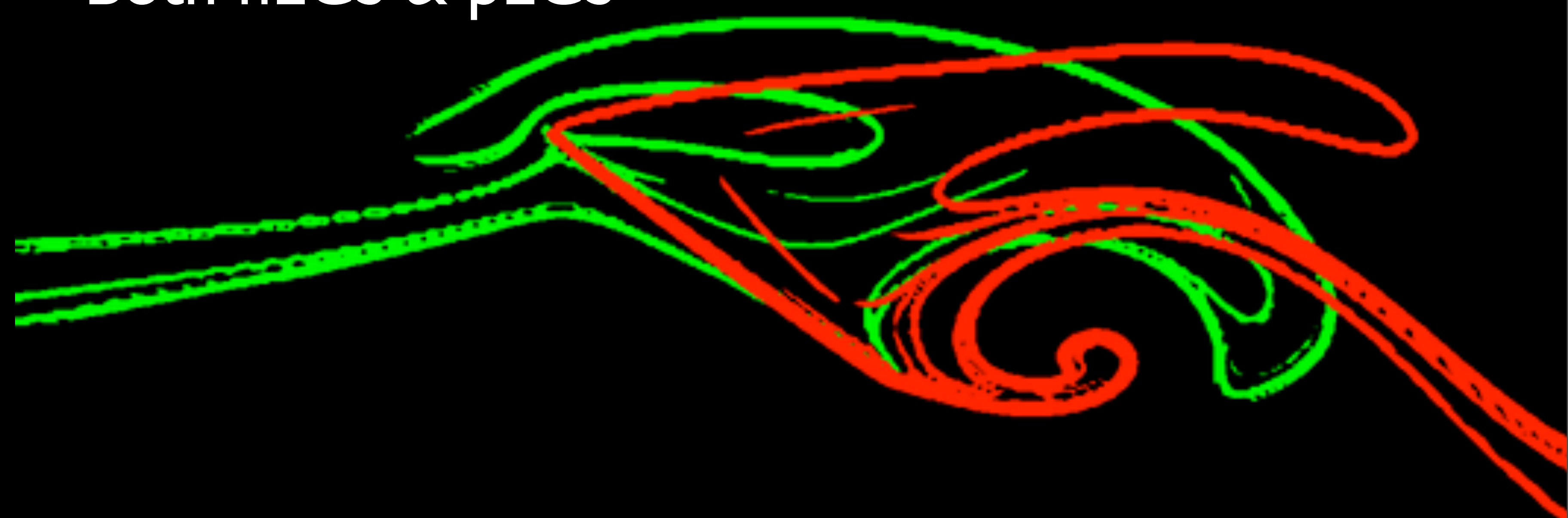

2D Model Problem

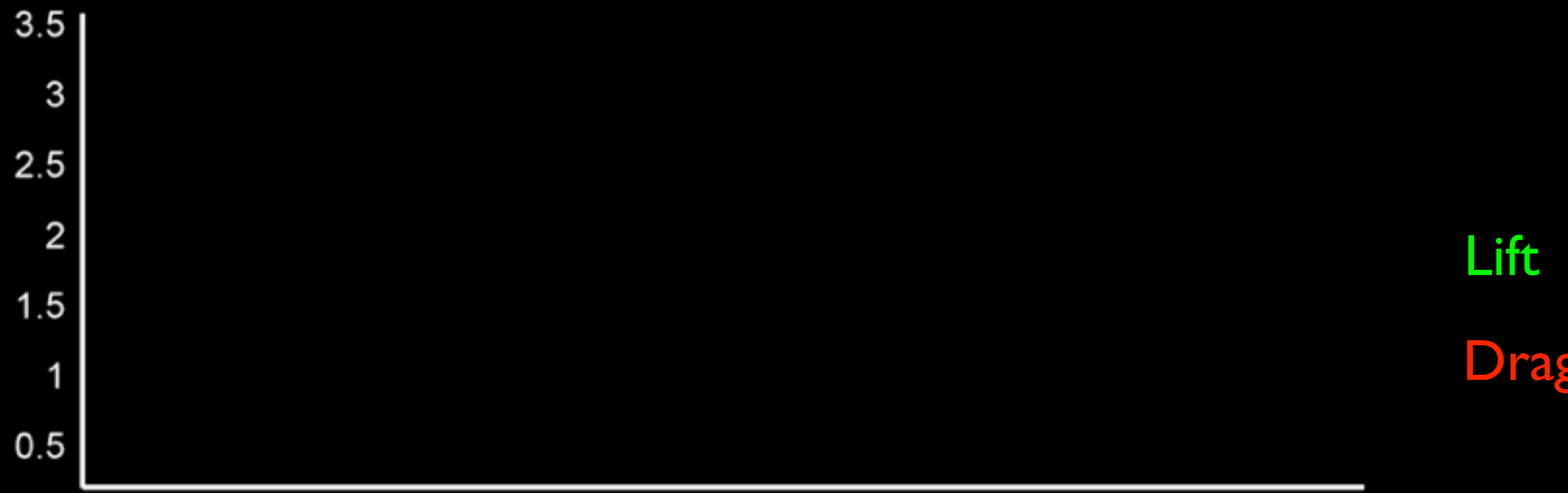

$\mathrm{Re} = 300$

$\alpha = 32^\circ$

2D Model Problem

Added-Mass

Transient

Periodic Vortex Shedding

Lift

Drag

$\mathrm{Re} = 300$

$\alpha = 32^\circ$

2D Model Problem

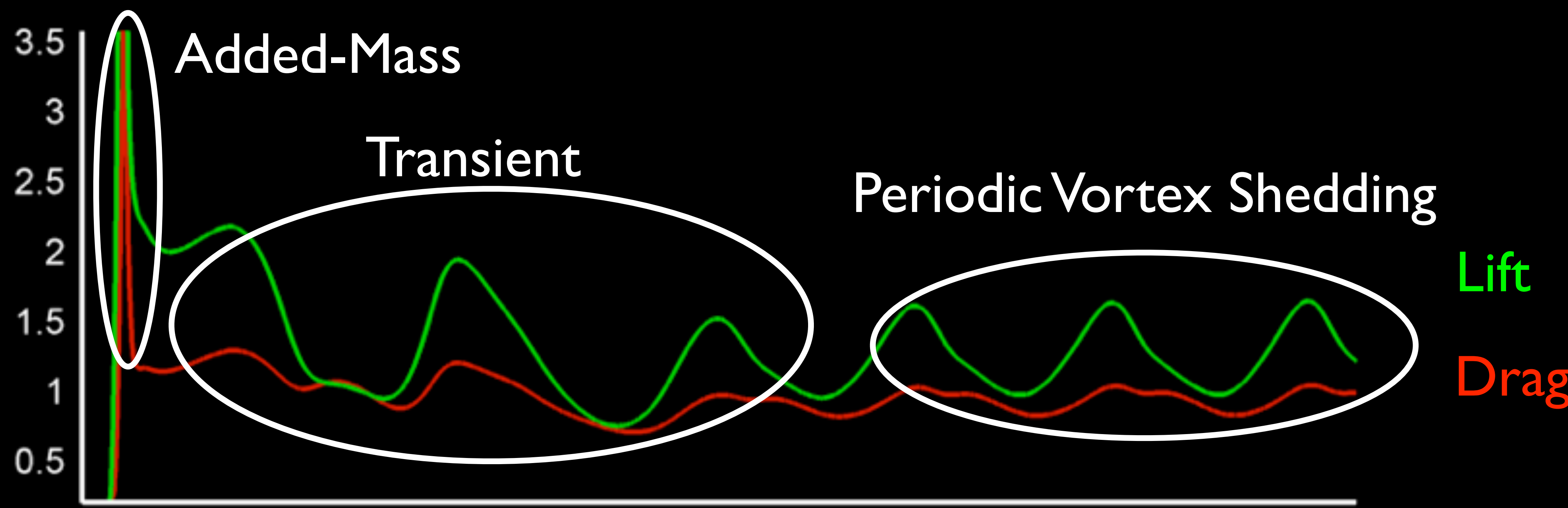

$\mathrm{Re} = 300$
$\alpha = 32^\circ$

Lift vs. Angle of Attack

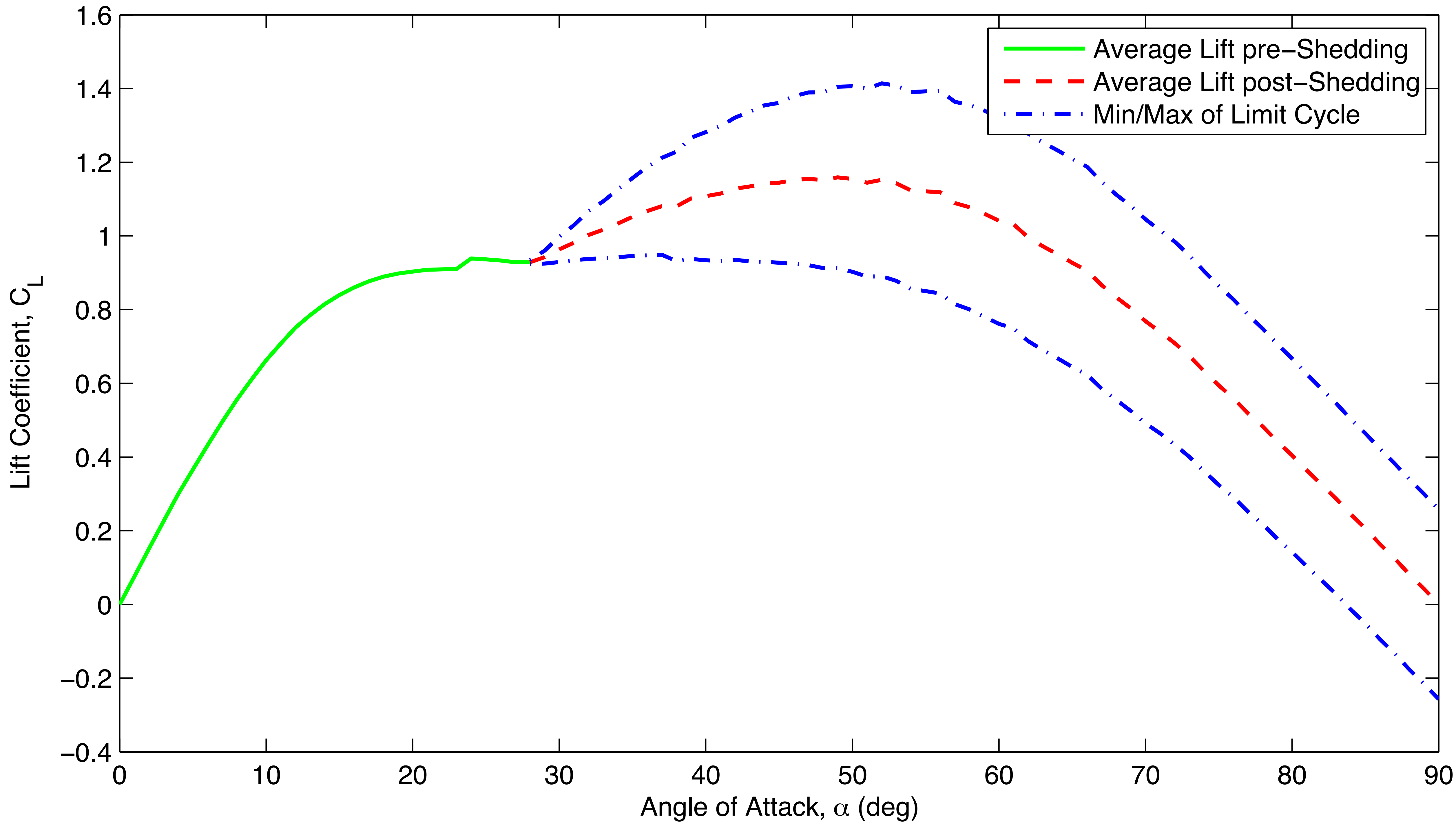

Low Reynolds number, (Re=100)

Hopf bifurcation at $\alpha_{\text{crit}} \approx 28^\circ$ **(pair of imaginary eigenvalues pass into right half plane)**

Lift vs. Angle of Attack

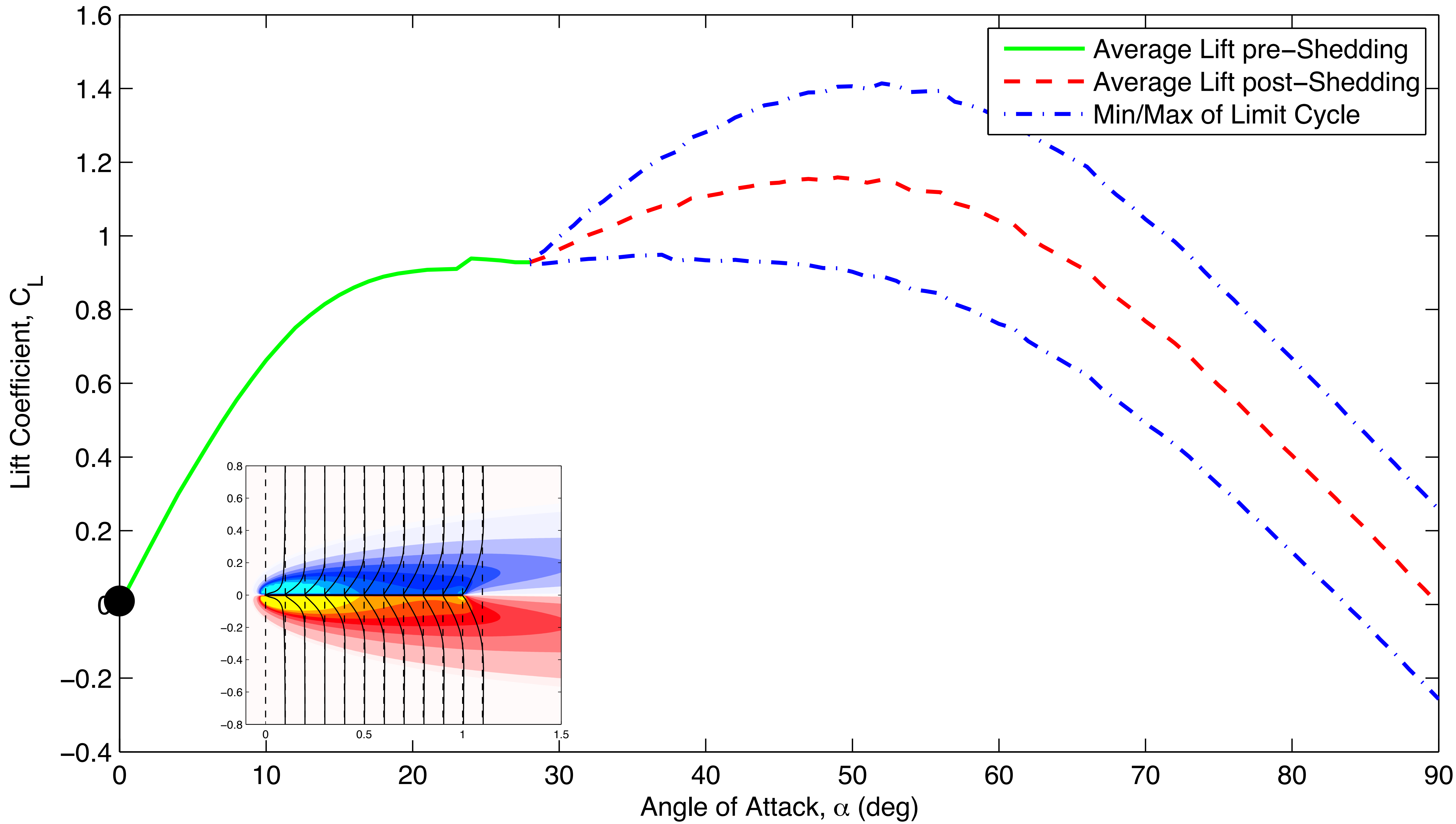

Low Reynolds number, (Re=100)

Hopf bifurcation at $\alpha_{\mathrm{crit}} \approx 28^\circ$ **(pair of imaginary eigenvalues pass into right half plane)**

Lift vs. Angle of Attack

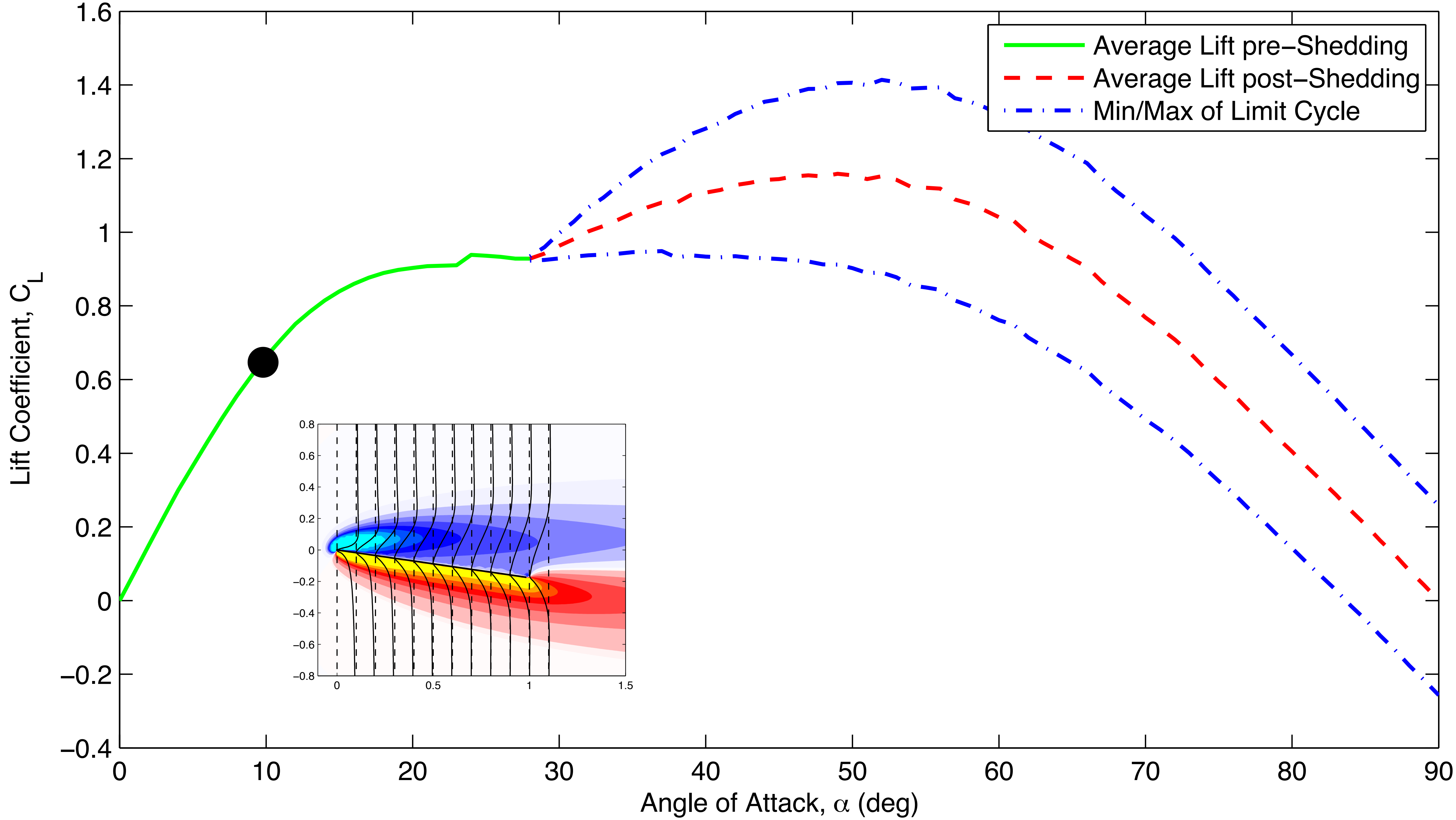

Low Reynolds number, (Re=100)

Hopf bifurcation at $\alpha_{\text{crit}} \approx 28^\circ$ **(pair of imaginary eigenvalues pass into right half plane)**

Lift vs. Angle of Attack

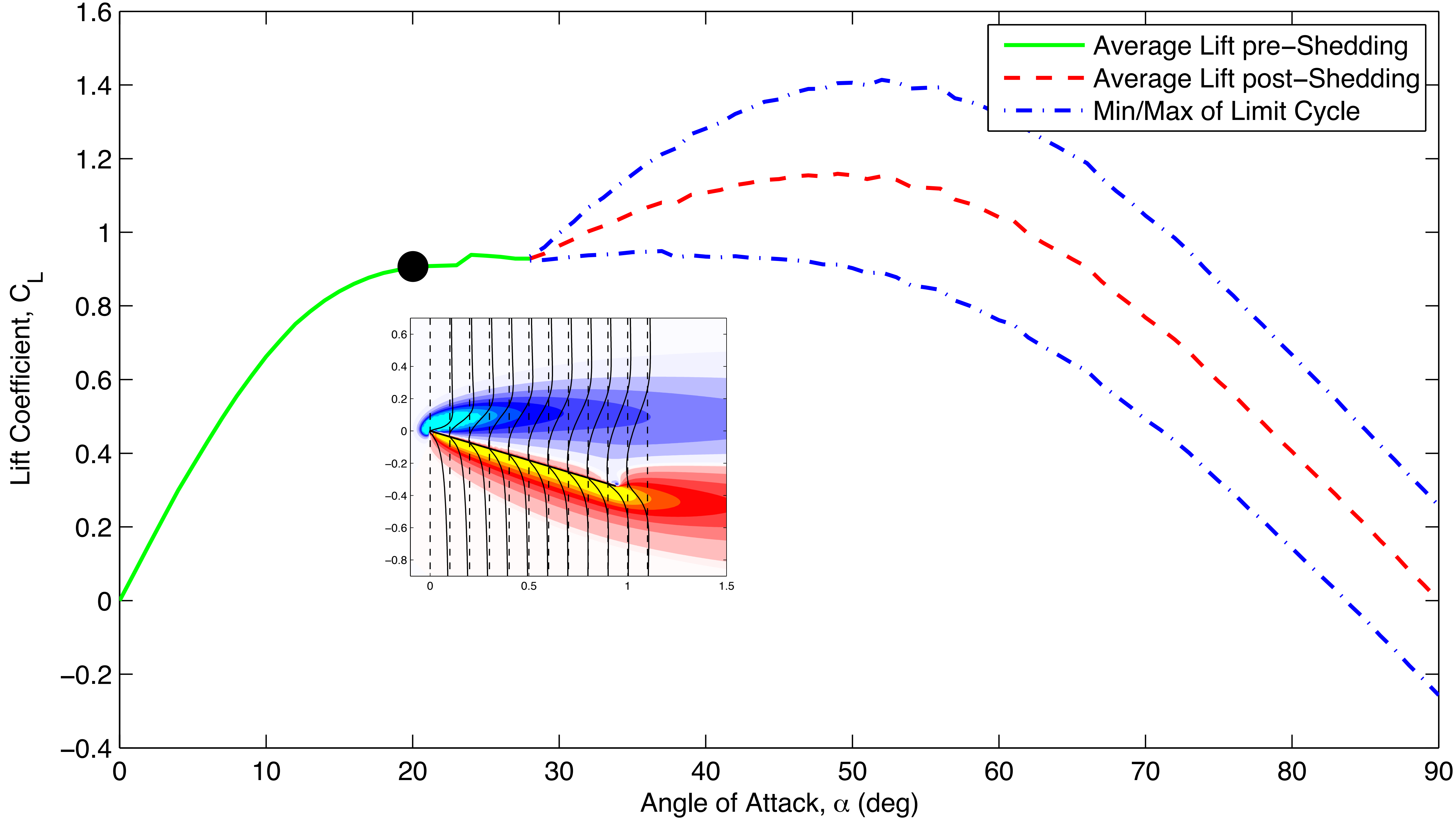

Low Reynolds number, (Re=100)

Hopf bifurcation at $\alpha_{\rm crit} \approx 28^\circ$ **(pair of imaginary eigenvalues pass into right half plane)**

Lift vs. Angle of Attack

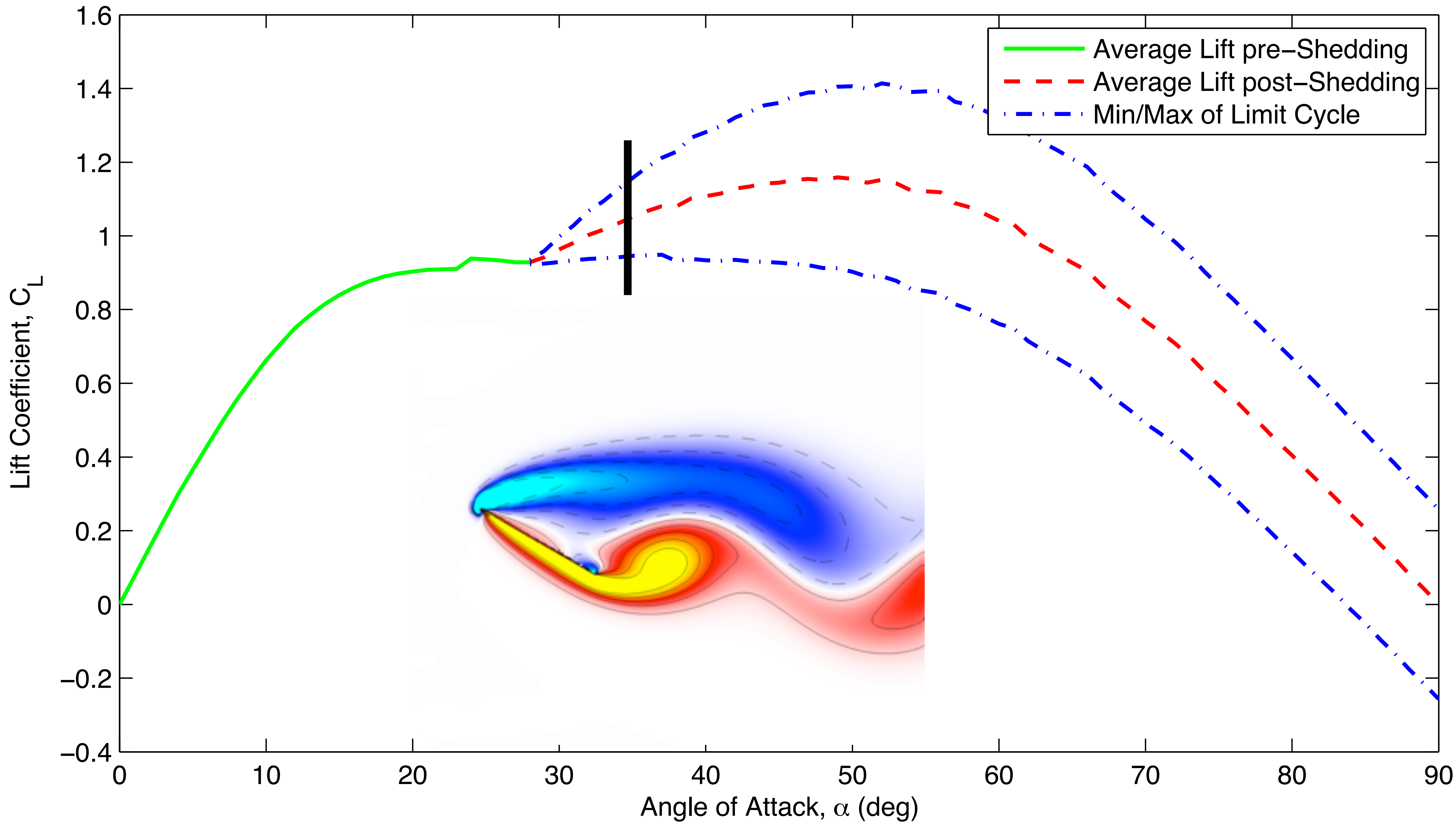

Low Reynolds number, (Re=100)

Hopf bifurcation at $\alpha_{\text{crit}} \approx 28^\circ$ **(pair of imaginary eigenvalues pass into right half plane)**

Lift vs Angle of Attack

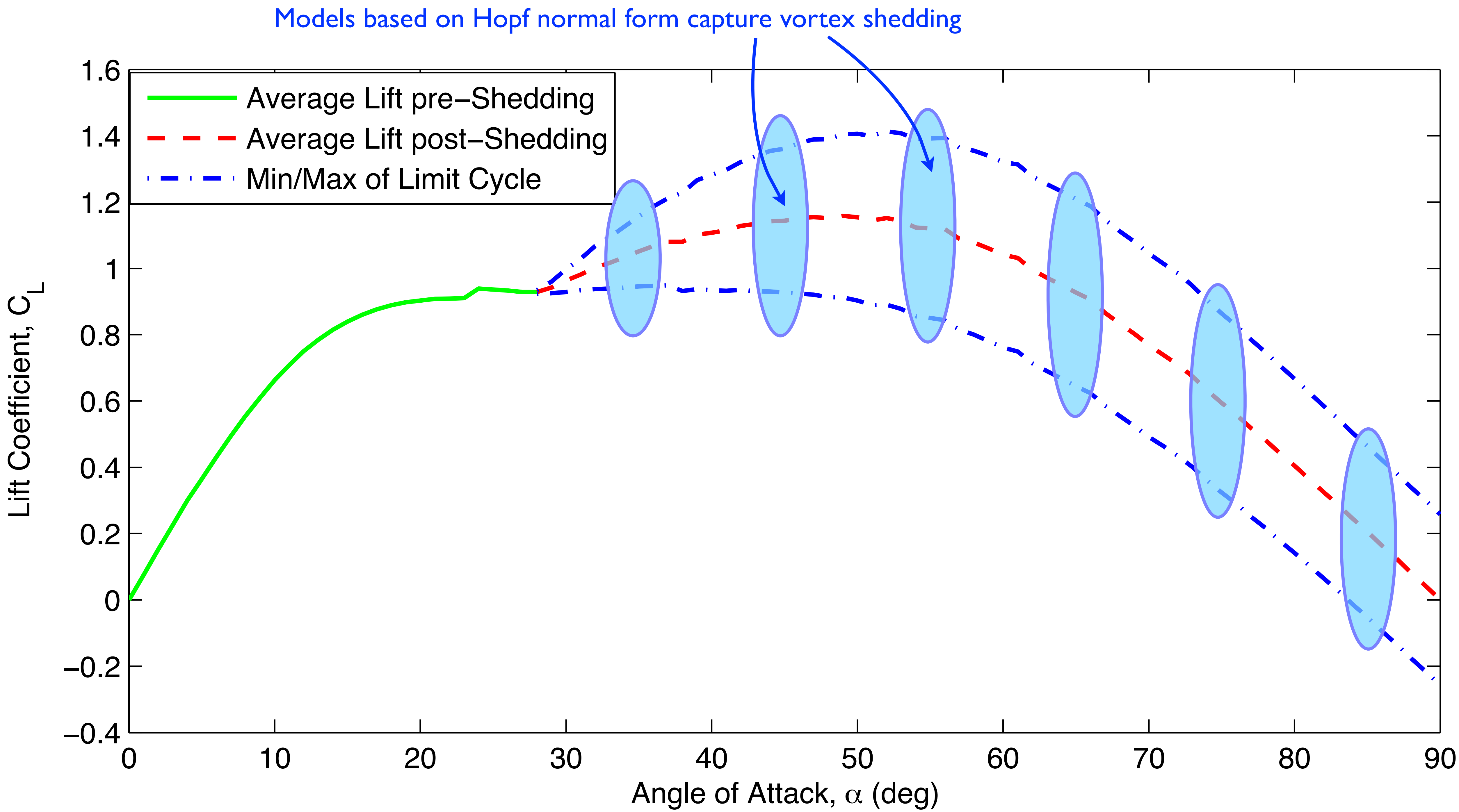

Low Reynolds number, (Re=100)

Hopf bifurcation at $\alpha_{\text{crit}} \approx 28^\circ$ **(pair of imaginary eigenvalues pass into right half plane)**

High angle of attack models

Heuristic Model

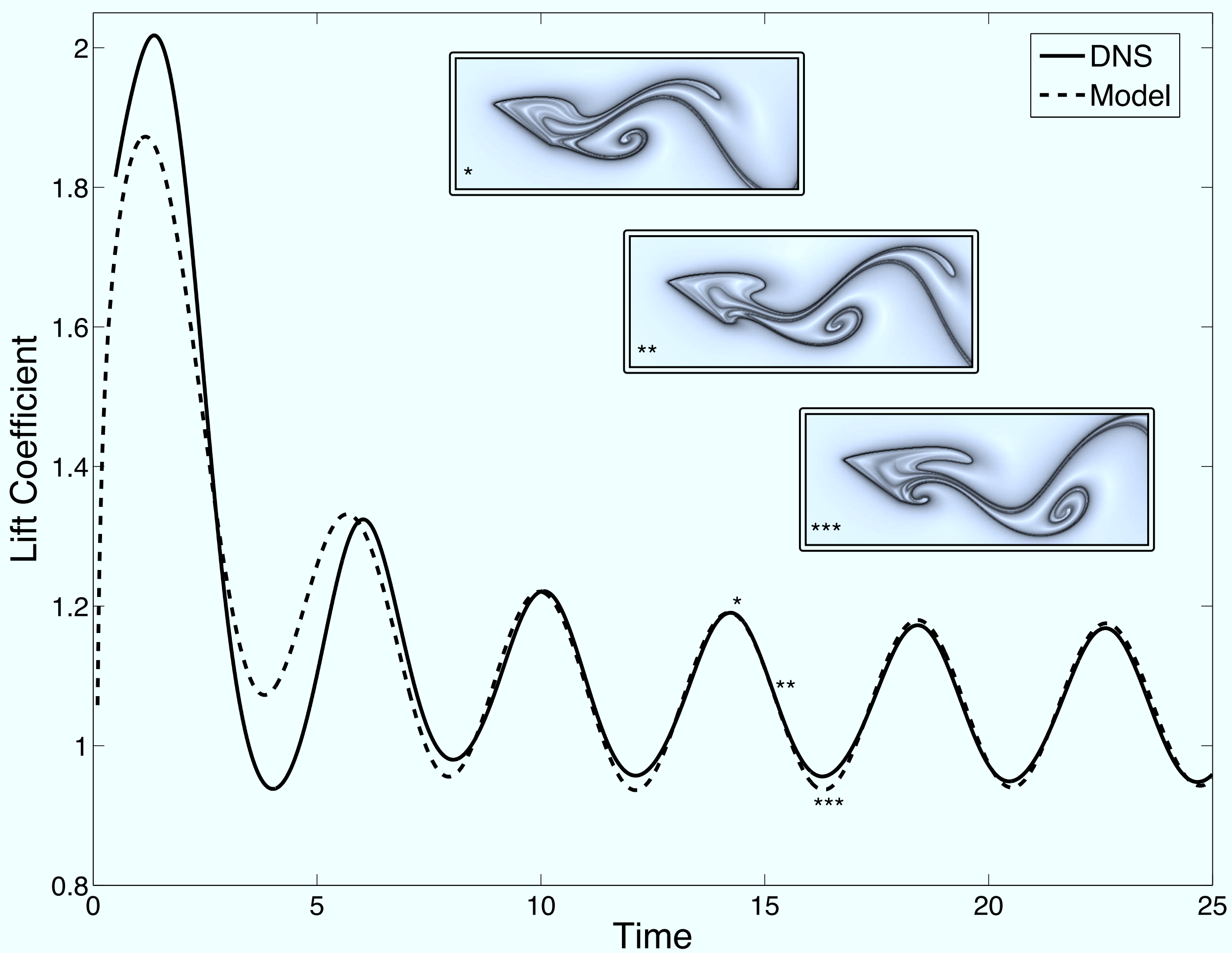

$$
\left.\begin{aligned}
\dot{x} &= (\alpha - \alpha_c)\mu x - \omega y - a x(x^2 + y^2) \\
\dot{y} &= (\alpha - \alpha_c)\mu y + \omega x - a y(x^2 + y^2) \\
\dot{z} &= -\lambda z
\end{aligned}\right\} \Longrightarrow
\begin{aligned}
\dot{r} &= r\left[(\alpha - \alpha_c)\mu - a r^2\right] \\
\dot{\theta} &= \omega \\
\dot{z} &= -\lambda z
\end{aligned}
$$

Galerkin Projection onto POD

Full DNS

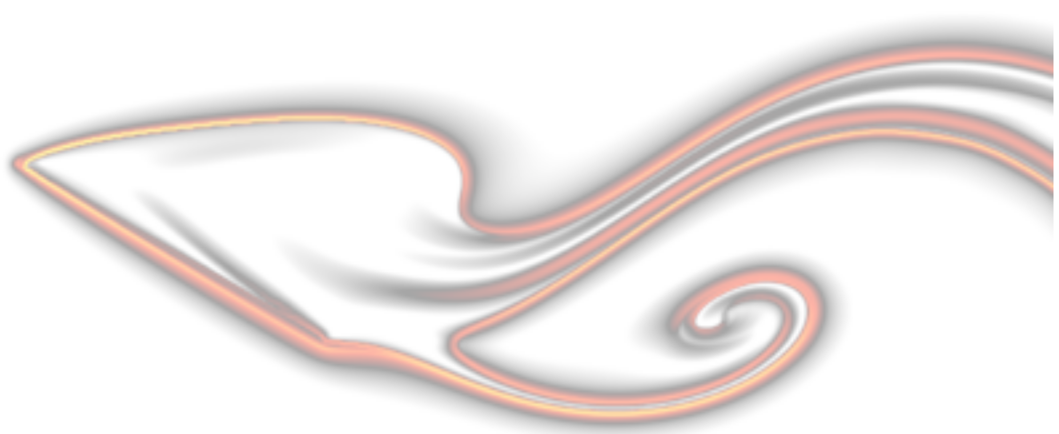

Reconstruction

High angle of attack models

Heuristic Model

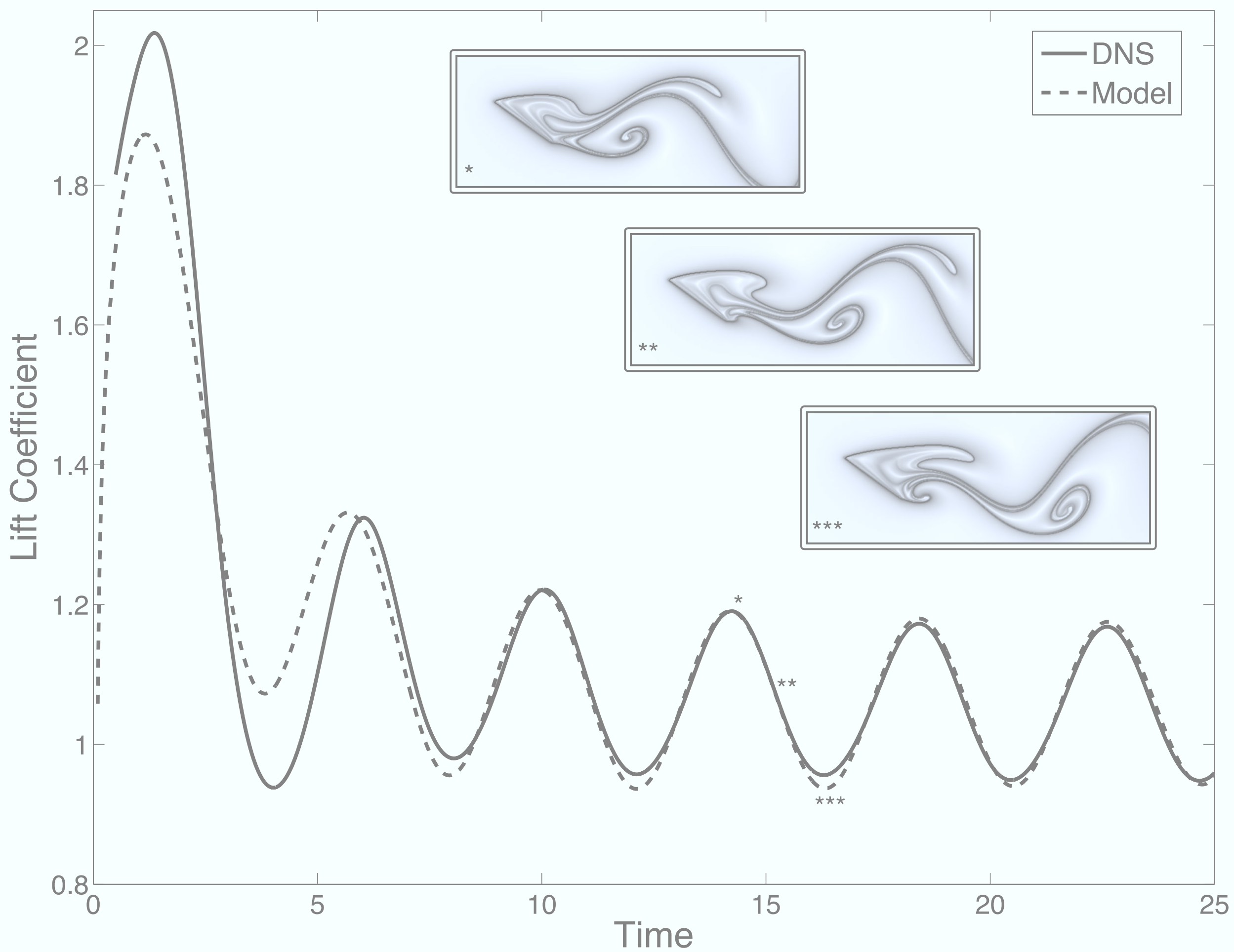

$$
\left.\begin{aligned}
\dot{x} &= (\alpha-\alpha_c)\mu x - \omega y - a x(x^2+y^2)\\
\dot{y} &= (\alpha-\alpha_c)\mu y + \omega x - a y(x^2+y^2)\\
\dot{z} &= -\lambda z
\end{aligned}\right\}
\implies
\begin{aligned}
\dot{r} &= r\left[(\alpha-\alpha_c)\mu - a r^2\right]\\
\dot{\theta} &= \omega\\
\dot{z} &= -\lambda z
\end{aligned}
$$

Galerkin Projection onto POD

Full DNS

Reconstruction

POD Modes for Stationary Plate

Full Flow

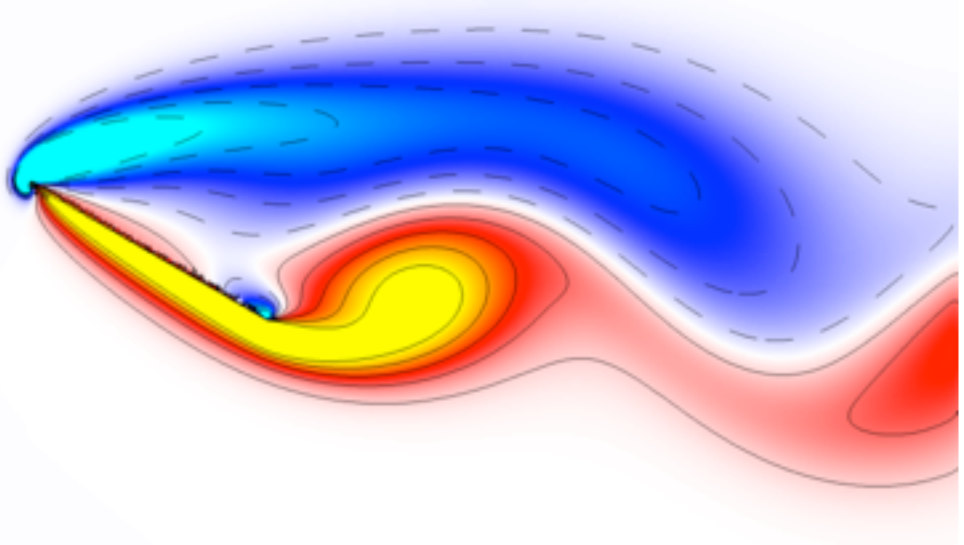

Mode 1

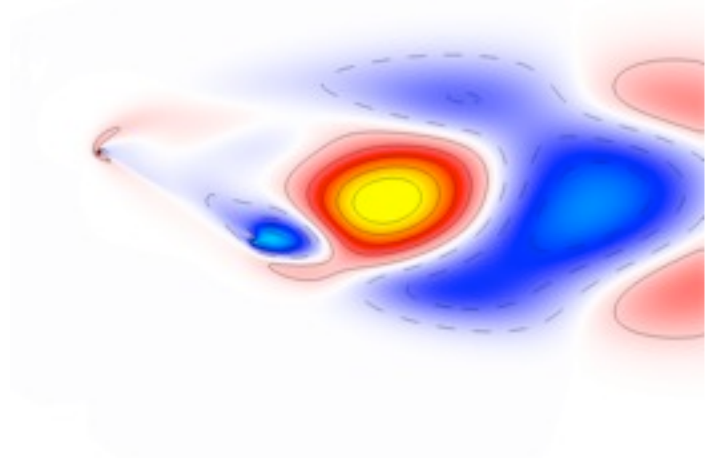

Mode 2

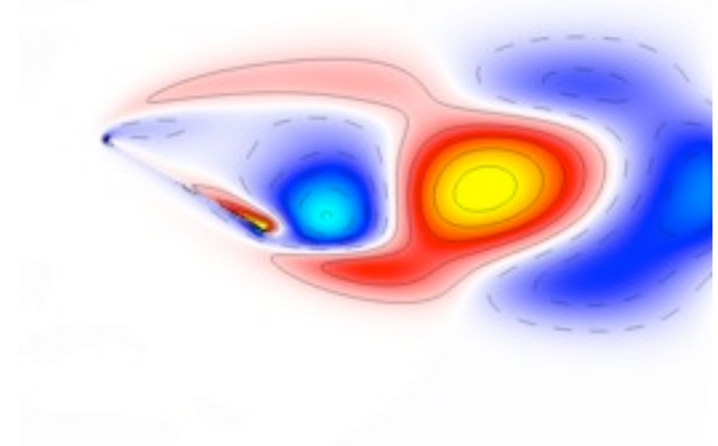

Mode 3

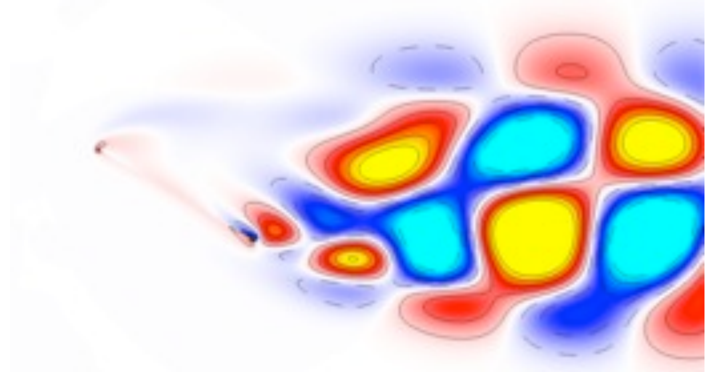

Mode 4

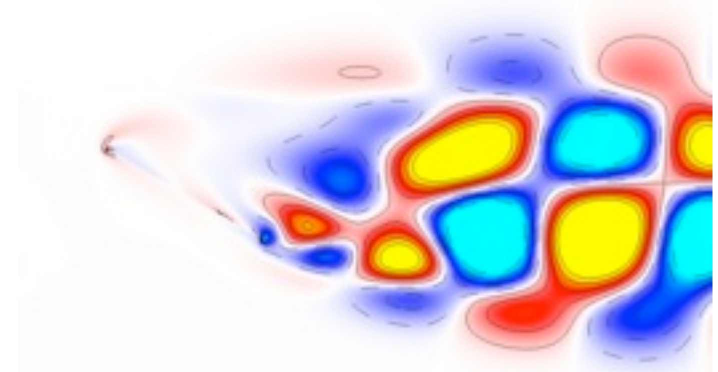

Mean Flow

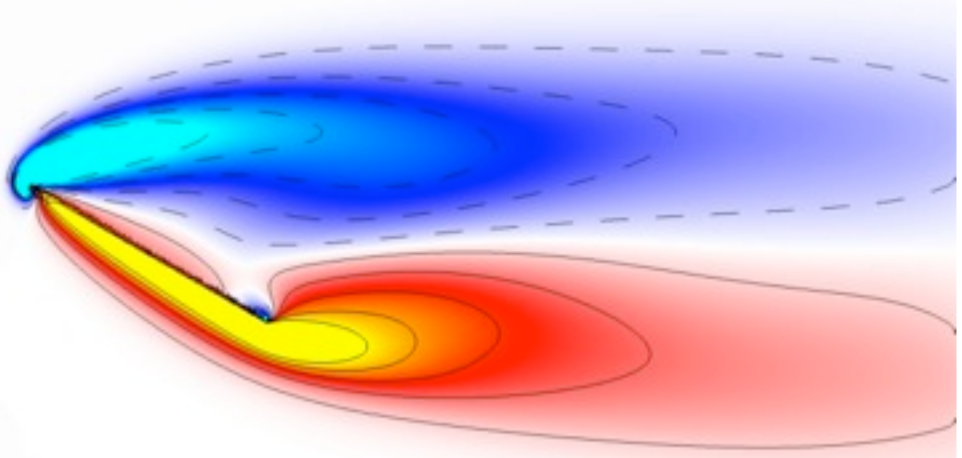

Mode 5

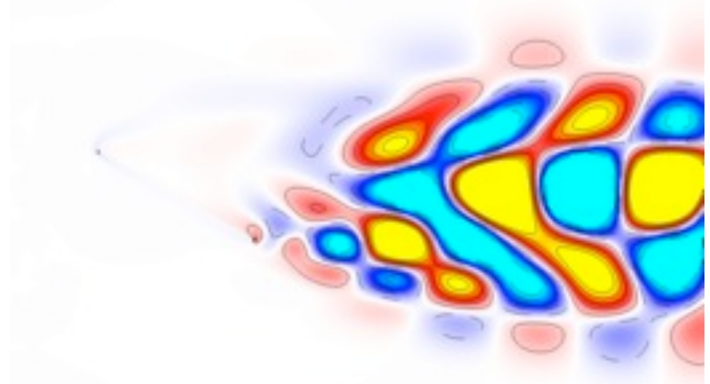

Mode 6

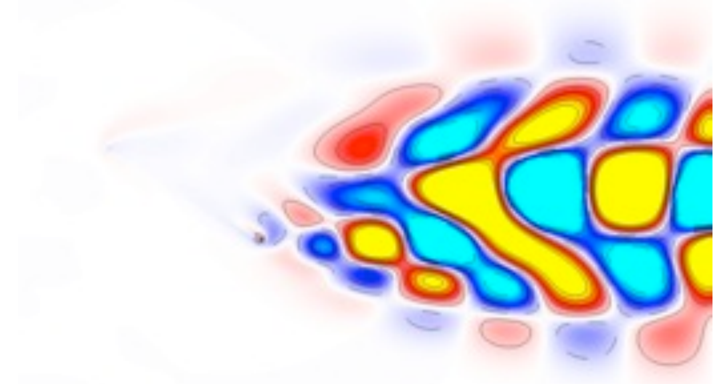

$\mathrm{Re} = 100$

$\alpha = 30^\circ$

Lift vs. Angle of Attack

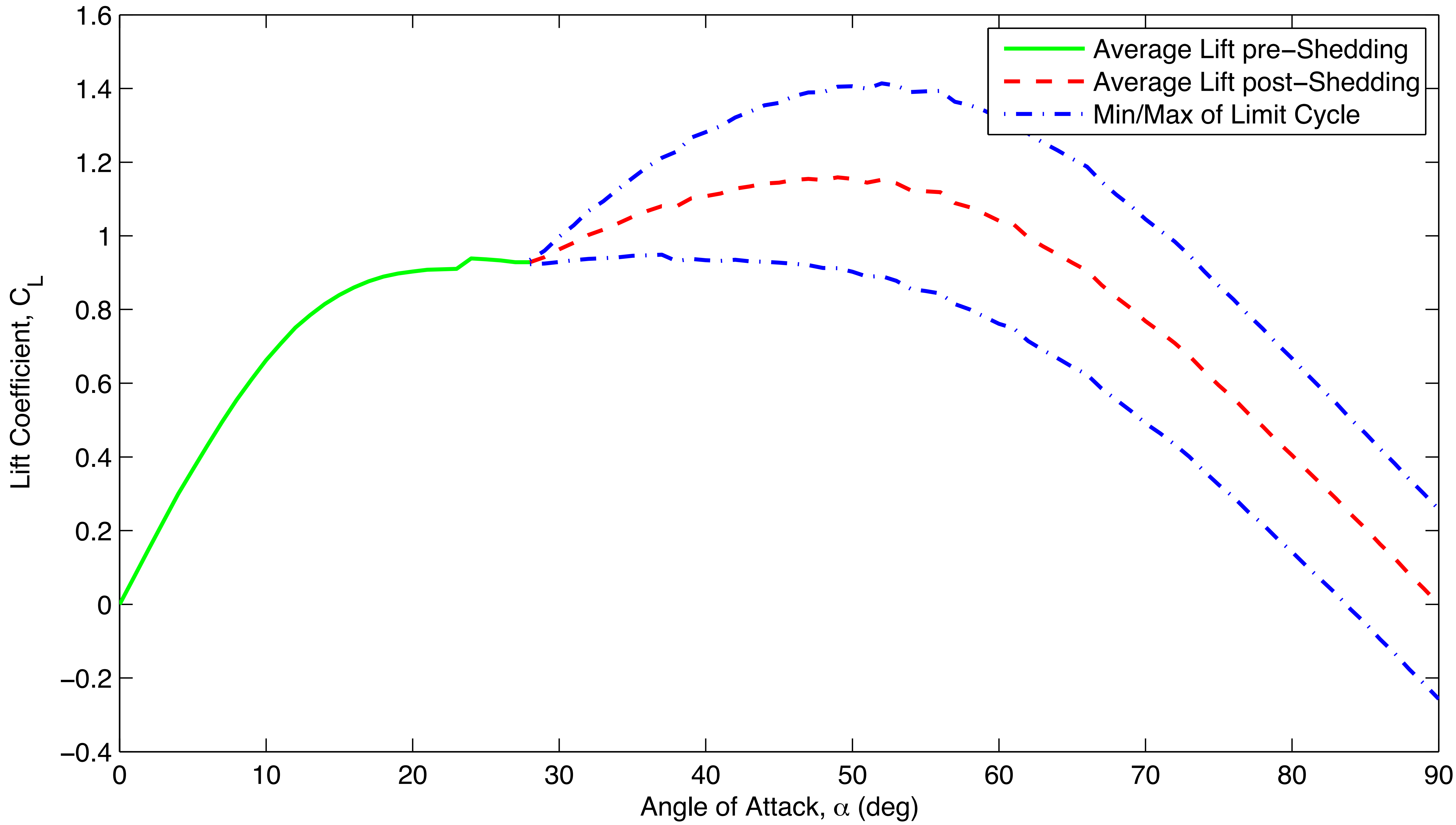

Need model that captures lift due to moving airfoil!

Lift vs. Angle of Attack

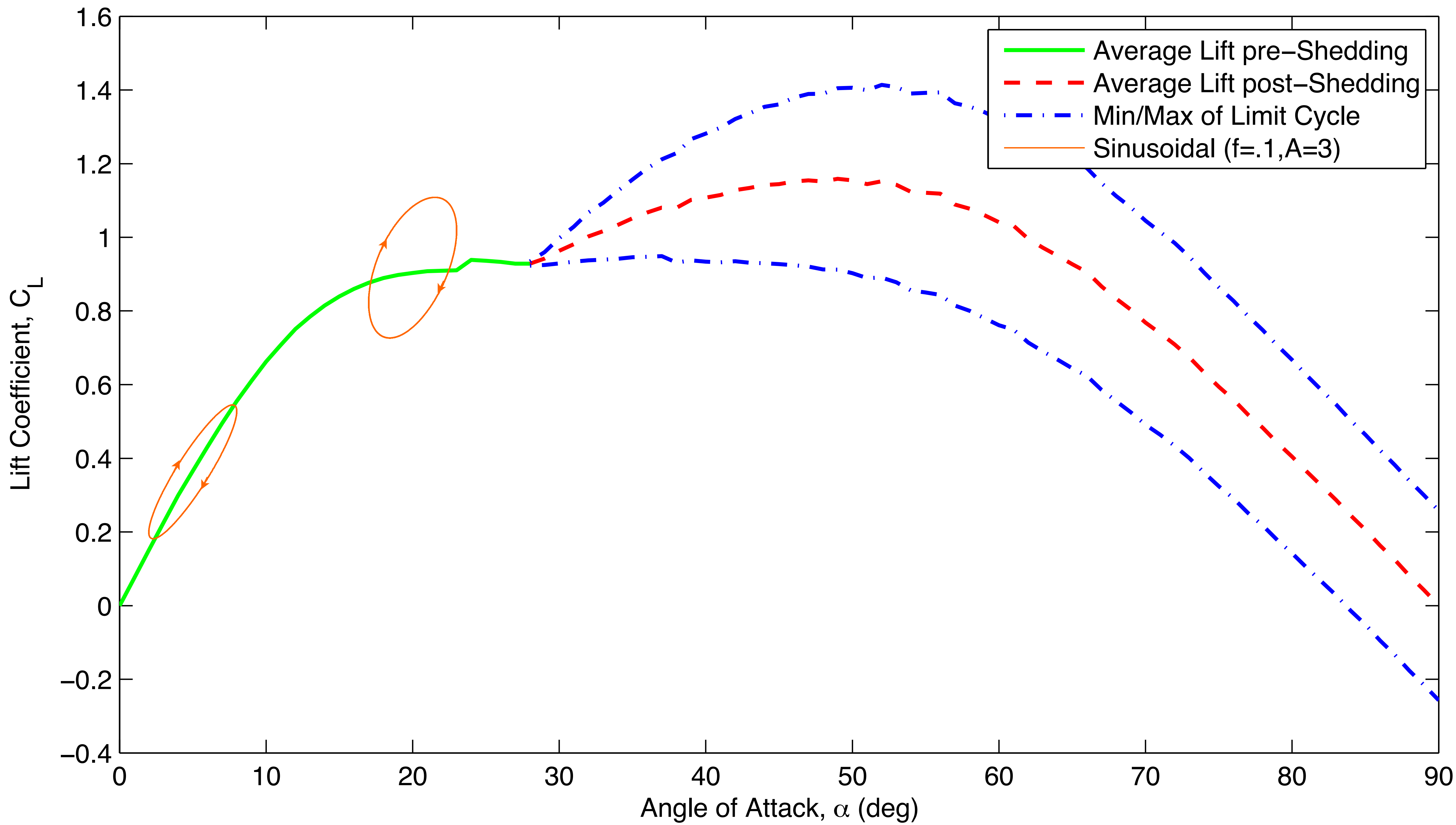

Need model that captures lift due to moving airfoil!

Lift vs. Angle of Attack

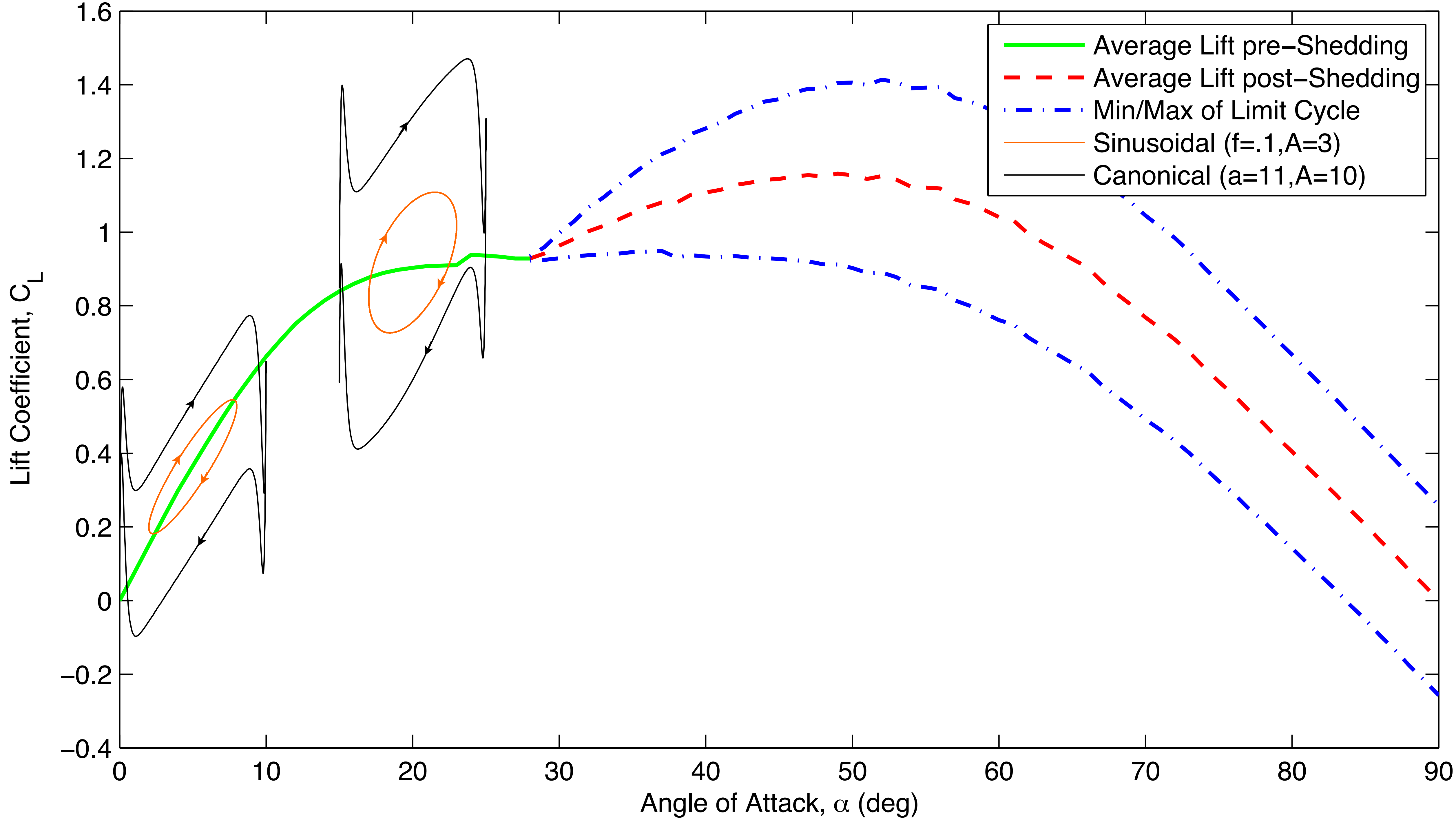

Need model that captures lift due to moving airfoil!

Lift vs. Angle of Attack

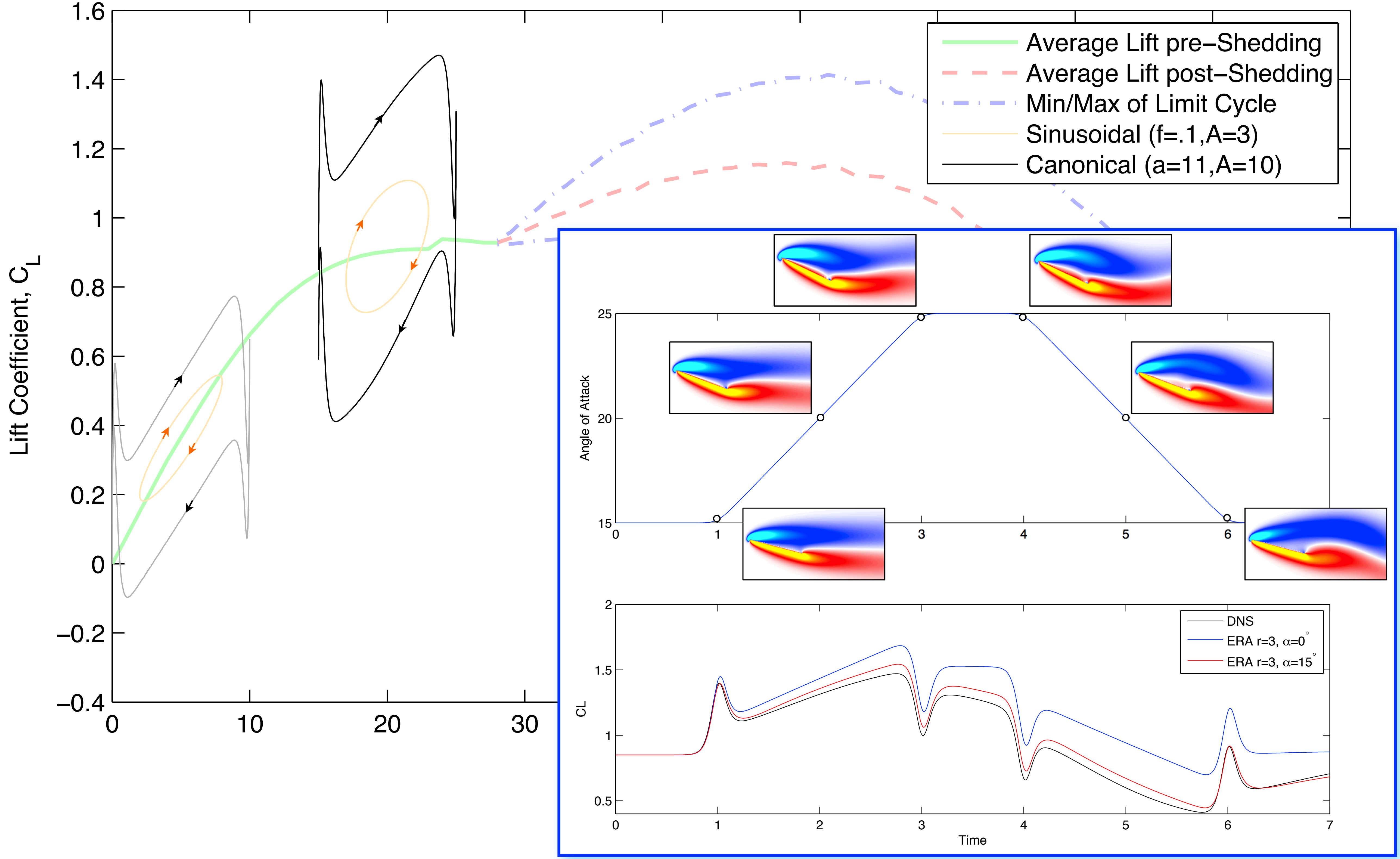

Need model that captures lift due to moving airfoil!

Lift vs. Angle of Attack

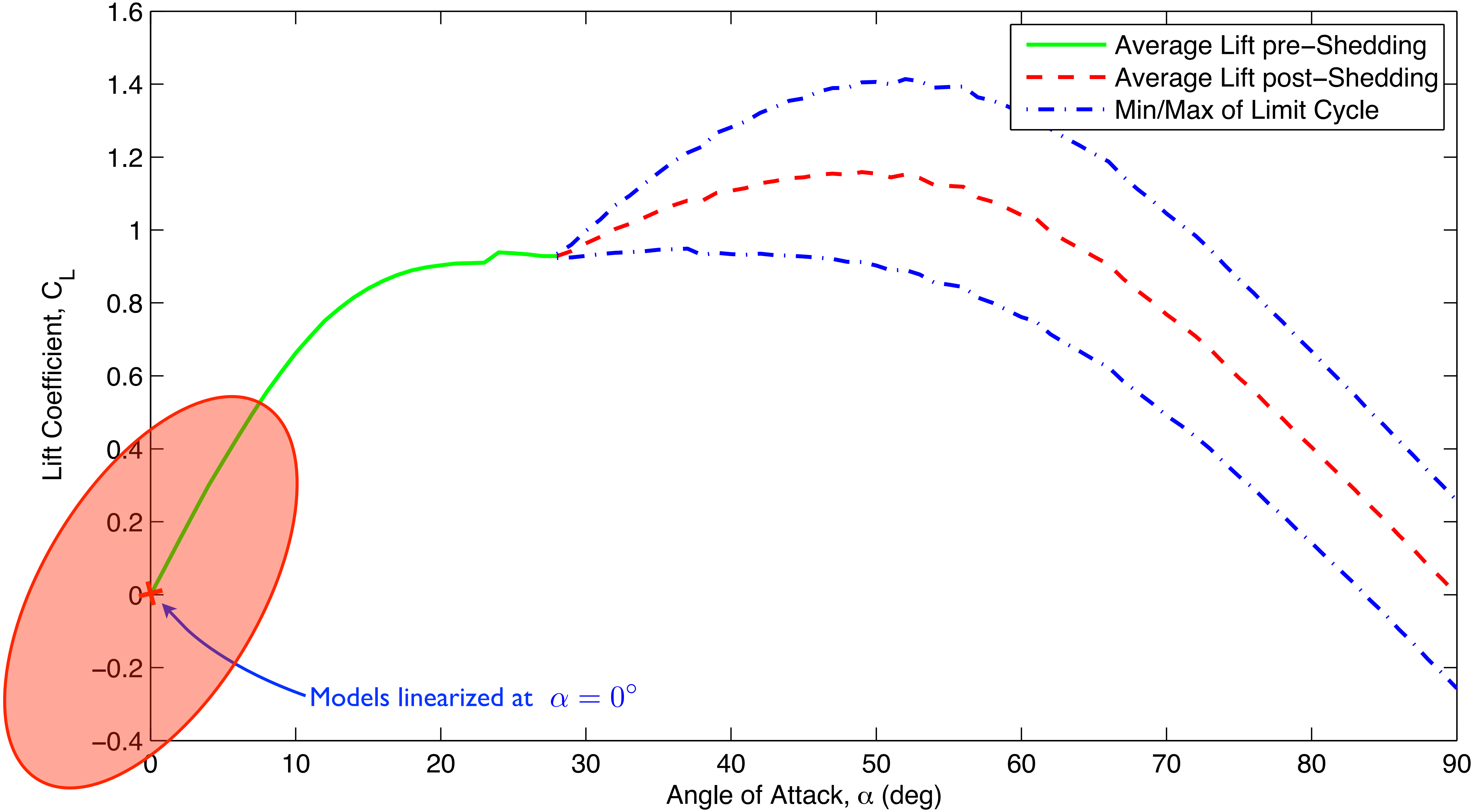

2D Model Problem

Added-Mass

Transient

Periodic Vortex Shedding

Lift

Drag

$\mathrm{Re} = 300$

$\alpha = 32^\circ$

2D Model Problem

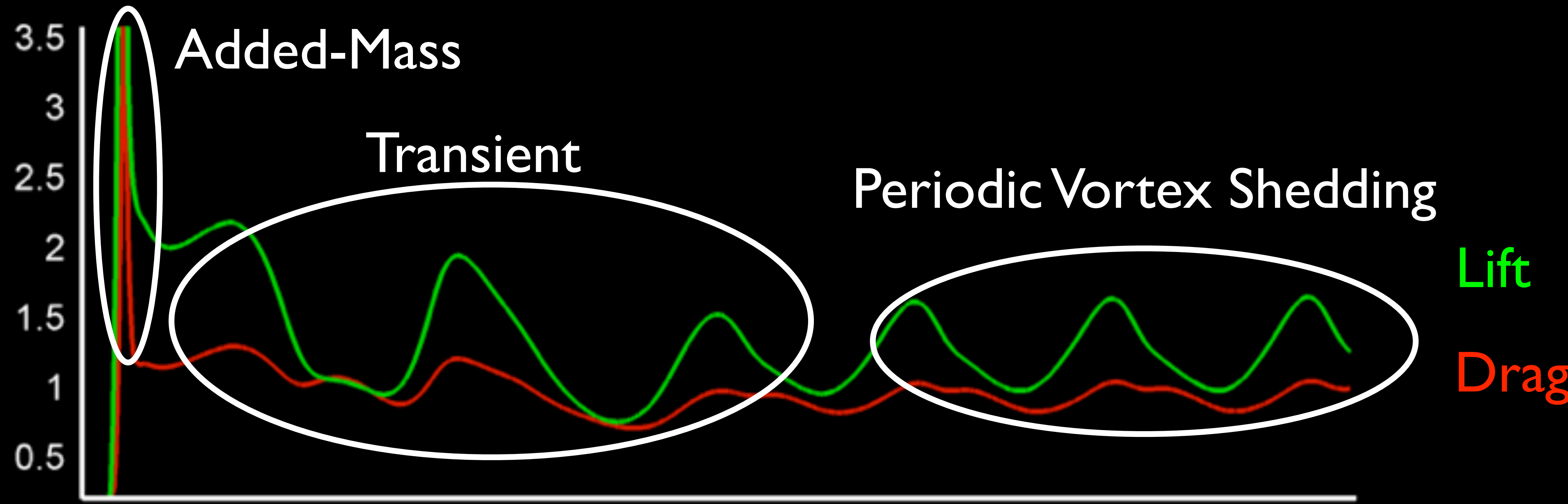

$\mathrm{Re} = 300$
$\alpha = 32^\circ$

Unsteady Aerodynamic Forces

Added Mass

Increasingly important for small/light aircraft

Unsteady potential flow forces (F=ma)

force needed to move air as plate accelerates

Circulatory/Viscous

Captures separation effects

Need improved models here

source of all lift in steady flight... and more

Unsteady Aerodynamic Forces

Added Mass

Increasingly important for small/light aircraft

Unsteady potential flow forces (F=ma)

force needed to move air as plate accelerates

Circulatory/Viscous

Captures separation effects

Need improved models here

source of all lift in steady flight... and more

The mass of the body and surrounding fluid are being accelerated, to different extents.

Kinetic energy T will be in some manner proportional to U (for potential and Stokes flows)

$$T = \rho \frac{I}{2} U^2 \qquad \text{where} \qquad I = \int_V \frac{u_i}{U} \cdot \frac{u_i}{U} dV$$

If body accelerates, T probably increases, and energy must be supplied:

$$\frac{dT}{dt} = -FU \quad \Longrightarrow \quad F_i = -\underbrace{\rho I_{ij}}_{\mathrm{AM}} \dot{U}_j$$

Lamb, 1945.

Milne-Thompson, 1962

Newman, 1977.

cylinder moving in Lab frame

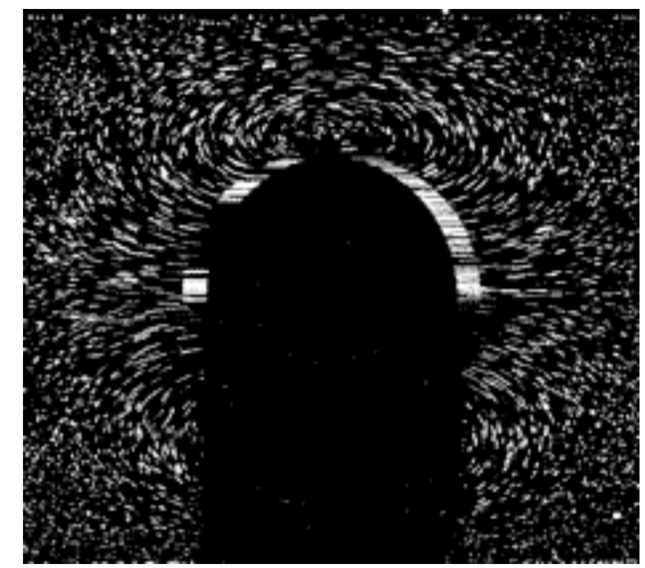

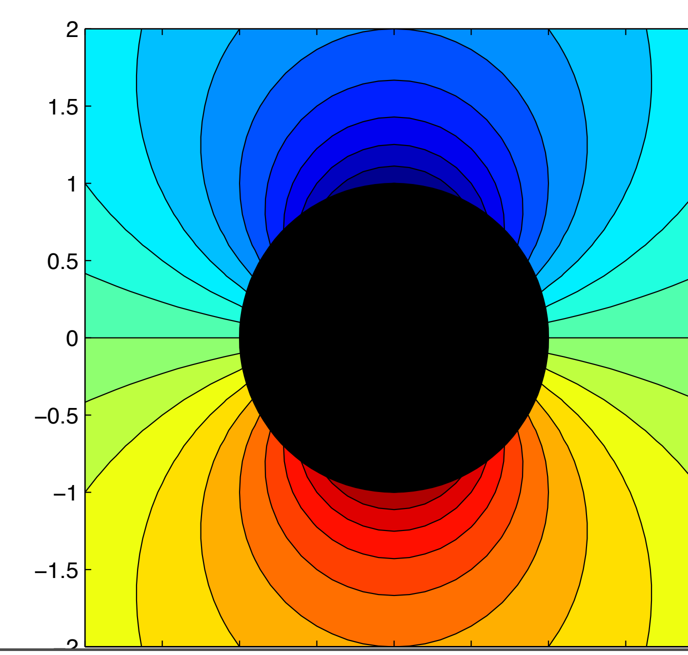

Unsteady Aerodynamic Forces

Added Mass

Increasingly important for small/light aircraft

Unsteady potential flow forces (F=ma)

force needed to move air as plate accelerates

Circulatory/Viscous

Captures separation effects

Need improved models here

source of all lift in steady flight... and more

The mass of the body and surrounding fluid are being accelerated, to different extents.

Kinetic energy T will be in some manner proportional to U (for potential and Stokes flows)

$$T = \rho \frac{I}{2} U^2 \qquad \text{where} \qquad I = \int_V \frac{u_i}{U} \cdot \frac{u_i}{U} dV$$

If body accelerates, T probably increases, and energy must be supplied:

$$\frac{dT}{dt} = -FU \quad \Longrightarrow \quad F_i = -\underbrace{\rho I_{ij}}_{\text{AM}} \dot{U}_j$$

Lamb, 1945.

Milne-Thompson, 1962

Newman, 1977.

Beer bubble acceleration

Unsteady Aerodynamic Forces

Added Mass

Increasingly important for small/light aircraft

Unsteady potential flow forces (F=ma)

force needed to move air as plate accelerates

Circulatory/Viscous

Captures separation effects

Need improved models here

source of all lift in steady flight... and more

Boundary layer

Laminar separation bubble

Leading edge vortex

Periodic Vortex Shedding

Milne-Thompson, 1973.

Stengel, 2004.

Theodorsen's Model - 1935

Added Mass

Increasingly important for small/light aircraft

Unsteady potential flow forces (F=ma)

force needed to move air as plate accelerates

Circulatory/Viscous

Captures separation effects

Need improved models here

source of all lift in steady flight... and more

$$C_L = \underbrace{\frac{\pi}{2}\left[\ddot{h} + \dot{\alpha} - \frac{a}{2}\ddot{\alpha}\right]}_{\text{Added-Mass}} + \underbrace{2\pi\left[\alpha + \dot{h} + \frac{1}{2}\dot{\alpha}\left(\frac{1}{2} - a\right)\right]}_{\text{Circulatory}} C(k)$$

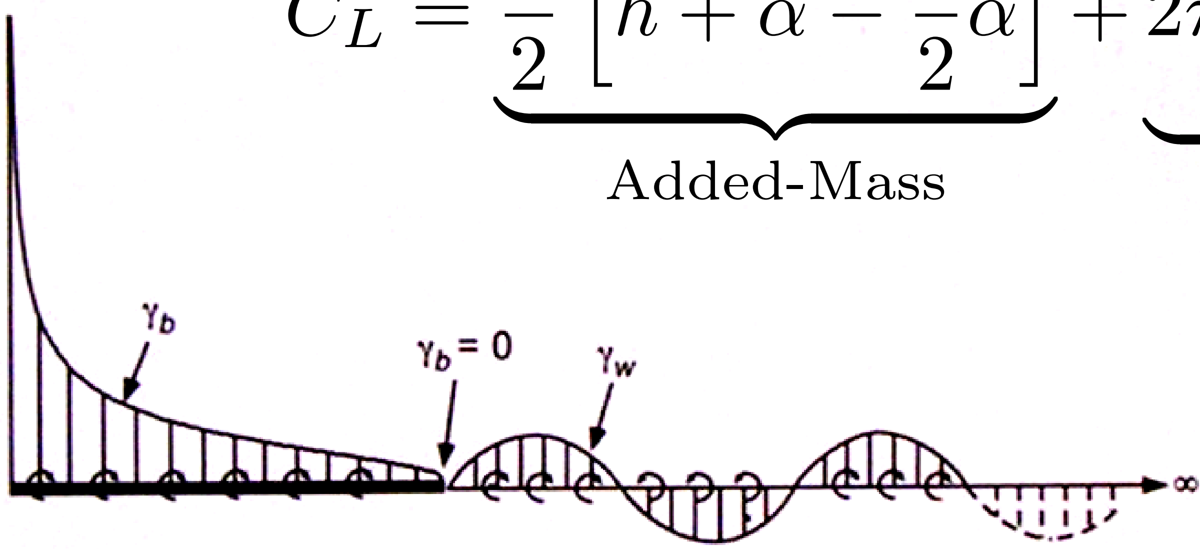

$$C(k) = \frac{H_1^{(2)}(k)}{H_1^{(2)}(k) + iH_0^{(2)}(k)}$$

2D Incompressible, inviscid model

Unsteady potential flow (w/ Kutta condition)

Linearized about zero angle of attack

$$\boxed{k = \frac{\pi f c}{U_\infty}}$$

Theodorsen, 1935.

Leishman, 2006.

Bode Plot of Theodorsen

$$C_L = \underbrace{\frac{\pi}{2}\left[\ddot{h} + \dot{\alpha} - \frac{a}{2}\ddot{\alpha}\right]}_{\text{Added-Mass}} + \underbrace{2\pi\left[\alpha + \dot{h} + \frac{1}{2}\dot{\alpha}\left(\frac{1}{2} - a\right)\right]}_{\text{Circulatory}} C(k)$$

$$\boxed{k = \frac{\pi f c}{U_\infty}}$$

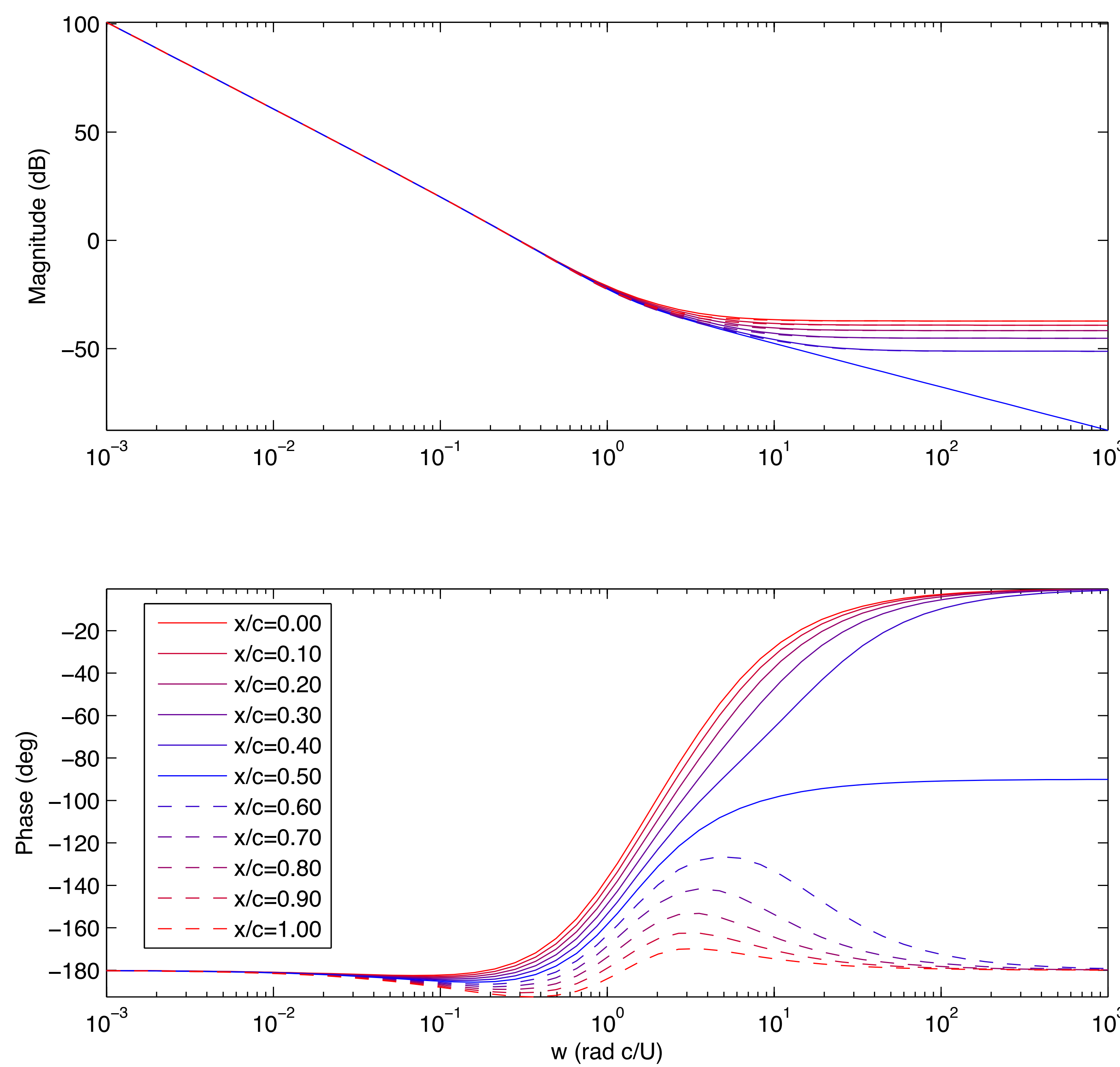

Frequency response

input is $\ddot{\alpha}$ **(** α **is angle of attack)**

output is lift coefficient $\mathrm{C_L}$

Low frequencies dominated by quasi-steady forces

High frequencies dominated by added-mass forces

Crossover region determined by Theodorsen's function $\mathrm{C(k)}$

Brunton and Rowley, AIAA ASM 2011

Zeros of Theodorsen's Model

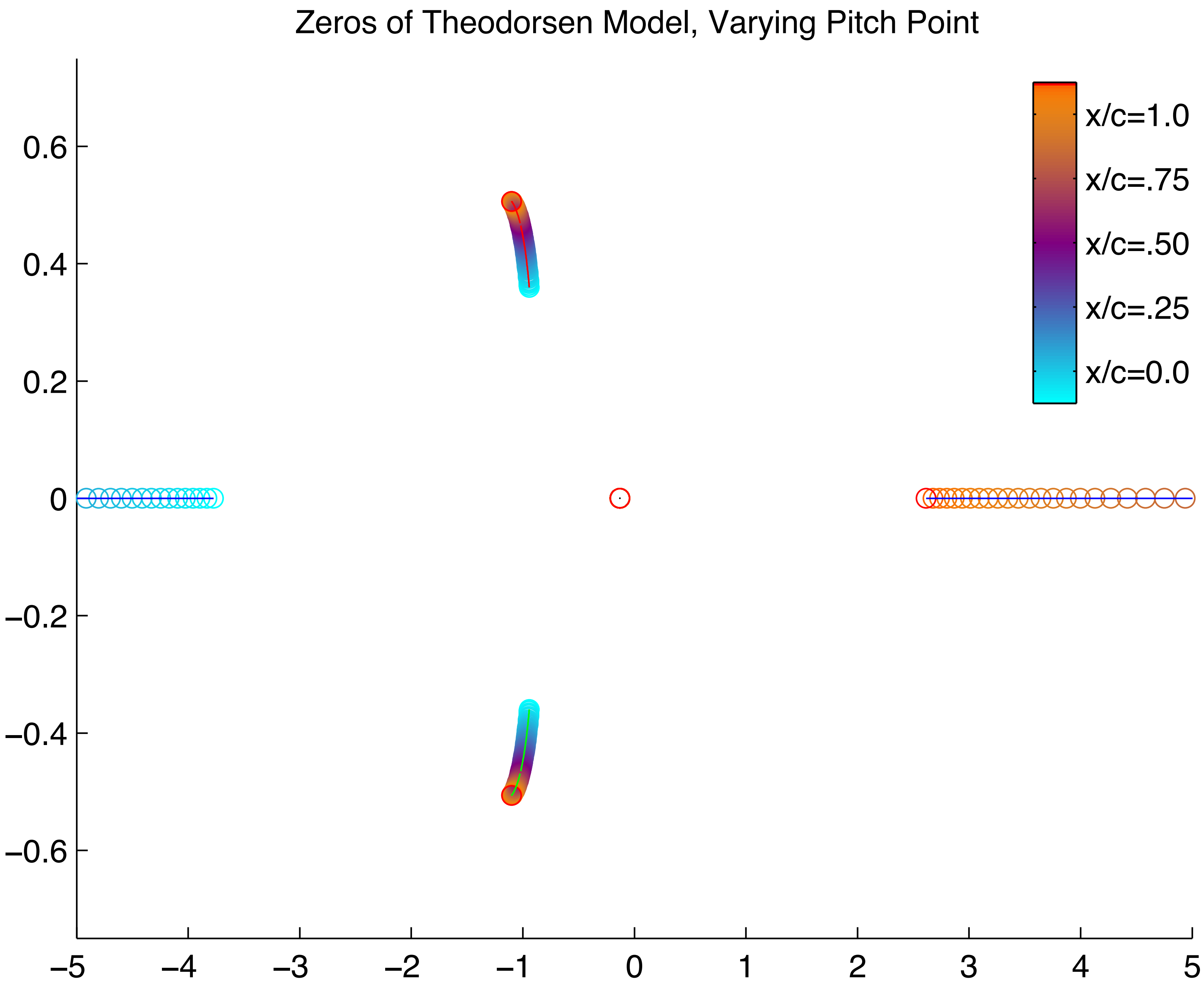

All Theodorsen pitch models have same poles, different zeros

As pitch point moves aft of center, zero enters RHP at +infinity.

non-minimum phase response:

Given a step in angle of attack, lift initially moves in opposite direction (because of negative added-mass forces), before the circulatory lift forces have a change to catch up and system relaxes to a positive lift steady state.

Brunton and Rowley, AIAA ASM 2011

Indicial Response Models

Given an impulse in angle of attack, $\alpha = \delta(t)$, the time history of Lift is $C_L^\delta(t)$

The response to an arbitrary input $\alpha(t)$ is given by linear superposition:

$$C_L(t) = \int_0^t C_L^\delta(t-\tau)\alpha(\tau)d\tau = \left(C_L^\delta * \alpha\right)(t)$$

Given a step in angle of attack, $\dot{\alpha} = \delta(t)$, the time history of Lift is $C_L^S(t)$

The response to an arbitrary input $\alpha(t)$ is given by:

$$C_L(t) = C_L^S(t)\alpha(0) + \int_0^t C_L^S(t-\tau)\dot{\alpha}(\tau)d\tau$$

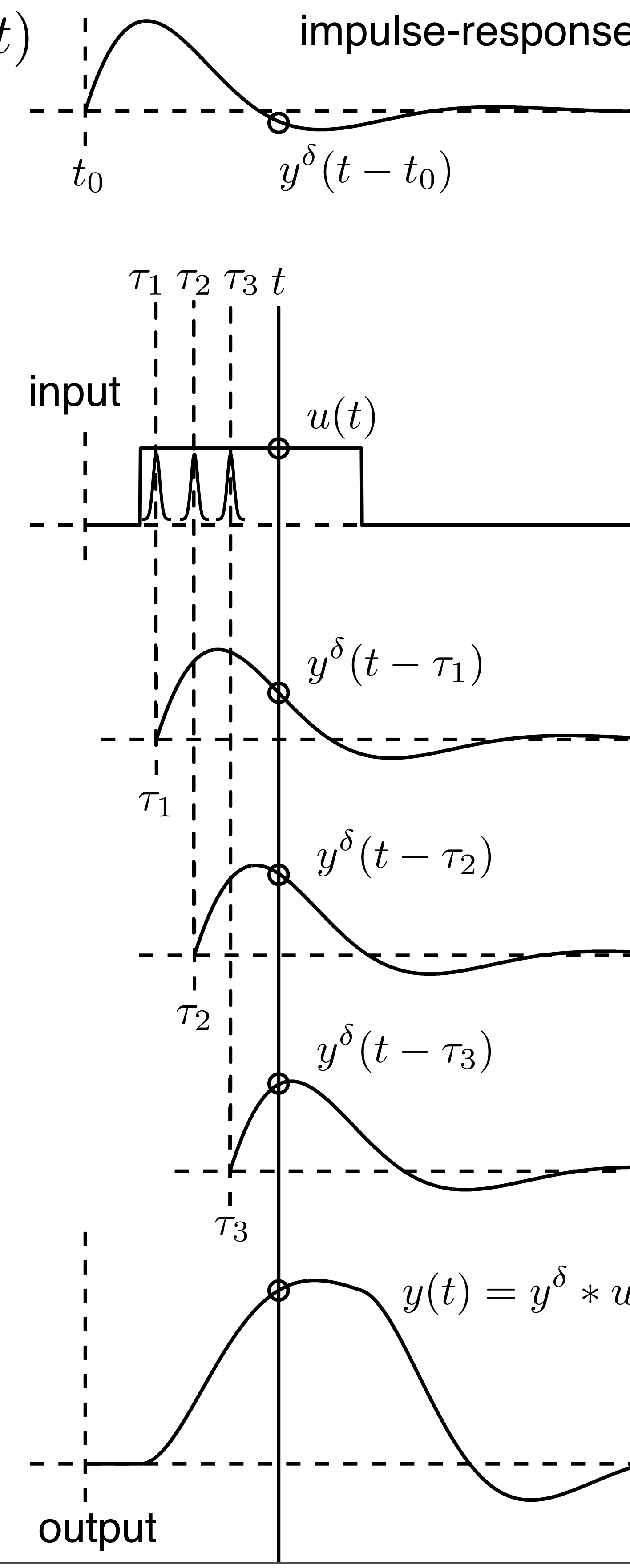

Model Summary

Reconstructs Lift for arbitrary input

Linear time-invariant (LTI) models

Based on experiment, simulation or theory

Wagner developed indicial response analytically using same approximations as Theodorsen

convolution integral inconvenient for feedback control design

Wagner, 1925.

Reisenthel, 1996.

Leishman, 2006.

Indicial Response Models

Given an impulse in angle of attack, $\alpha = \delta(t)$, the time history of Lift is $C_L^{\delta}(t)$

The response to an arbitrary input $\alpha(t)$ is given by linear superposition:

$$C_L(t) = \int_0^t C_L^{\delta}(t-\tau)\alpha(\tau)d\tau = \left(C_L^{\delta} * \alpha\right)(t)$$

Given a step in angle of attack, $\dot{\alpha} = \delta(t)$, the time history of Lift is $C_L^S(t)$

The response to an arbitrary input $\alpha(t)$ is given by:

$$C_L(t) = C_L^S(t)\alpha(0) + \int_0^t C_L^S(t-\tau)\dot{\alpha}(\tau)d\tau$$

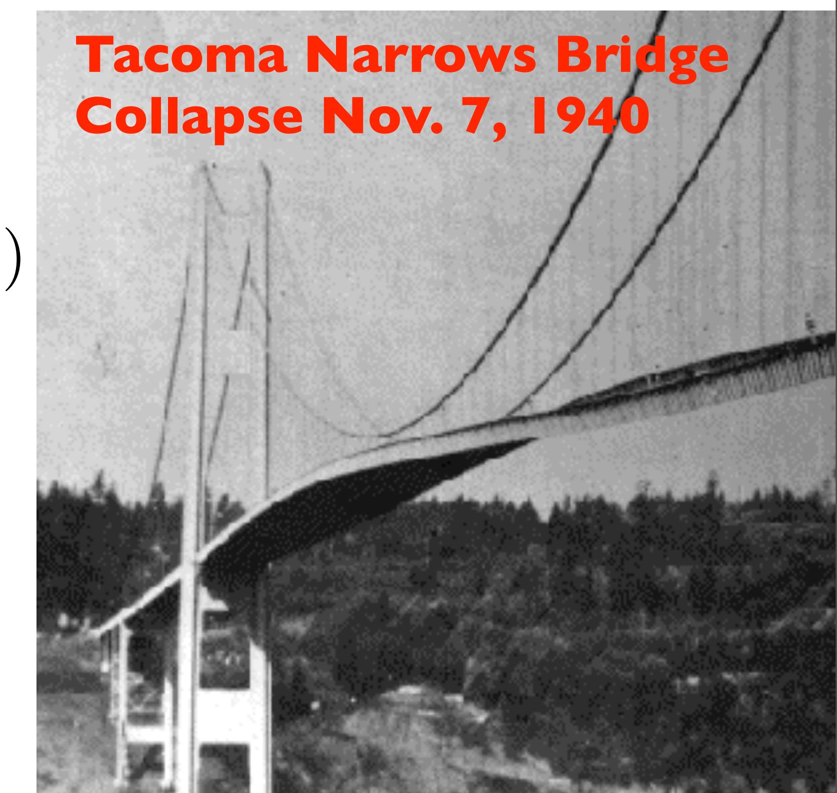

Model Summary

Reconstructs Lift for arbitrary input

Linear time-invariant (LTI) models

Based on experiment, simulation or theory

Wagner developed indicial response analytically using same approximations as Theodorsen

convolution integral inconvenient for feedback control design

Wagner, 1925.

Reisenthel, 1996.

Leishman, 2006.

State-Space Indicial Response

Indicial Response

Tuned to specific geometry, Re #

$$C_L(t) = C_L^\delta(t)\alpha(0) + \int_0^t C_L^\delta(t-\tau)\dot{\alpha}(\tau)d\tau$$

Theodorsen's Model

Physically motivated components

Parametrized by pitch point

Frequency domain, idealized assumptions

$$C_L = \underbrace{\frac{\pi}{2}\left[\ddot{h} + \dot{\alpha} - \frac{a}{2}\ddot{\alpha}\right]}_{\text{Added-Mass}} + \underbrace{2\pi\left[\alpha + \dot{h} + \frac{1}{2}\dot{\alpha}\left(\frac{1}{2} - a\right)\right]}_{\text{Circulatory}} C(k)$$

State-Space Model

Captures input output dynamics accurately

Computationally tractable

fits into control framework

transient dynamics

$$\frac{d}{dt}\begin{bmatrix}\mathbf{x}\\ \alpha\\ \dot{\alpha}\end{bmatrix} = \begin{bmatrix}A_r & 0 & 0\\ 0 & 0 & 1\\ 0 & 0 & 0\end{bmatrix}\begin{bmatrix}\mathbf{x}\\ \alpha\\ \dot{\alpha}\end{bmatrix} + \begin{bmatrix}B_r\\ 0\\ 1\end{bmatrix}\ddot{\alpha}$$

$$C_L = \begin{bmatrix}C_r & C_{L_\alpha} & C_{L_{\dot{\alpha}}}\end{bmatrix}\begin{bmatrix}\mathbf{x}\\ \alpha\\ \dot{\alpha}\end{bmatrix} + C_{L_{\ddot{\alpha}}}\ddot{\alpha}$$

quasi-steady and added-mass

State-Space Indicial Response

Stability derivatives plus fast dynamics

$$C_L(\alpha, \dot{\alpha}, \ddot{\alpha}, \mathbf{x}) = C_{L_\alpha}\alpha + C_{L_{\dot{\alpha}}}\dot{\alpha} + C_{L_{\ddot{\alpha}}}\ddot{\alpha} + C\mathbf{x}$$

Quasi-steady and added-mass

Transient dynamics

Transfer Function

$$Y(s) = \left[\frac{C_{L_\alpha}}{s^2} + \frac{C_{L_{\dot{\alpha}}}}{s} + C_{L_{\ddot{\alpha}}} + G(s)\right] s^2 U(s)$$

State-Space Model

Captures input output dynamics accurately

Computationally tractable

fits into control framework

transient dynamics

$$\frac{d}{dt}\begin{bmatrix}\mathbf{x}\\ \alpha \\ \dot{\alpha}\end{bmatrix} = \begin{bmatrix} A_r & 0 & 0 \\ 0 & 0 & 1 \\ 0 & 0 & 0 \end{bmatrix}\begin{bmatrix}\mathbf{x}\\ \alpha \\ \dot{\alpha}\end{bmatrix} + \begin{bmatrix} B_r \\ 0 \\ 1\end{bmatrix}\ddot{\alpha}$$

$$C_L = \begin{bmatrix} C_r & C_{L_\alpha} & C_{L_{\dot{\alpha}}}\end{bmatrix}\begin{bmatrix}\mathbf{x}\\ \alpha \\ \dot{\alpha}\end{bmatrix} + C_{L_{\ddot{\alpha}}}\ddot{\alpha}$$

quasi-steady and added-mass

State-Space Indicial Response

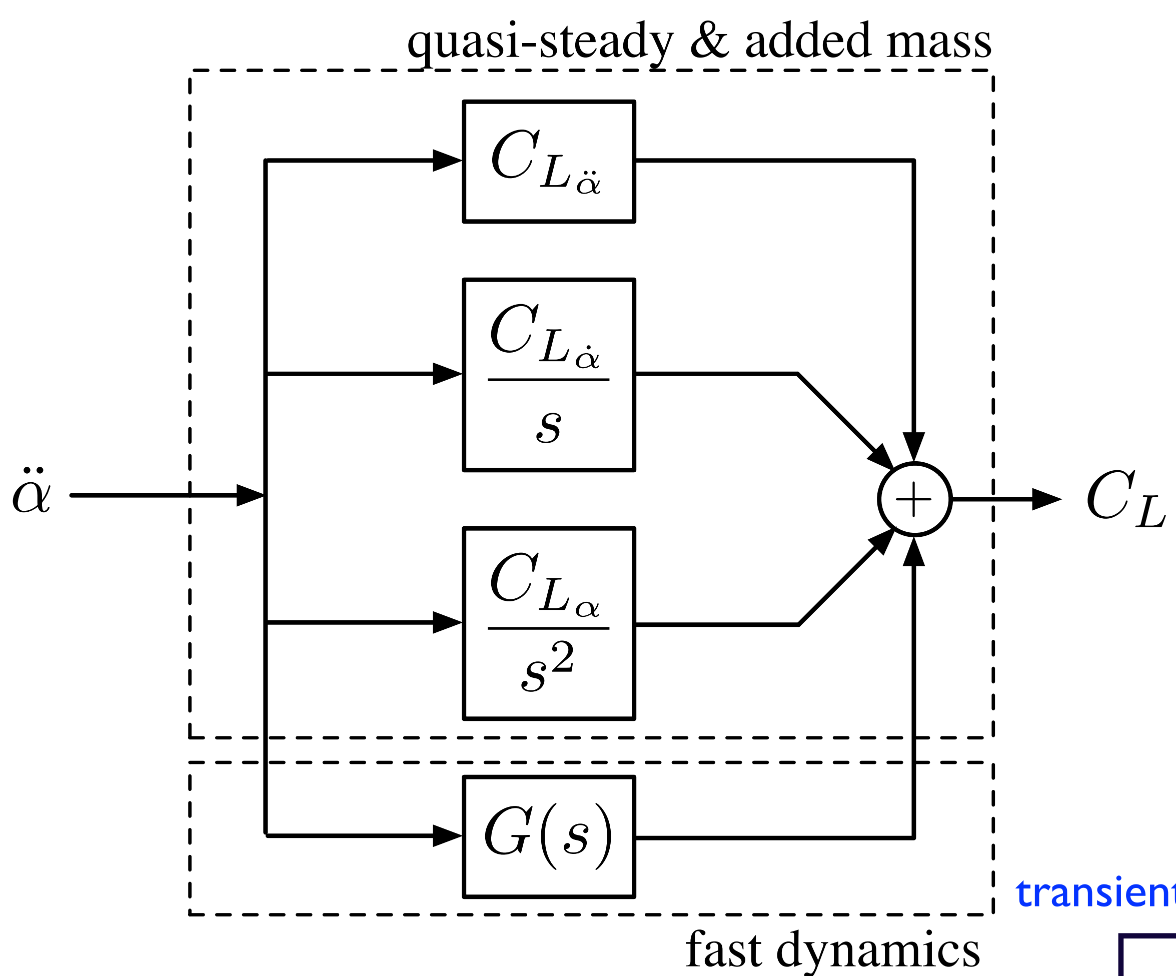

Model Summary

Linearized about $\alpha = 0$

Based on experiment, simulation or theory

Recovers stability derivatives $C_{L_\alpha}, C_{L_{\dot{\alpha}}}, C_{L_{\ddot{\alpha}}}$ associated with quasi-steady and added-mass

ODE model ideal for control design

transient dynamics

$$\frac{d}{dt}\begin{bmatrix}\mathbf{x}\\ \alpha\\ \dot{\alpha}\end{bmatrix} = \begin{bmatrix}A_r & 0 & 0\\ 0 & 0 & 1\\ 0 & 0 & 0\end{bmatrix}\begin{bmatrix}\mathbf{x}\\ \alpha\\ \dot{\alpha}\end{bmatrix} + \begin{bmatrix}B_r\\ 0\\ 1\end{bmatrix}\ddot{\alpha}$$

$$C_L = \begin{bmatrix}C_r & C_{L_\alpha} & C_{L_{\dot{\alpha}}}\end{bmatrix}\begin{bmatrix}\mathbf{x}\\ \alpha\\ \dot{\alpha}\end{bmatrix} + C_{L_{\ddot{\alpha}}}\ddot{\alpha}$$

quasi-steady and added-mass

Brunton and Rowley, *in preparation.*

Identifying Model from Simulations

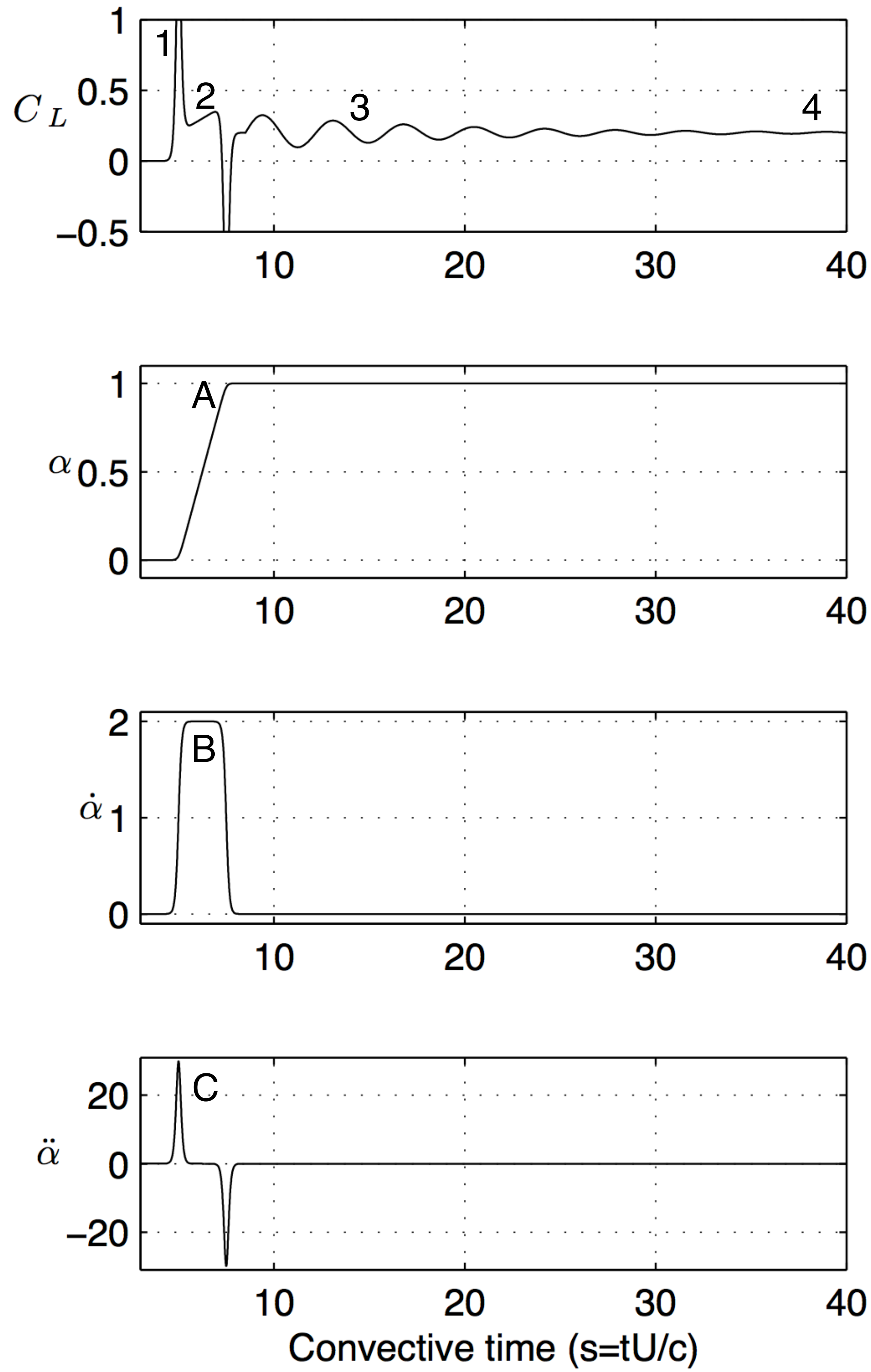

1 - added-mass from $\ddot{\alpha}$ (C)

2 - added-mass from $\dot{\alpha}$ (B) and quasi-steady α (A)

3 - fast dynamics (G) and quasi-steady from α (A)

4 - quasi-steady from α (A)

Cartoon illustration of aerodynamic step response

4-6 orders of magnitude frequency and scale separation in response

Method I

step maneuver in α
$\dot{\alpha} = \delta$ (resolved in time)

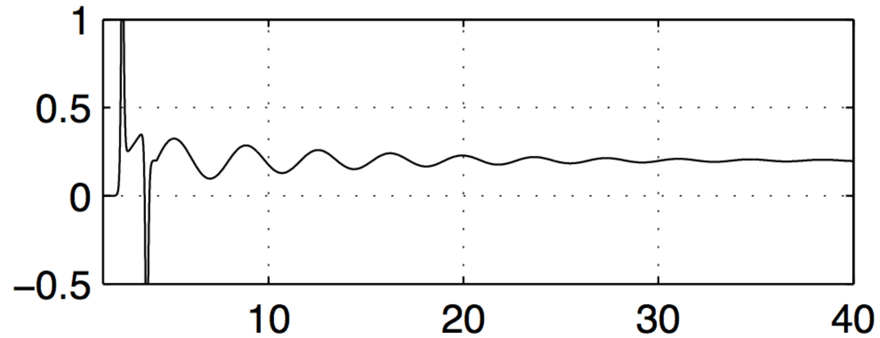

subtract off $\alpha \cdot C_{L_\alpha}$
(low frequency asymptote)

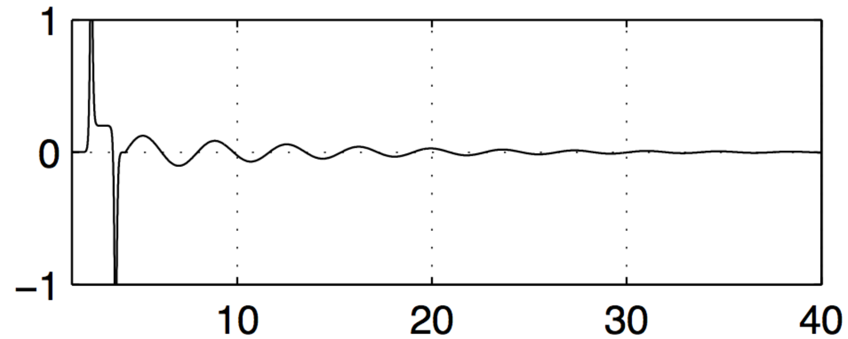

subtract off $\ddot{\alpha} \cdot C_{\ddot{\alpha}}$
(high frequency asymptote)

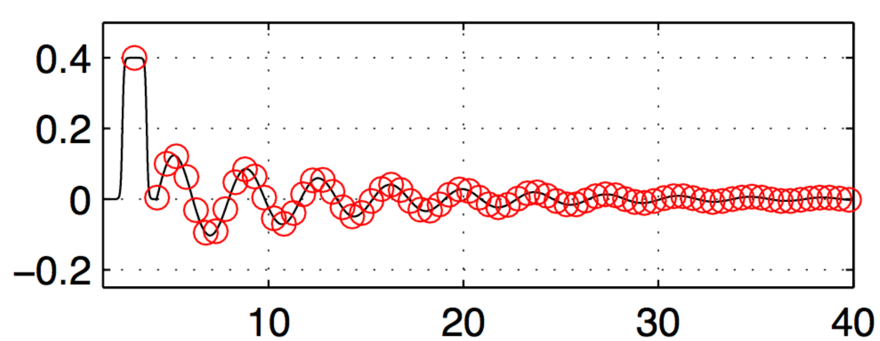

$$\frac{d}{dt}\begin{bmatrix} x \\ \alpha \\ \dot{\alpha} \end{bmatrix} = \begin{bmatrix} A & 0 & B \\ 0 & 0 & 1 \\ 0 & 0 & 0 \end{bmatrix}\begin{bmatrix} x \\ \alpha \\ \dot{\alpha} \end{bmatrix} + \begin{bmatrix} 0 \\ 0 \\ 1 \end{bmatrix}\ddot{\alpha}$$

$$y = \begin{bmatrix} C & C_\alpha & C_{\dot{\alpha}} \end{bmatrix}\begin{bmatrix} x \\ \alpha \\ \dot{\alpha} \end{bmatrix} + D\ddot{\alpha}$$

Transient dynamics modeled using ERA model

$$\dot{\alpha} \to (A, B, C, C_{\dot{\alpha}}) \to C_L$$

Method II

step maneuver in α
$\dot{\alpha} = \delta$ (resolved in time)

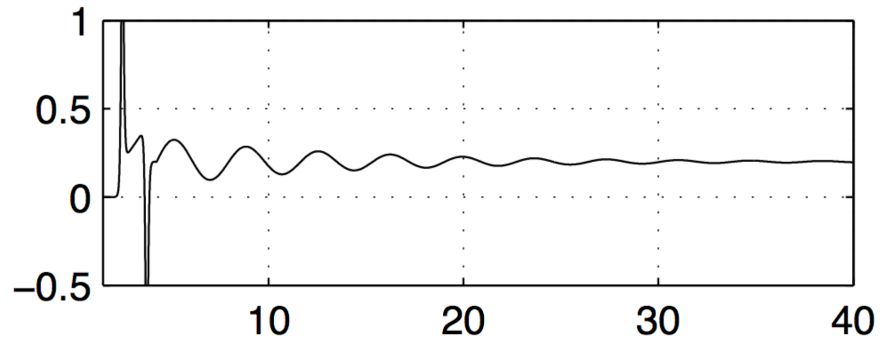

subtract off $\alpha \cdot C_{L_\alpha}$
(low frequency asymptote)

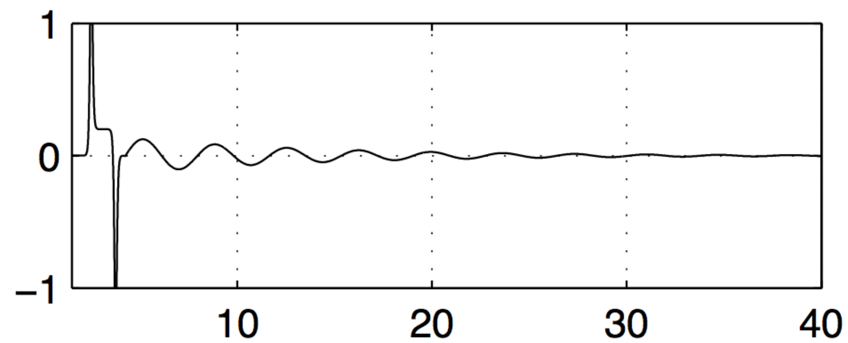

subtract off $\dot{\alpha} \cdot C_{\dot{\alpha}}$

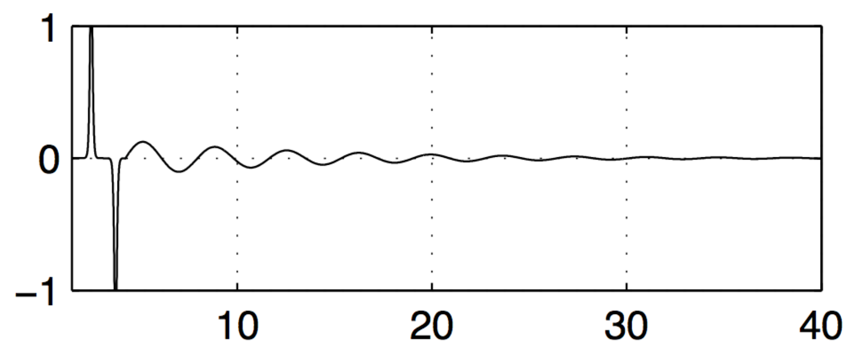

integrate to obtain $\ddot{\alpha} = \delta$
(less C_{L_α} and $C_{\dot{\alpha}}$ terms)

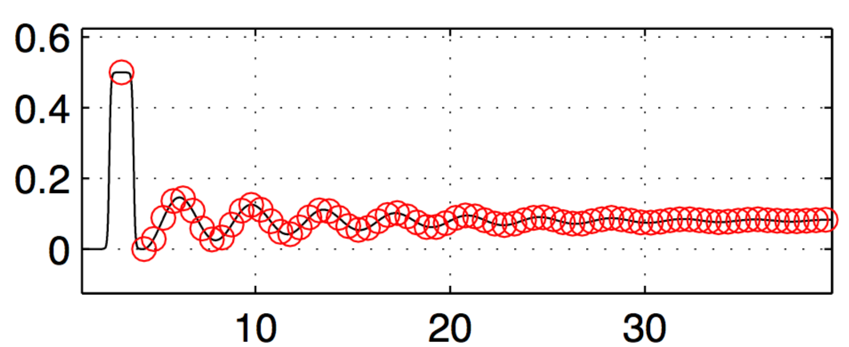

$$\frac{d}{dt}\begin{bmatrix} x \\ \alpha \\ \dot{\alpha} \end{bmatrix} = \begin{bmatrix} A & 0 & 0 \\ 0 & 0 & 1 \\ 0 & 0 & 0 \end{bmatrix} \begin{bmatrix} x \\ \alpha \\ \dot{\alpha} \end{bmatrix} + \begin{bmatrix} B \\ 0 \\ 1 \end{bmatrix} \ddot{\alpha}$$

$$y = \begin{bmatrix} C & C_\alpha & C_{\dot{\alpha}} \end{bmatrix} \begin{bmatrix} x \\ \alpha \\ \dot{\alpha} \end{bmatrix} + D\ddot{\alpha}$$

Transient dynamics modeled using ERA model

$$\dot{\alpha} \rightarrow (A, B, C, D) \rightarrow C_L$$

Summary of Methods

Method I

$$\frac{d}{dt}\begin{bmatrix} x \\ \alpha \\ \dot{\alpha} \end{bmatrix} = \begin{bmatrix} A & 0 & B \\ 0 & 0 & 1 \\ 0 & 0 & 0 \end{bmatrix}\begin{bmatrix} x \\ \alpha \\ \dot{\alpha} \end{bmatrix} + \begin{bmatrix} 0 \\ 0 \\ 1 \end{bmatrix}\ddot{\alpha}$$

$$y = \begin{bmatrix} C & C_\alpha & C_{\dot{\alpha}} \end{bmatrix}\begin{bmatrix} x \\ \alpha \\ \dot{\alpha} \end{bmatrix} + D\ddot{\alpha}$$

Method II

$$\frac{d}{dt}\begin{bmatrix} x \\ \alpha \\ \dot{\alpha} \end{bmatrix} = \begin{bmatrix} A & 0 & 0 \\ 0 & 0 & 1 \\ 0 & 0 & 0 \end{bmatrix}\begin{bmatrix} x \\ \alpha \\ \dot{\alpha} \end{bmatrix} + \begin{bmatrix} B \\ 0 \\ 1 \end{bmatrix}\ddot{\alpha}$$

$$y = \begin{bmatrix} C & C_\alpha & C_{\dot{\alpha}} \end{bmatrix}\begin{bmatrix} x \\ \alpha \\ \dot{\alpha} \end{bmatrix} + D\ddot{\alpha}$$

General procedure

1. **Obtain time-resolved step response in pitch angle**
2. **Identify some or all of the quasi-steady and added mass parameters** $C_{L_\alpha}, C_{\dot{\alpha}}, C_{\ddot{\alpha}}$
3. **Model remaining transient dynamic with Eigensystem realization algorithm (ERA)**

recently shown to be equivalent to balanced proper orthogonal decomposition (BPOD)

Highly flexible

1. **Extensions for pitch, plunge, and surge motions**
2. **Multiple input, multiple output models possible with ERA**

Bode Plot - Pitch (LE)

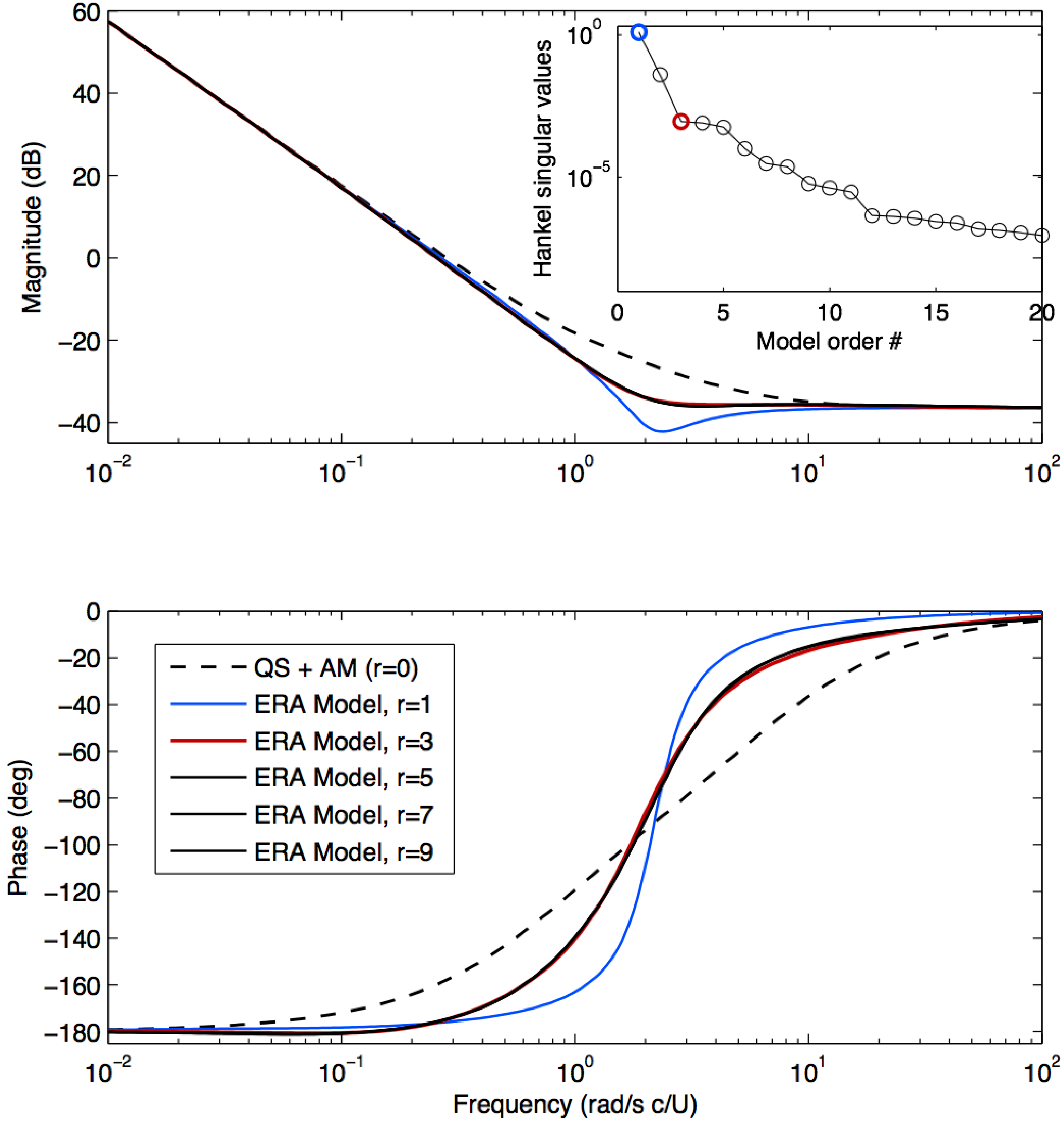

Frequency response

input is $\ddot{\alpha}$ (α is angle of attack)

output is lift coefficient C_L

Pitching at leading edge

Model without additional dynamics [QS+AM (r=0)] is inaccurate in crossover region

Models with fast dynamics of ERA model order >3 are converged

Punchline: additional fast dynamics (ERA model) are essential

Brunton and Rowley, *in preparation*.

Bode Plot - Pitch (QC)

Frequency response

input is $\ddot{\alpha}$ (α is angle of attack)

output is lift coefficient C_L

Pitching at quarter chord

Reduced order model with ERA r=7 accurately reproduces Indicial Response

Indicial Response and model agree better with DNS than Theodorsen's model.

Asymptotes are correct for Indicial Response because it is based on simulations

Model for pitch/plunge dynamics [ERA, r=7 (MIMO)] works as well, for the same order model

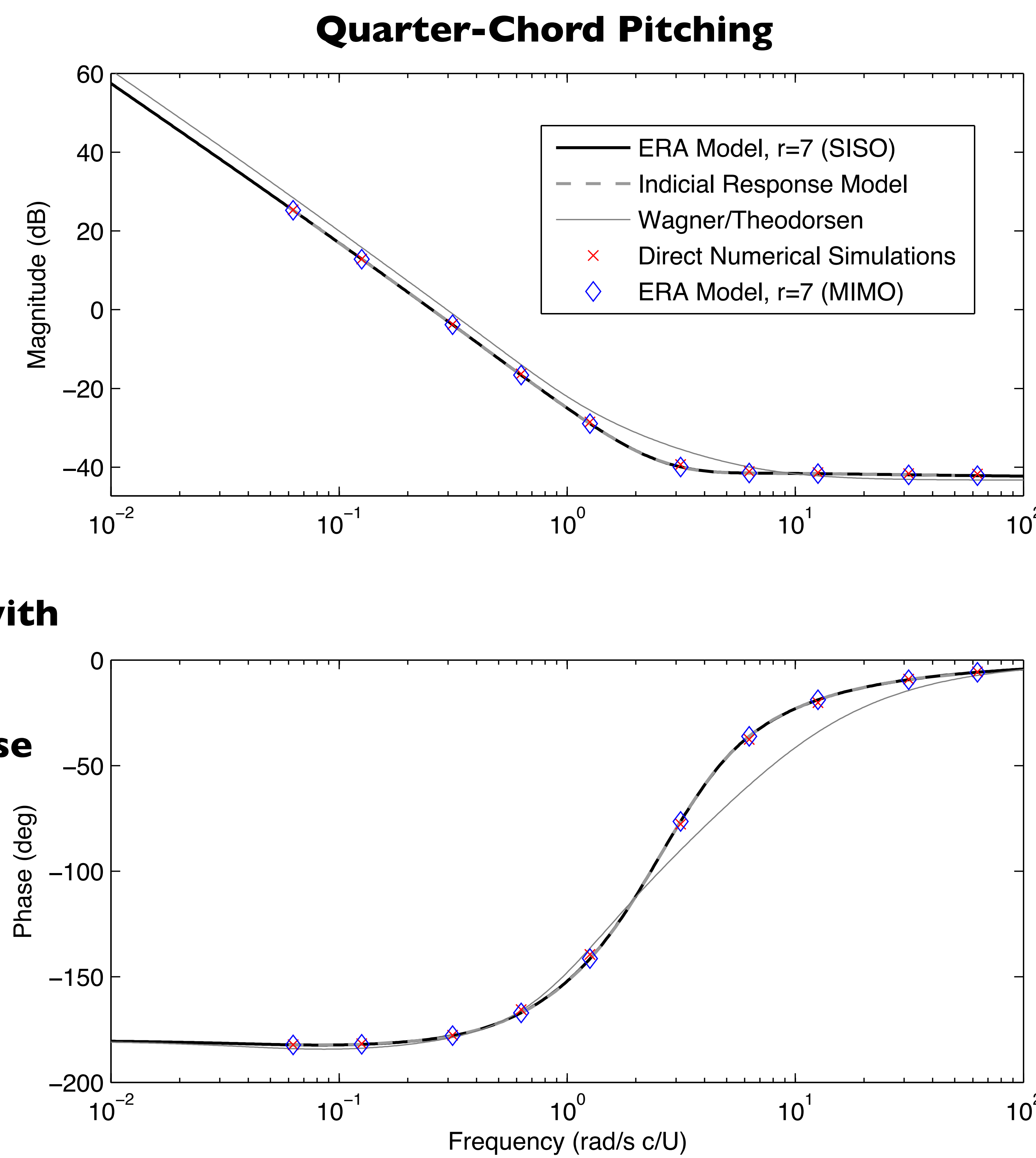

Brunton and Rowley, *in preparation*.

Parametrized by Pitch Point

$$\frac{d}{dt}\begin{bmatrix}\mathbf{x}\\ \alpha\\ \dot\alpha\\ \dot h\end{bmatrix} = \begin{bmatrix}A & 0 & 0 & 0\\ 0 & 0 & 1 & 0\\ 0 & 0 & 0 & 0\\ 0 & 0 & 0 & 0\end{bmatrix}\begin{bmatrix}\mathbf{x}\\ \alpha\\ \dot\alpha\\ \dot h\end{bmatrix} + \begin{bmatrix}B_1 - \frac{a}{2}B_2 & B_2\\ 0 & 0\\ 1 & 0\\ -\frac{a}{2} & 1\end{bmatrix}\begin{bmatrix}\ddot\alpha\\ \ddot h\end{bmatrix}$$

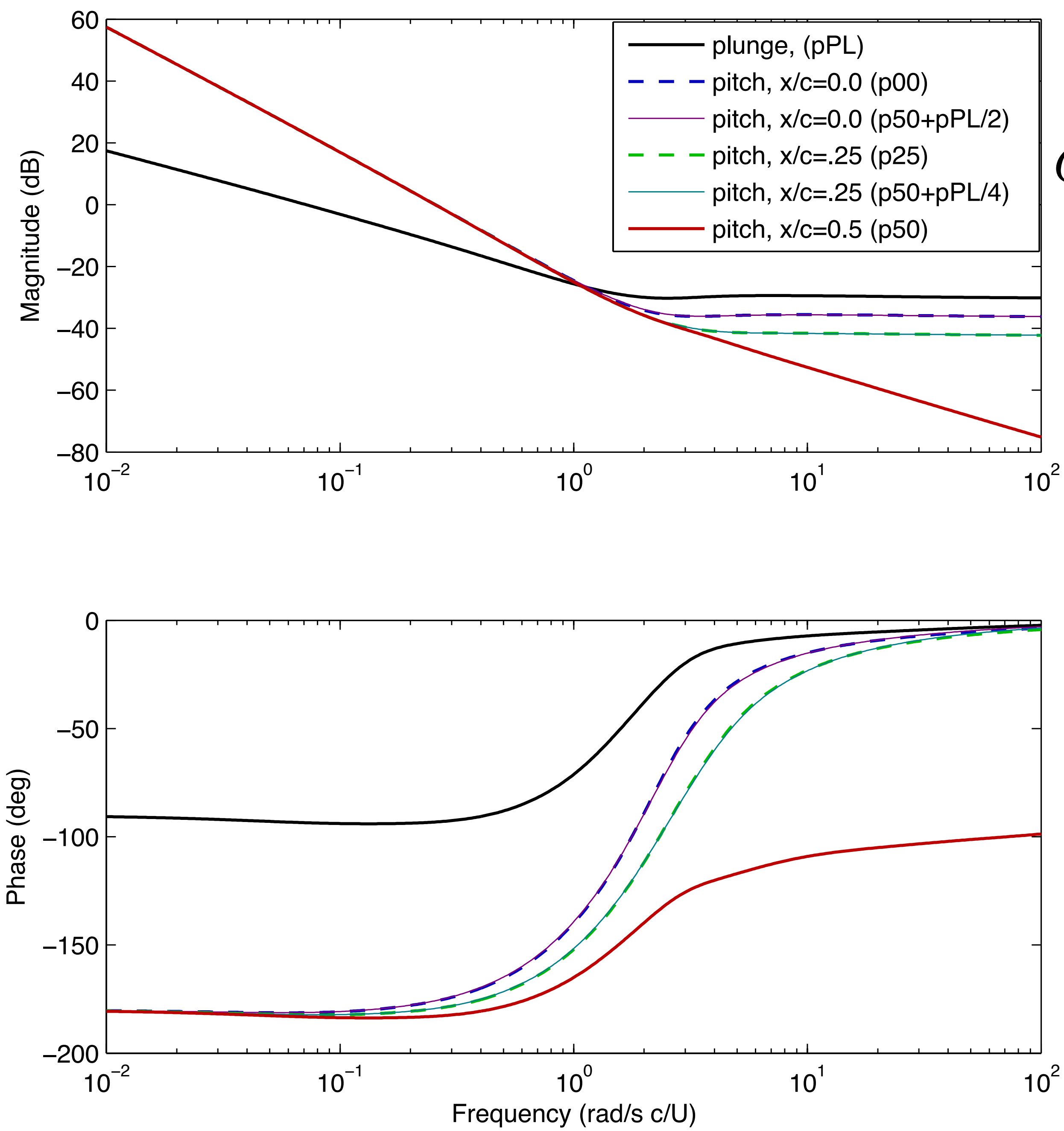

$$C_L = \begin{bmatrix}C & C_\alpha & C_{\dot\alpha} & C_{\dot h}\end{bmatrix}\begin{bmatrix}\mathbf{x}\\ \alpha\\ \dot\alpha\\ \dot h\end{bmatrix} + \begin{bmatrix}C_{\ddot\alpha} - \frac{a}{2}C_{\ddot h} & C_{\ddot h}\end{bmatrix}\begin{bmatrix}\ddot\alpha\\ \ddot h\end{bmatrix}$$

(A, B_1, C) **model for pitch at mid-chord**

(A, B_2, C) **model for plunge**

Pitch about any point is linear combination of pitch at mid-chord and plunge motion

Models all have same poles, different zeros (similar to Theodorsen's model)

Pitch/Plunge Maneuver

Canonical pitch-up, hold, pitch-down maneuver, followed by step-down in vertical position

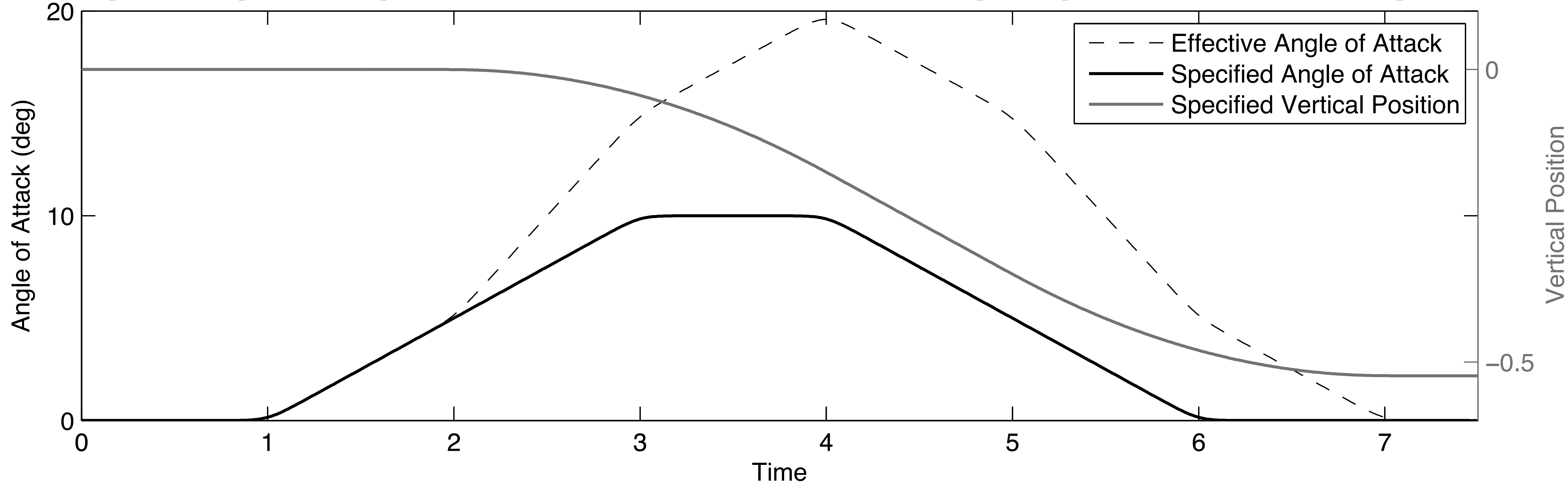

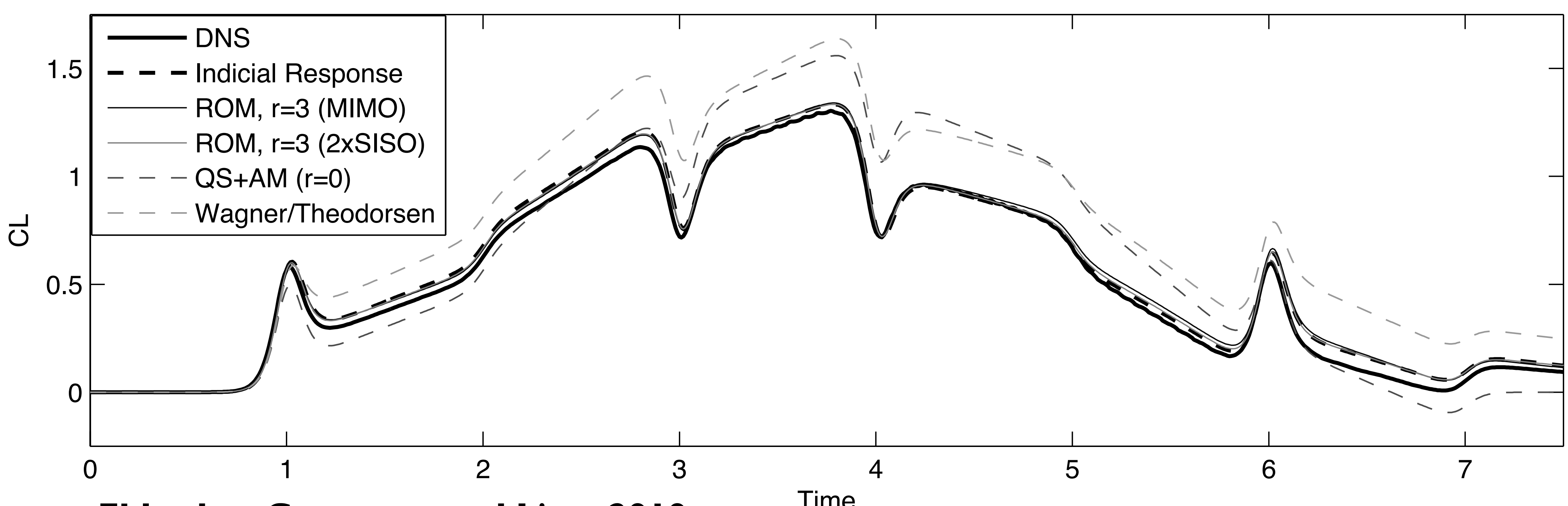

OL, Altman, Eldredge, Garmann, and Lian, 2010

Brunton and Rowley, *in preparation*.

Reduced order model for indicial response accurately captures lift coefficient history from DNS

Lift vs. Angle of Attack

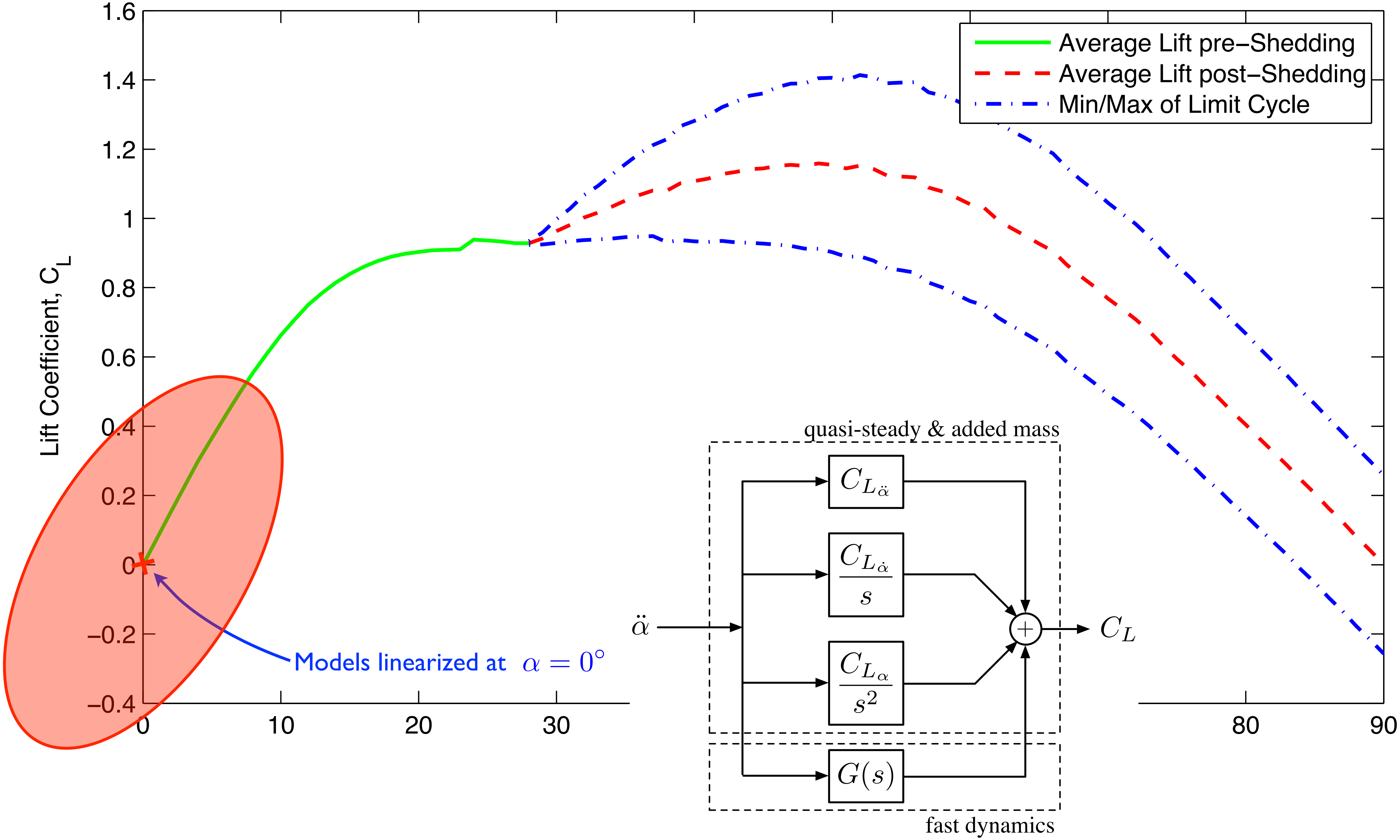

Lift vs. Angle of Attack

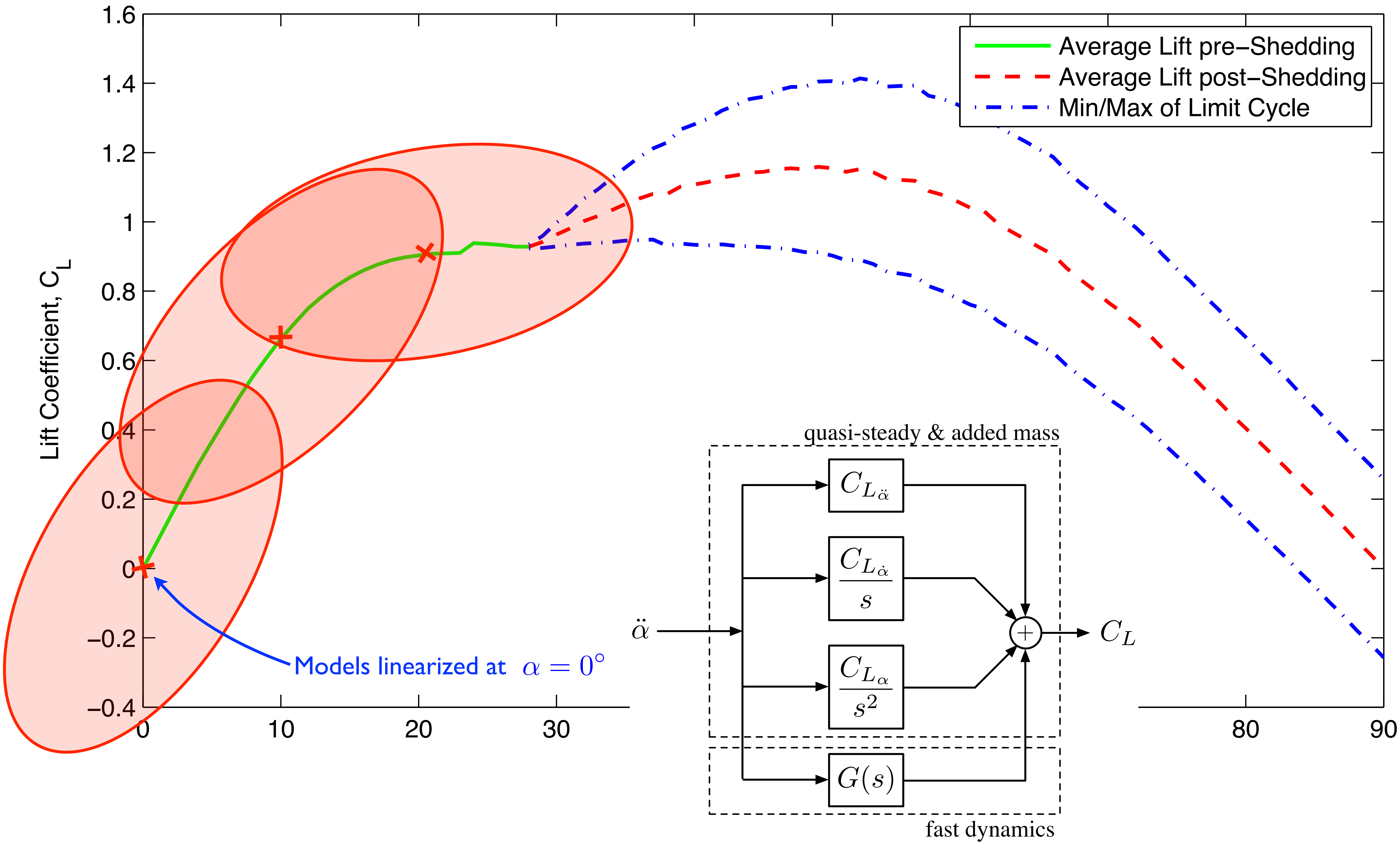

Models at various angle of attack

Impulse response simulations after rapid step-up $\alpha \in [0^\circ, 27^\circ]$

Initial lift $C_L(\alpha_0)$ **subtracted off**

Model with order r=7 required to capture this flow feature, eventually develops into vortex shedding mode

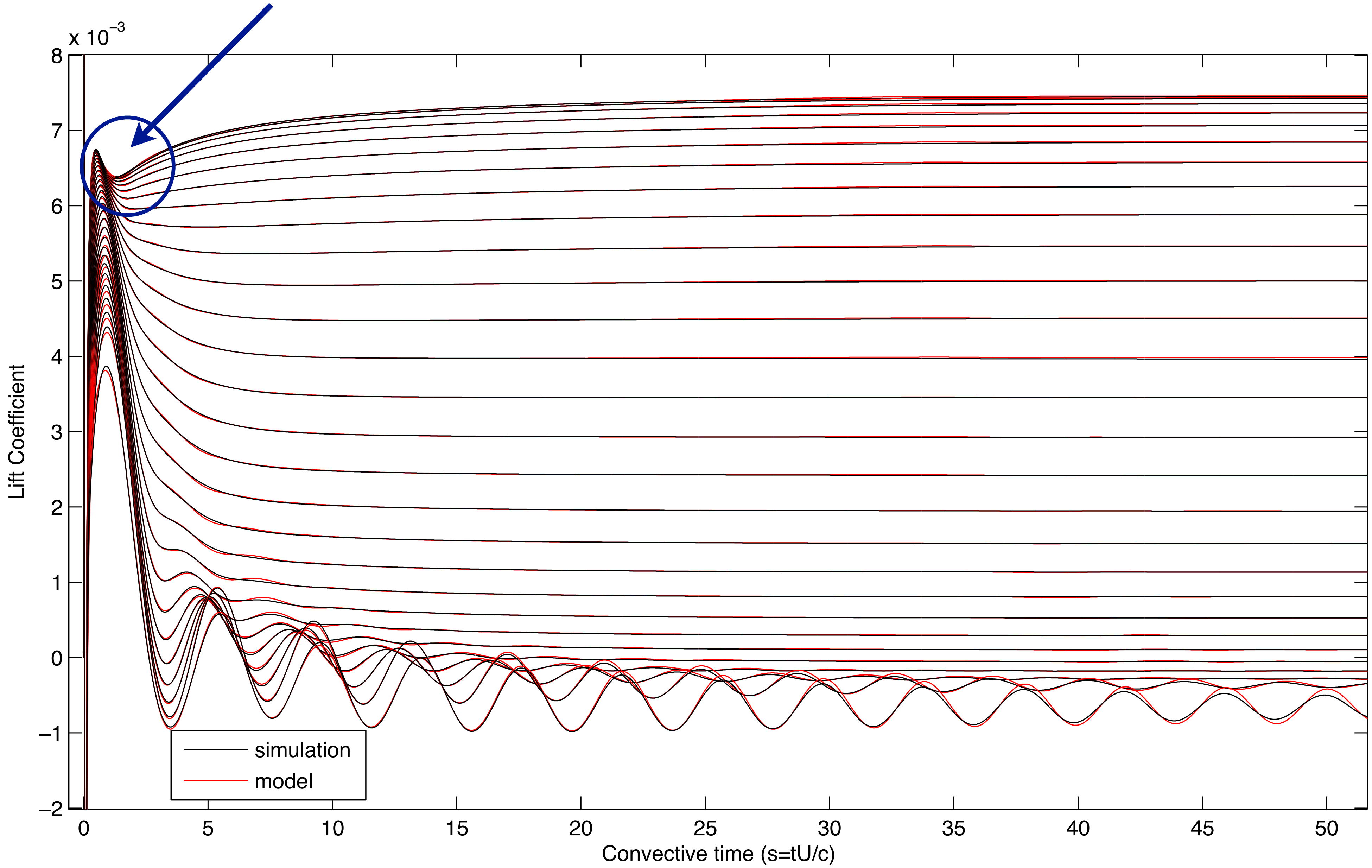

$\alpha = 0^\circ$

$\alpha = 27^\circ$

Bode Plot of ERA Models

Results

Lift slope decreases for increasing angle of attack, so magnitude of low frequency motions decreases for increasing angle of attack.

At larger angle of attack, phase converges to -180 at much lower frequencies. I.e., solutions take longer to reach equilibrium in time domain.

Consistent with fact that for large angle of attack, system is closer to Hopf instability, and a pair of eigenvalues are moving closer to imaginary axis.

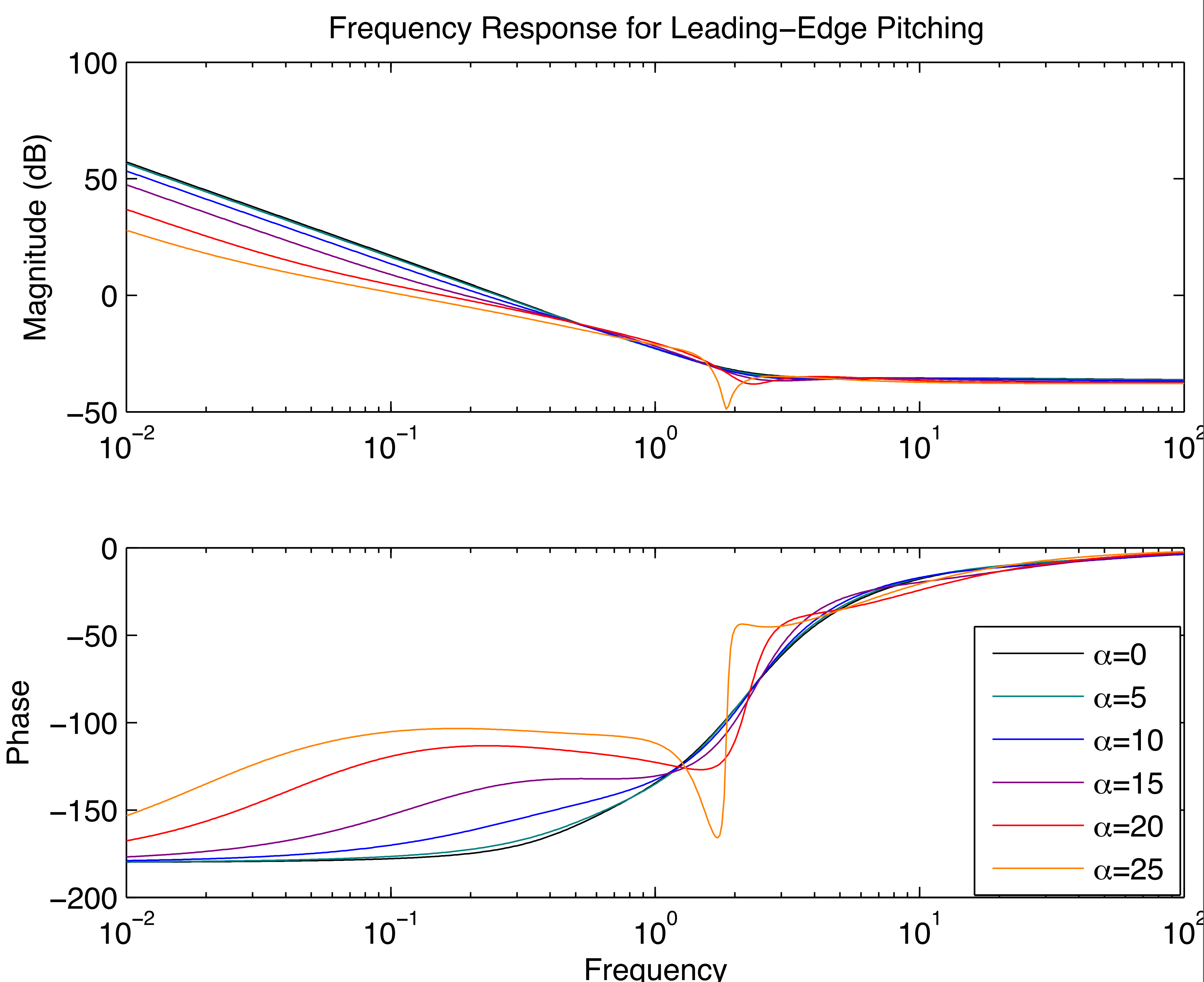

Poles and Zeros of ERA Models

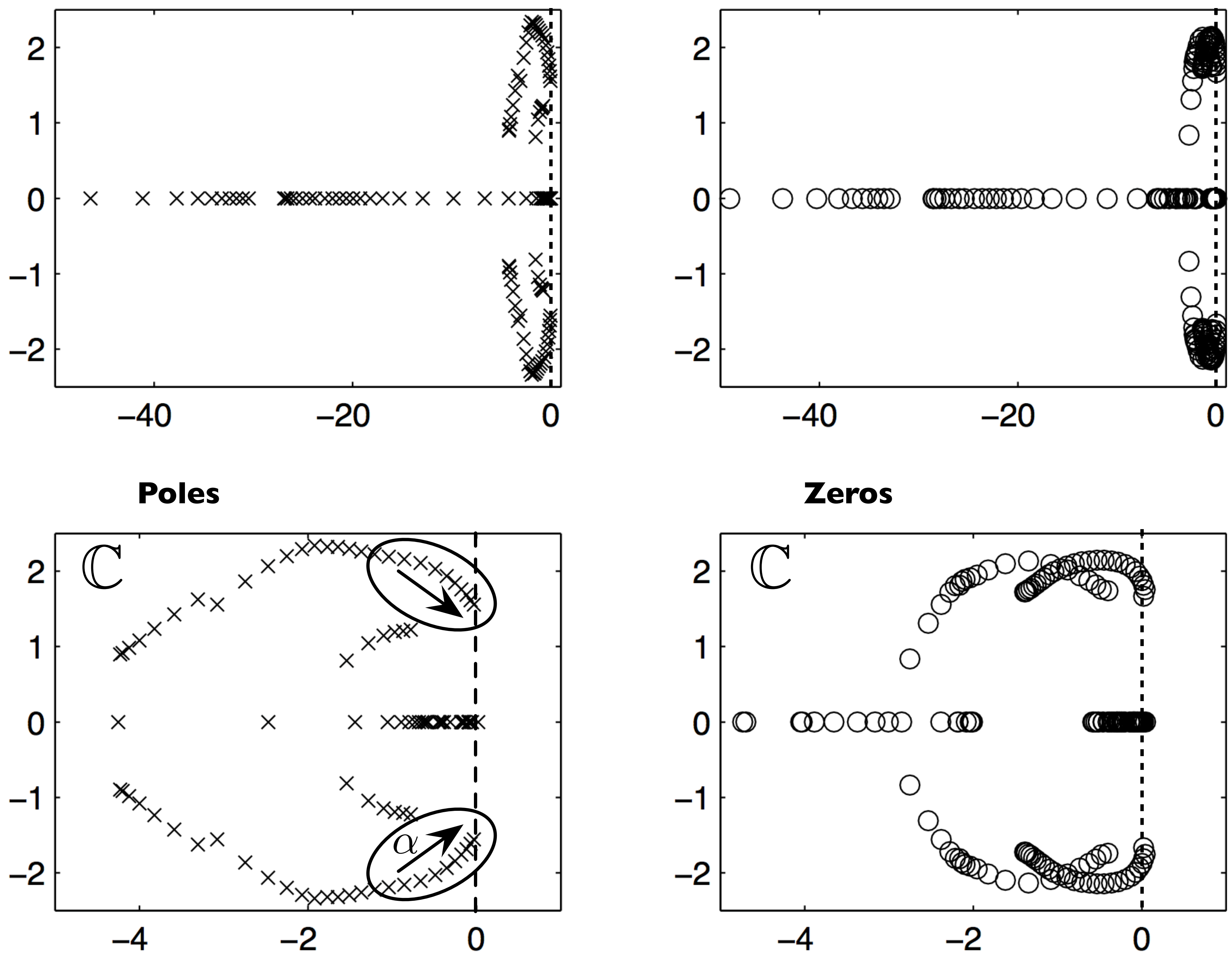

As angle of attack increases, pair of poles (and pair of zeros) march towards imaginary axis.

This is a good thing, because a Hopf bifurcation occurs at $\alpha_{\text{crit}} \approx 28^\circ$

Brunton and Rowley, AIAA ASM 2011

Bode Plot of Model (-) vs Data (x)

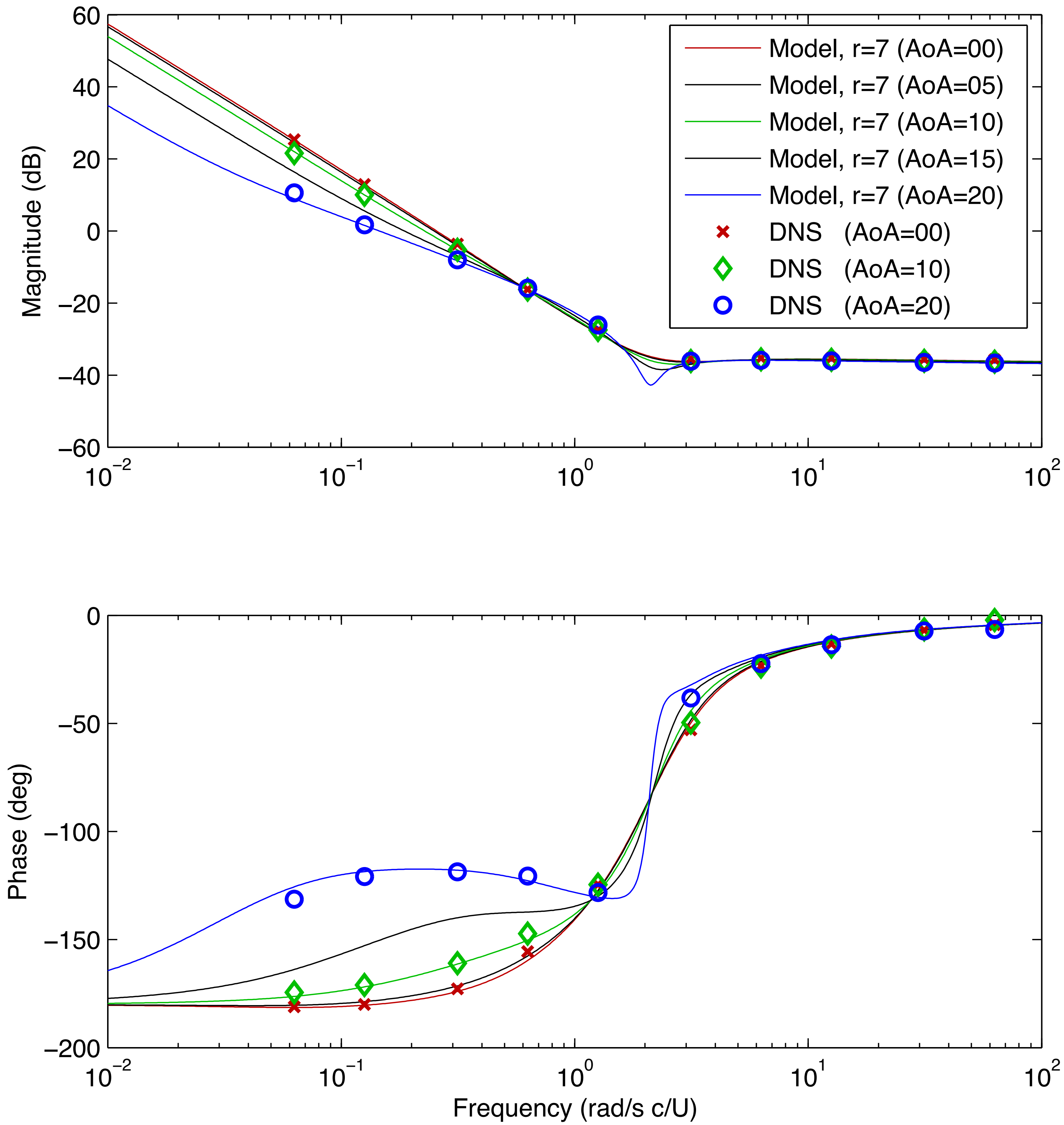

Direct numerical simulation confirms that local linearized models are accurate for small amplitude sinusoidal maneuvers

Brunton and Rowley, AIAA ASM 2011

Large Amplitude Maneuver

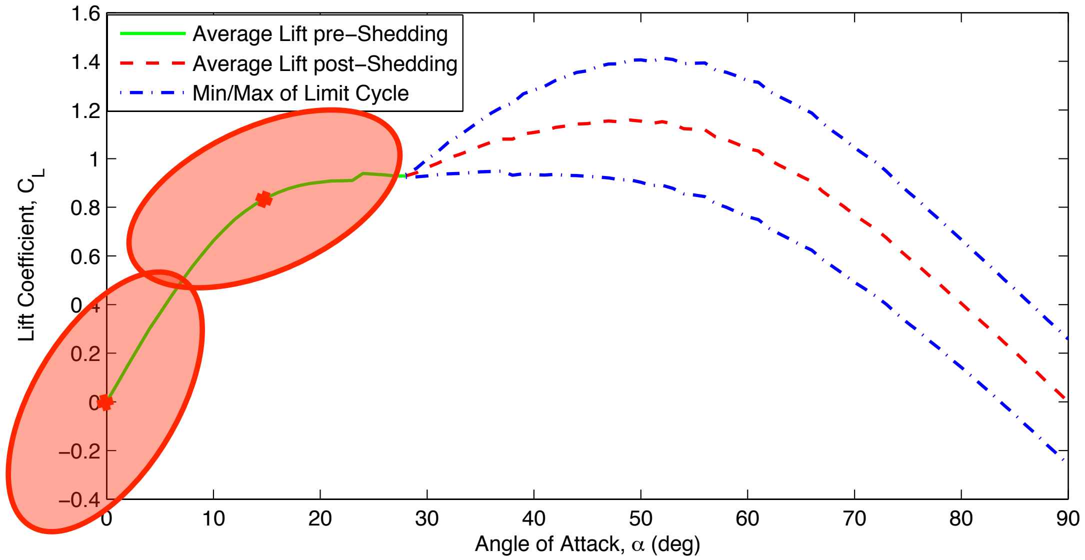

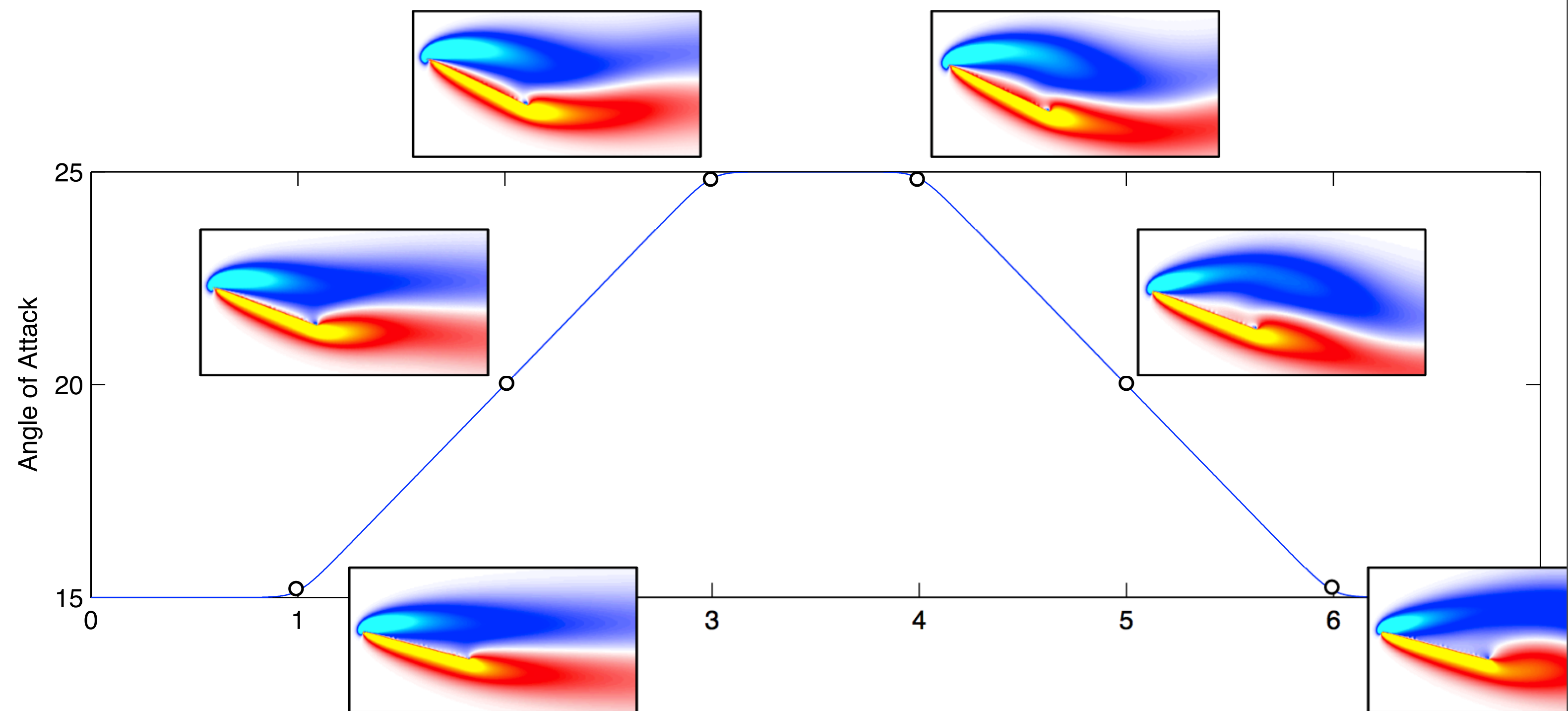

Compare models linearized at

$\alpha = 0^\circ$ **and** $\alpha = 15^\circ$

For pitching maneuver with

$$\alpha \in [15^\circ, 25^\circ]$$

Model linearized at $\alpha = 15^\circ$

captures lift response more accurately

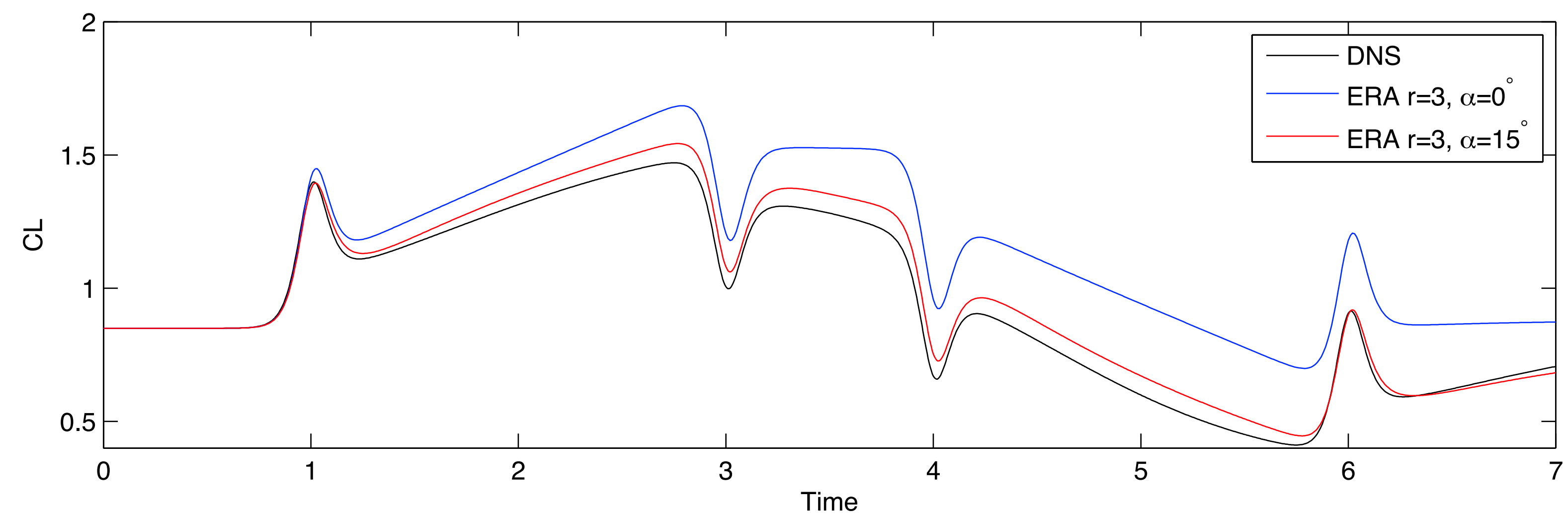

$$G(t) = \log\left[\frac{\cosh(a(t-t_1))\cosh(a(t-t_4))}{\cosh(a(t-t_2))\cosh(a(t-t_3))}\right] \qquad \alpha(t) = \alpha_0 + \alpha_{\max}\frac{G(t)}{\max(G(t))}$$

Brunton and Rowley, AIAA ASM 2011 **OL, Altman, Eldredge, Garmann, and Lian, 2010**

(Indicial) Step Response

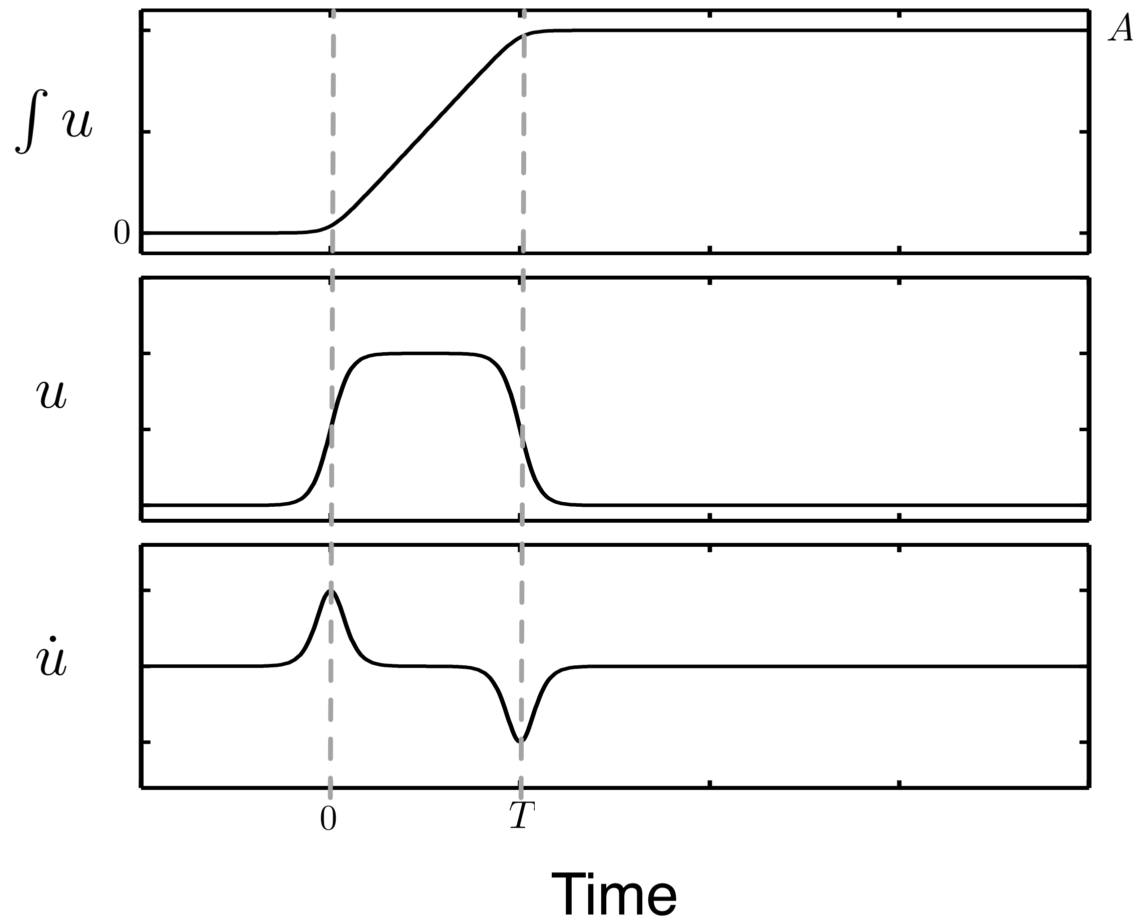

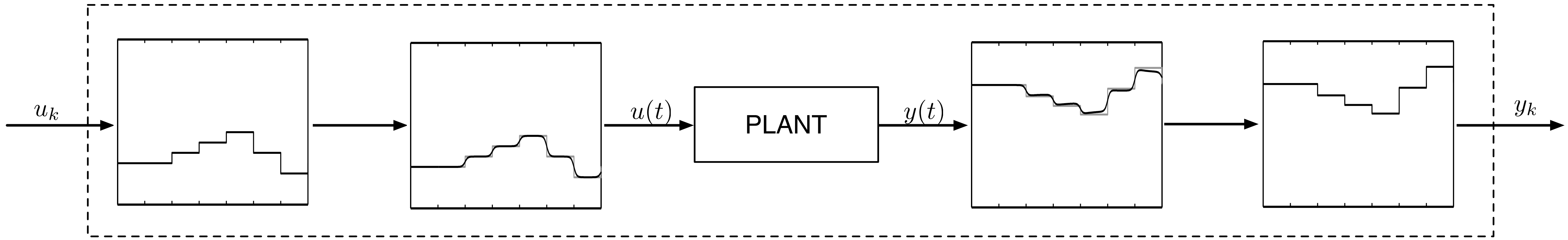

Previously, models are based on aerodynamic step response

Idea: Have pilot fly aircraft around for 5-10 minutes, back out the Markov parameters, and construct ERA model.

Random Input Maneuver

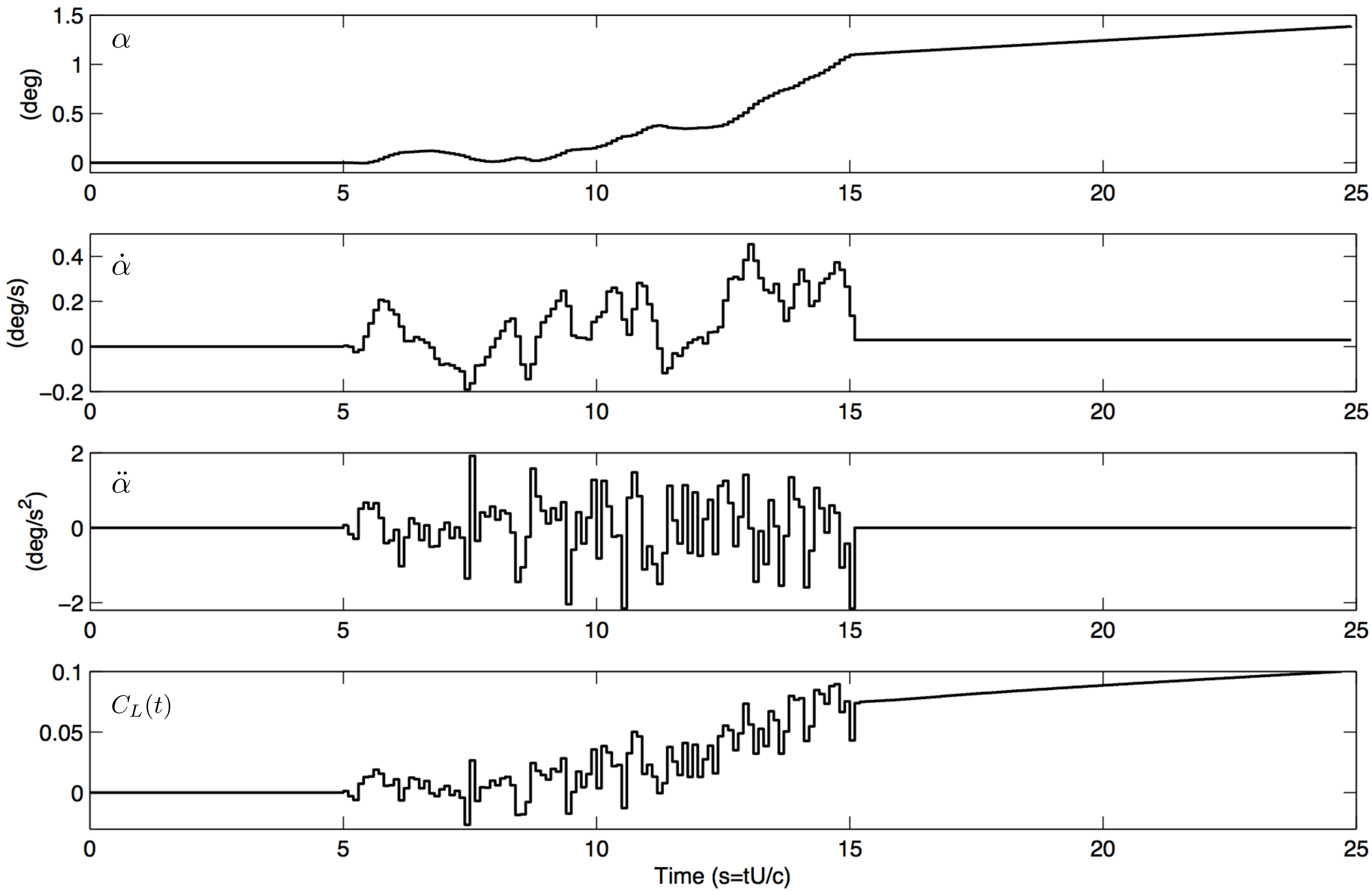

Observer/Kalman filter identification (OKID) works best, so far.

Idea: Have pilot fly aircraft around for 5-10 minutes, back out the Markov parameters, and construct ERA model.

Comparison of Methods

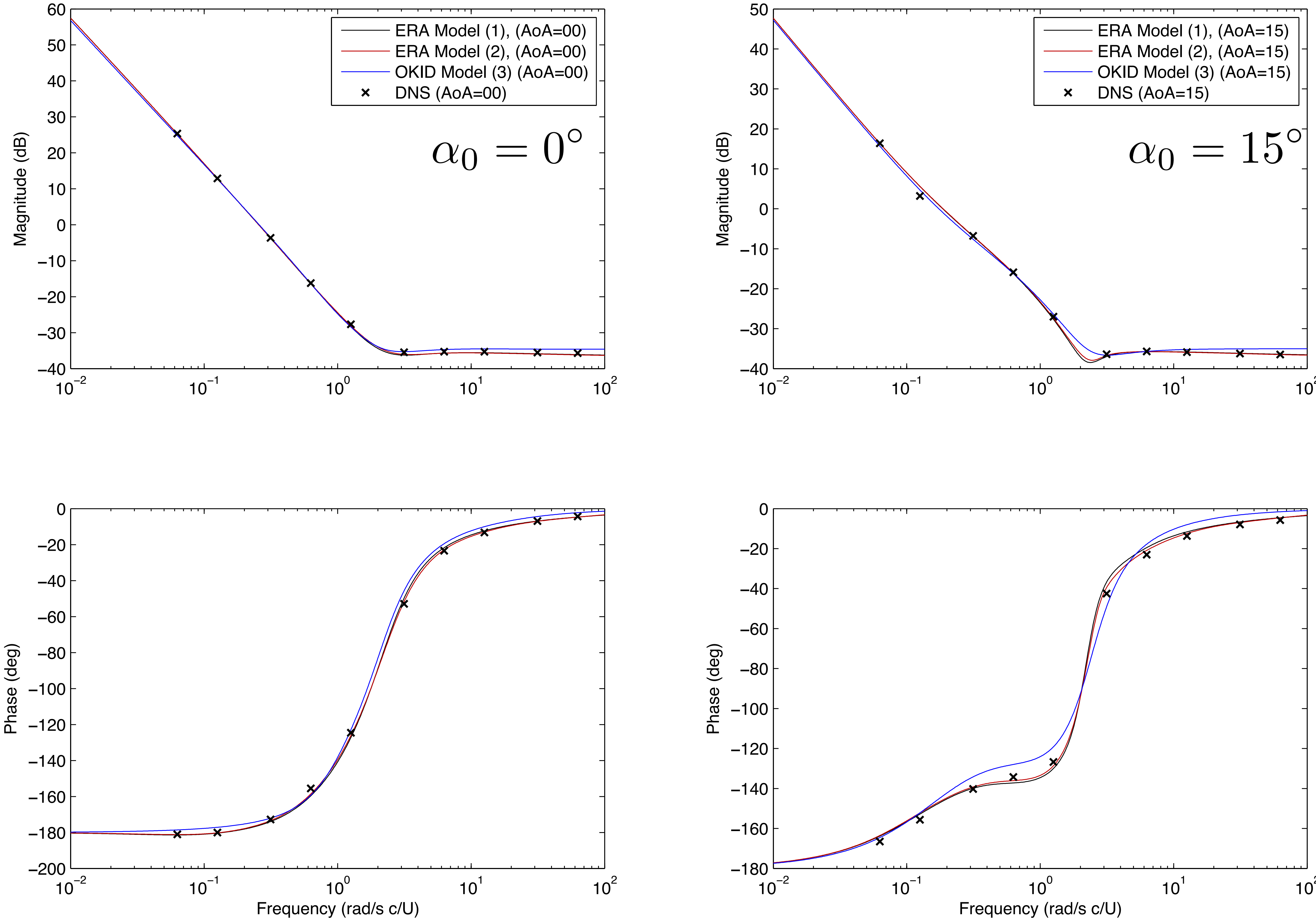

Wind Tunnel Experiments

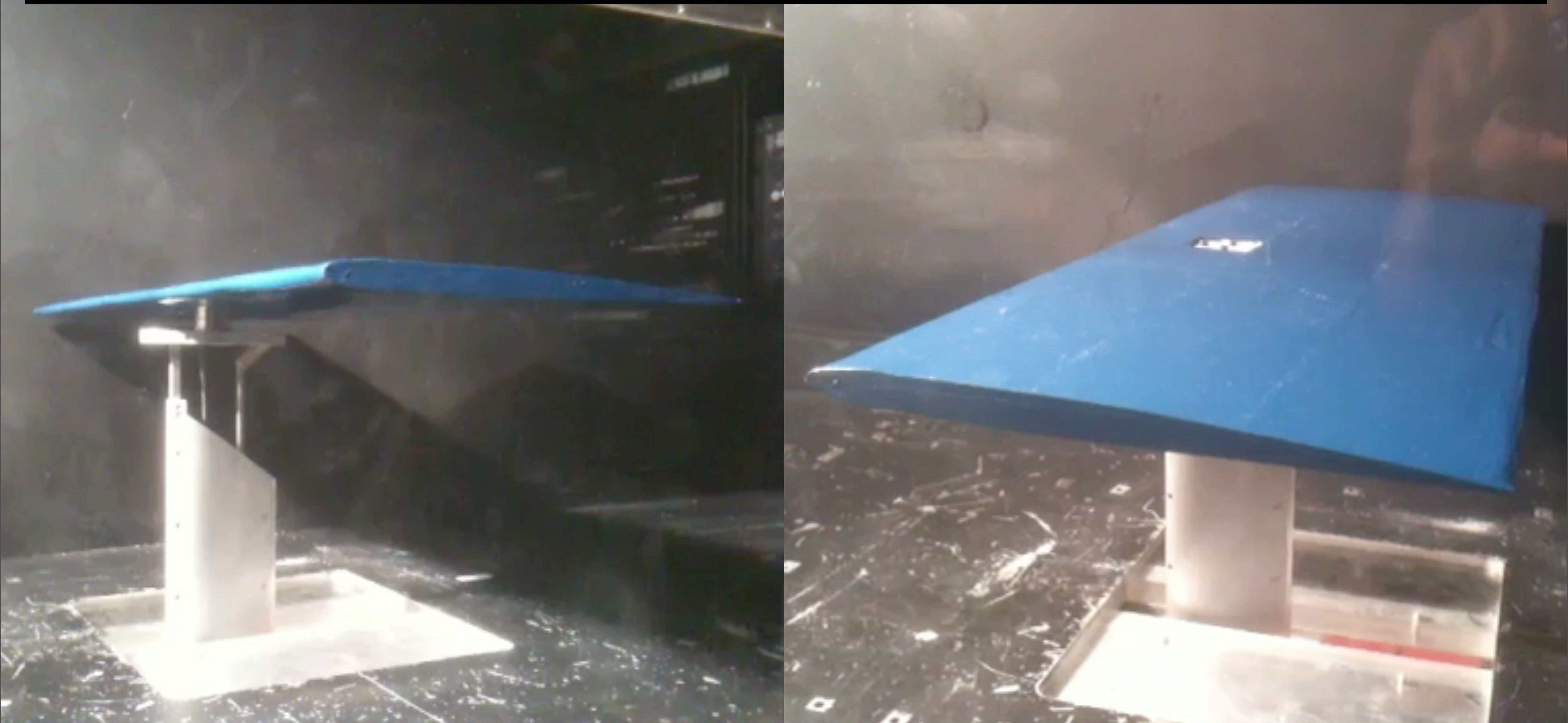

Andrew Fejer Unsteady Flow Wind Tunnel

Principle Investigator - Dave Williams

NACA 0006 Airfoil

Chord Length: 0.246 m

Free Stream Velocity: 4.00 m/s

Reynolds Number: 65,000

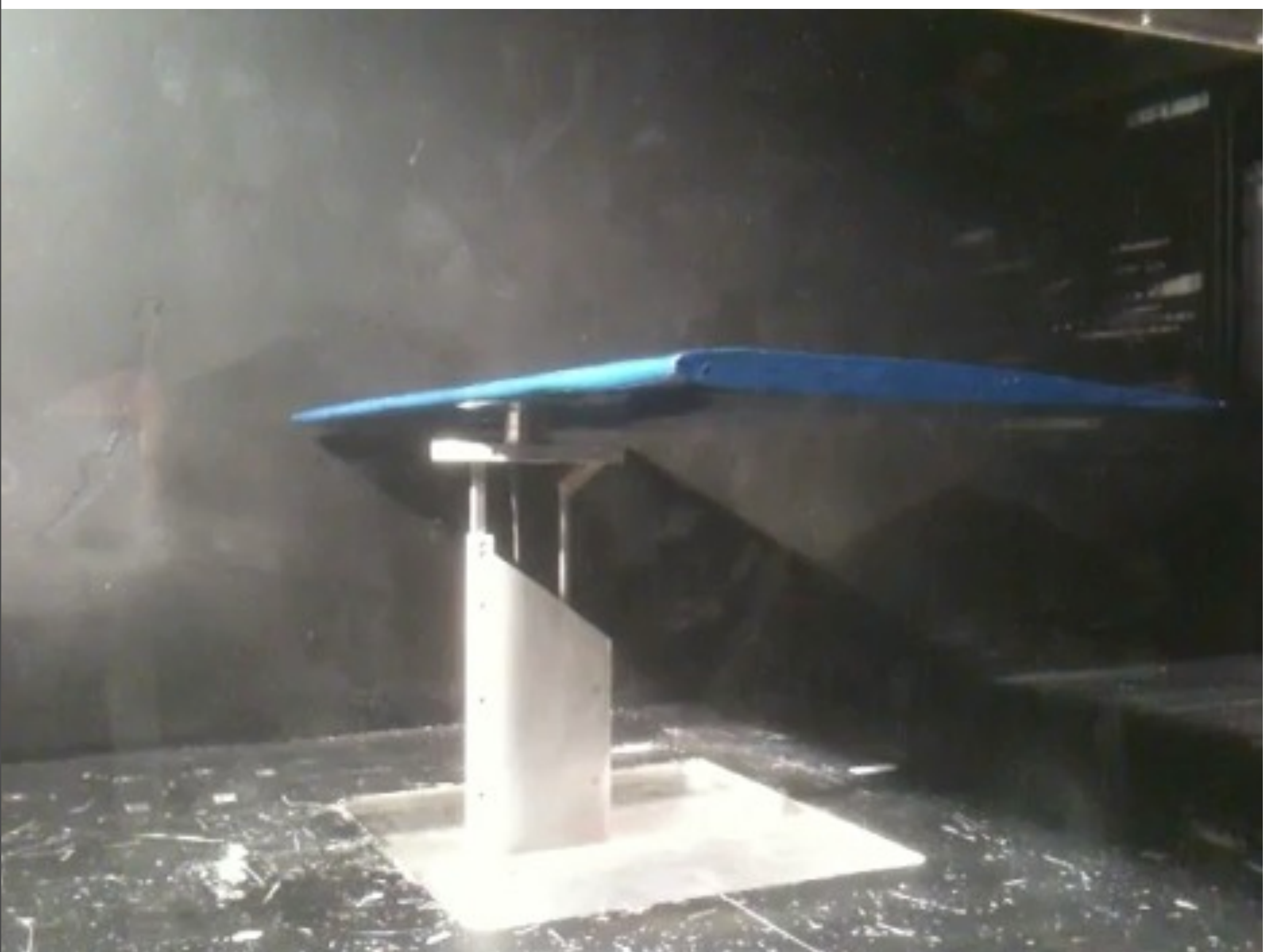

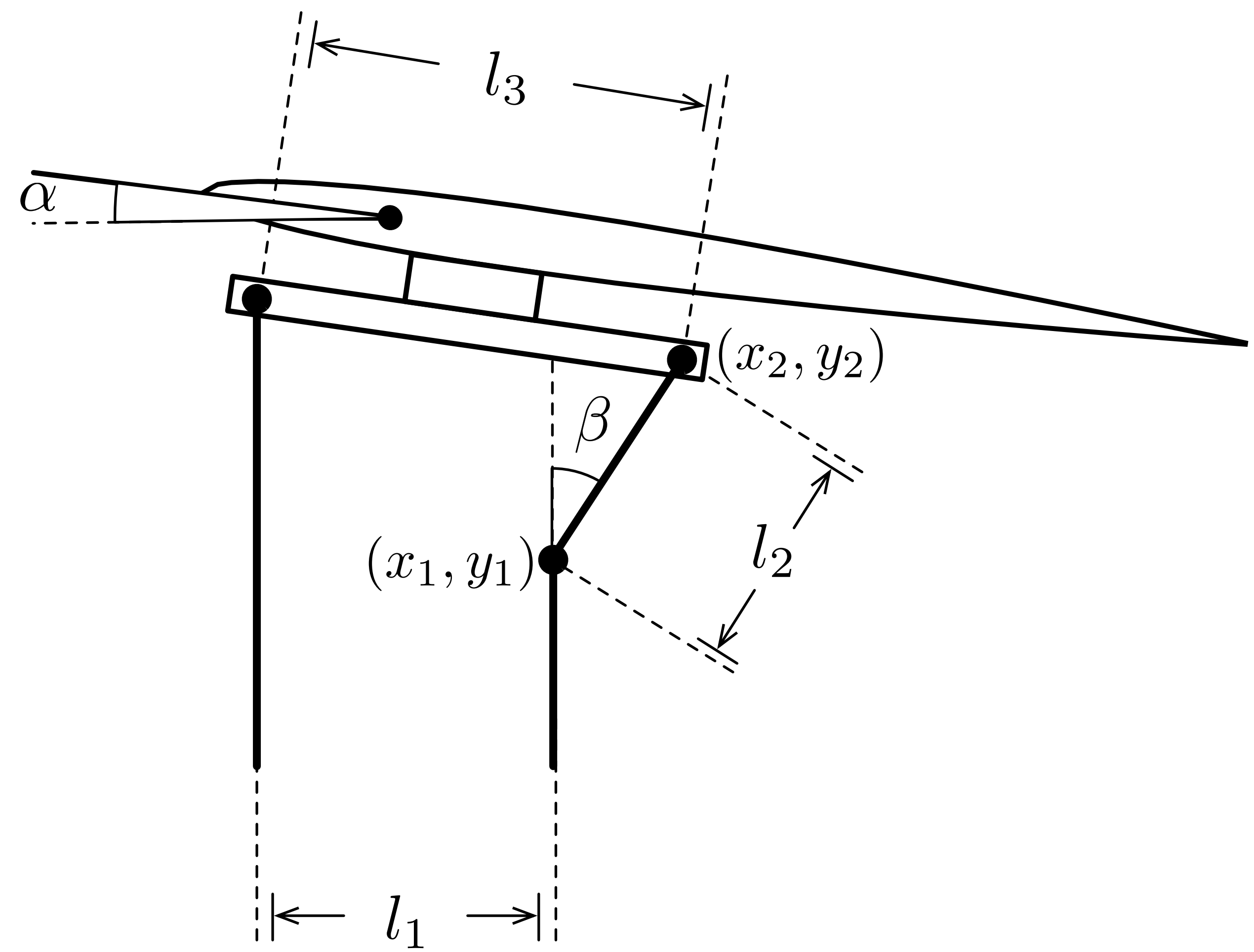

Summary

1. Account for hinge constraint nonlinearity
2. Rotate force vectors to obtain lift force
3. Subtract out point mass effects (mechanical)

$$\begin{bmatrix} L \\ D \end{bmatrix} = \underbrace{\begin{bmatrix} \cos(\alpha) & -\sin(\alpha) \\ \sin(\alpha) & \cos(\alpha) \end{bmatrix}}_{R_\alpha} \begin{bmatrix} N \\ P \end{bmatrix}$$

Phase Averaged Data

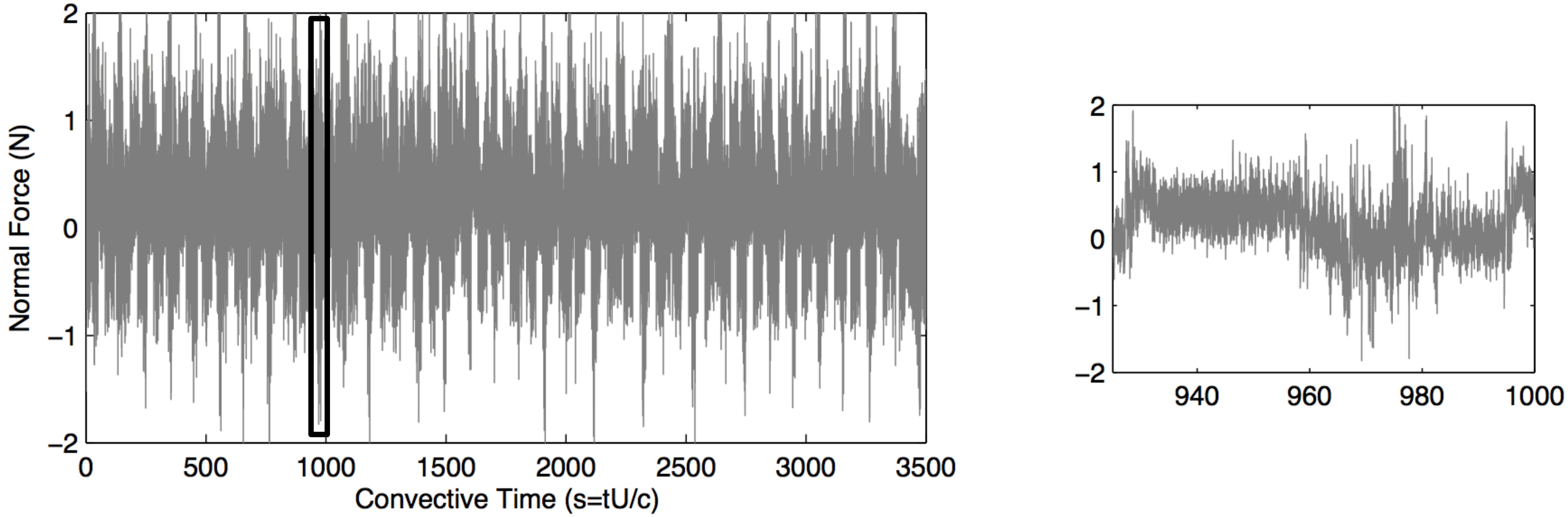

5 degree step-up, step-down maneuver

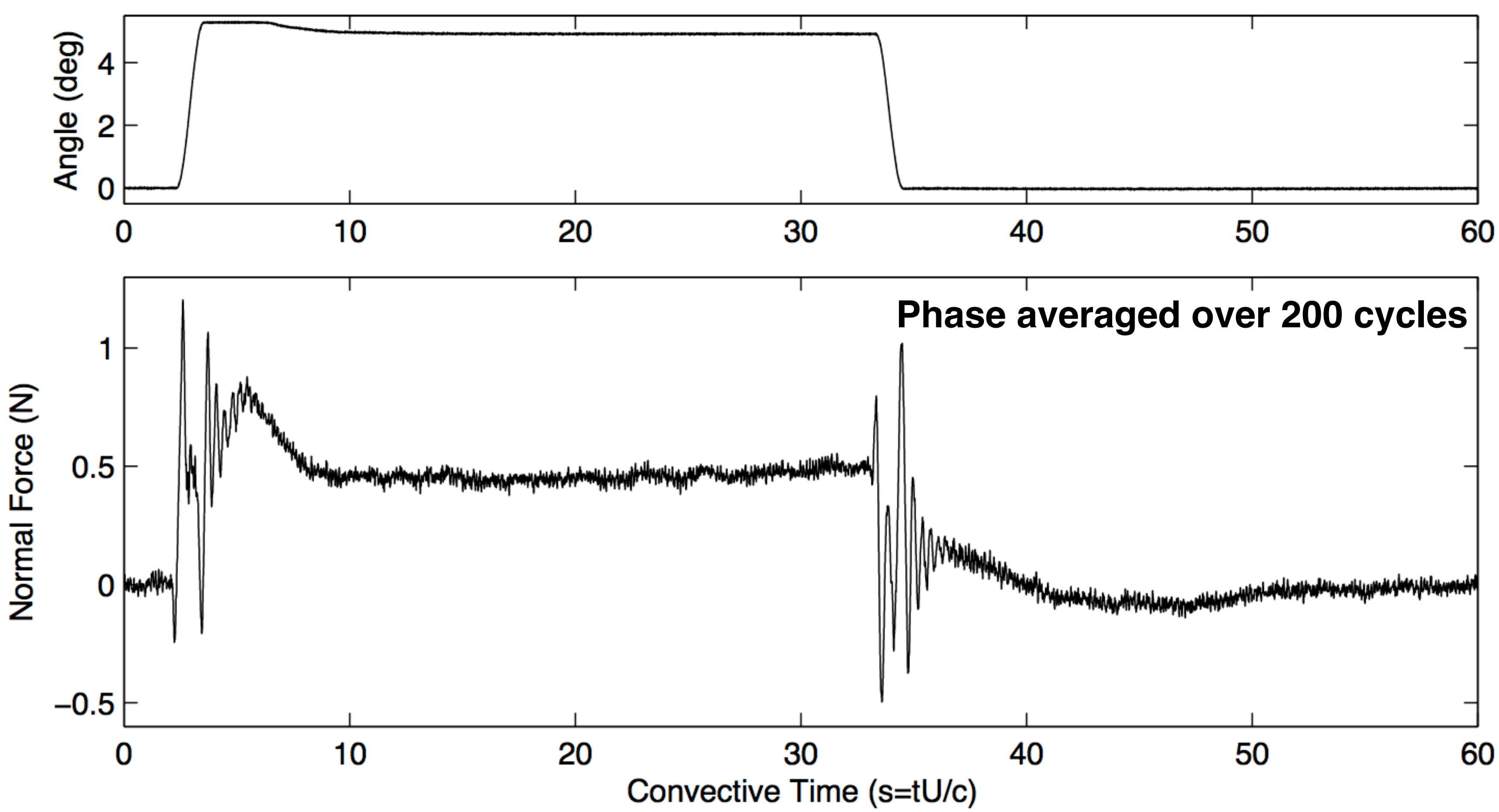

Wing Maneuver

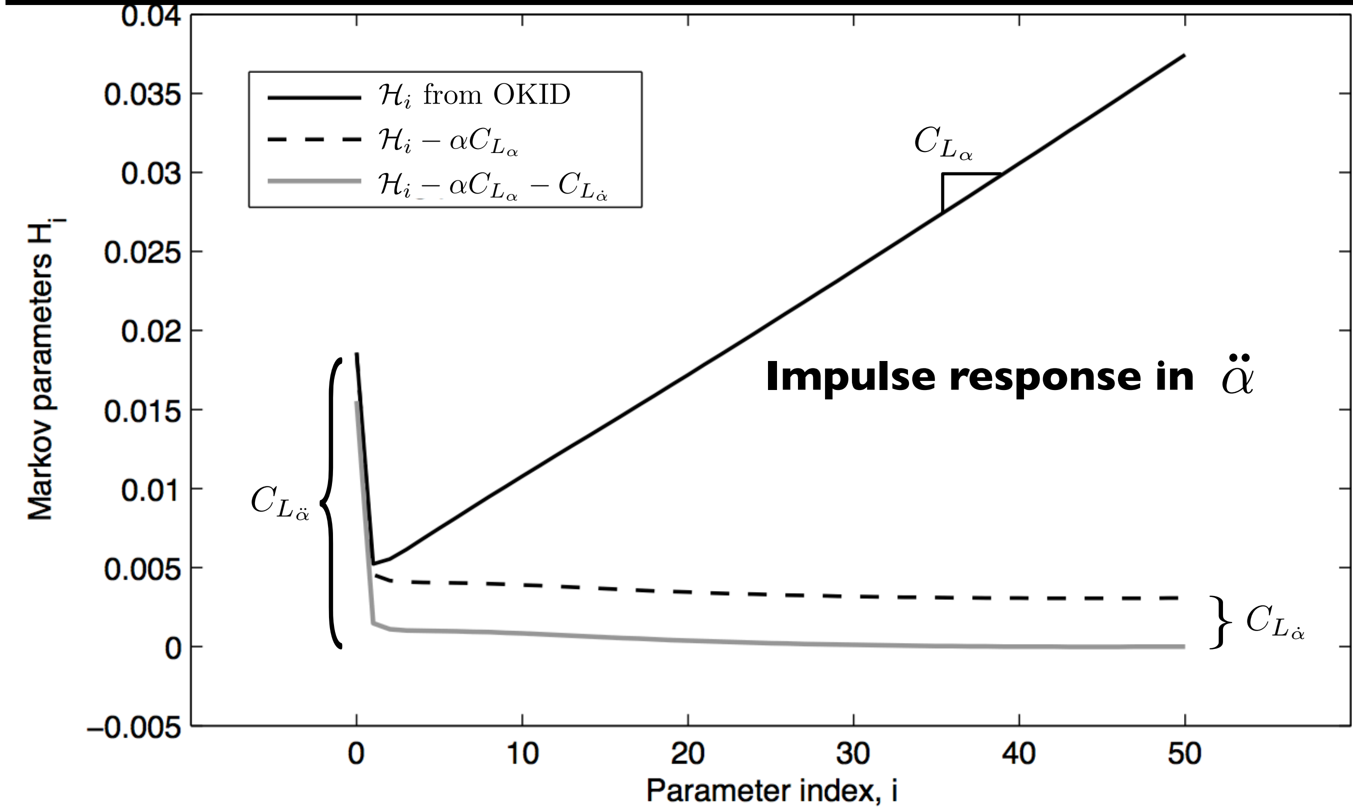

$$\frac{d}{dt}\begin{bmatrix}\mathbf{x}\\ \alpha\\ \dot{\alpha}\end{bmatrix} = \begin{bmatrix}A_r & 0 & 0\\ 0 & 0 & 1\\ 0 & 0 & 0\end{bmatrix}\begin{bmatrix}\mathbf{x}\\ \alpha\\ \dot{\alpha}\end{bmatrix} + \begin{bmatrix}B_r\\ 0\\ 1\end{bmatrix}\ddot{\alpha}$$

$$C_L = \begin{bmatrix}C_r & C_{L_\alpha} & C_{L_{\dot\alpha}}\end{bmatrix}\begin{bmatrix}\mathbf{x}\\ \alpha\\ \dot{\alpha}\end{bmatrix} + C_{L_{\ddot\alpha}}\ddot{\alpha}$$

Pseudo-random sequence of ramp-hold maneuvers (aggressive maneuver)

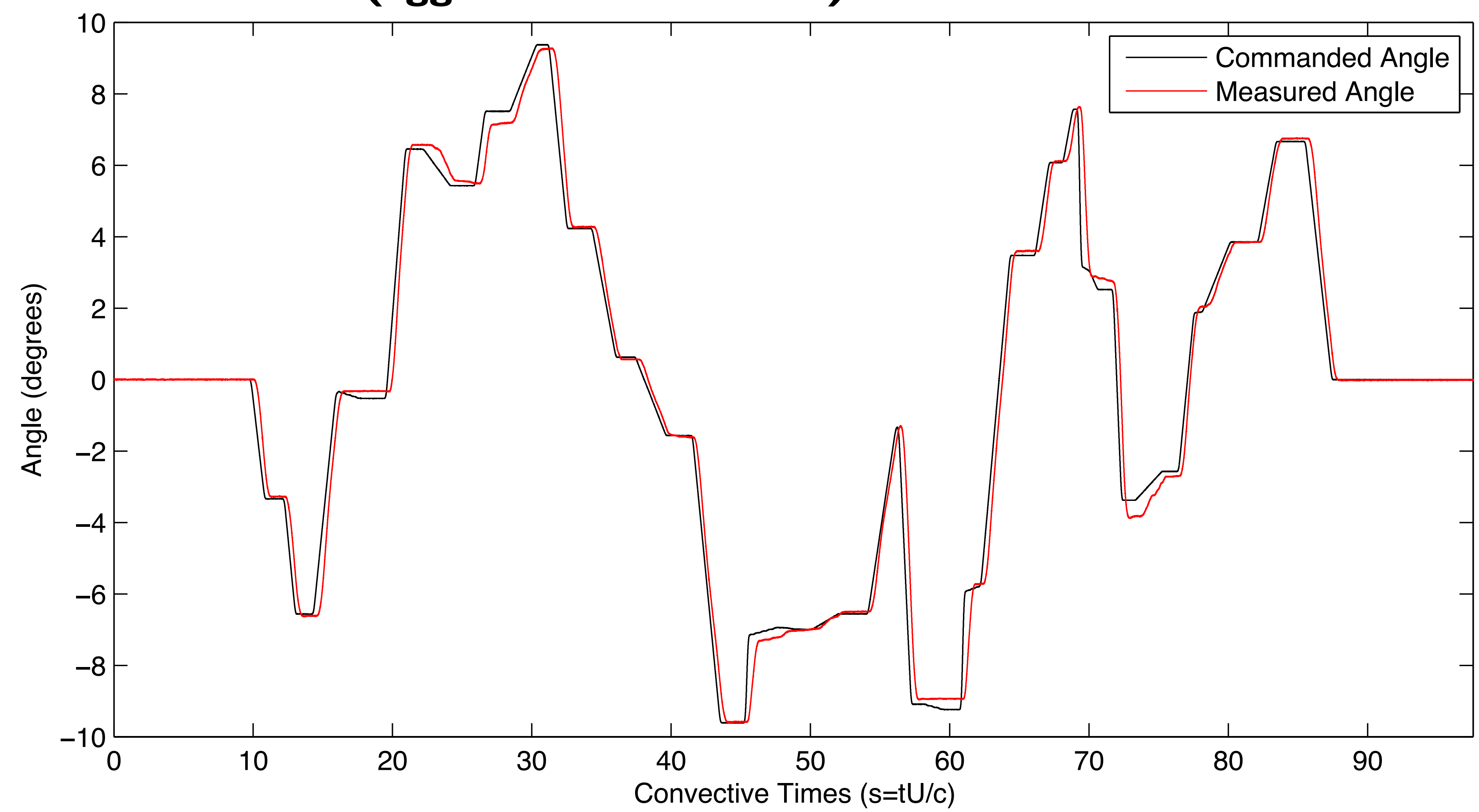

Single ramp-hold maneuver

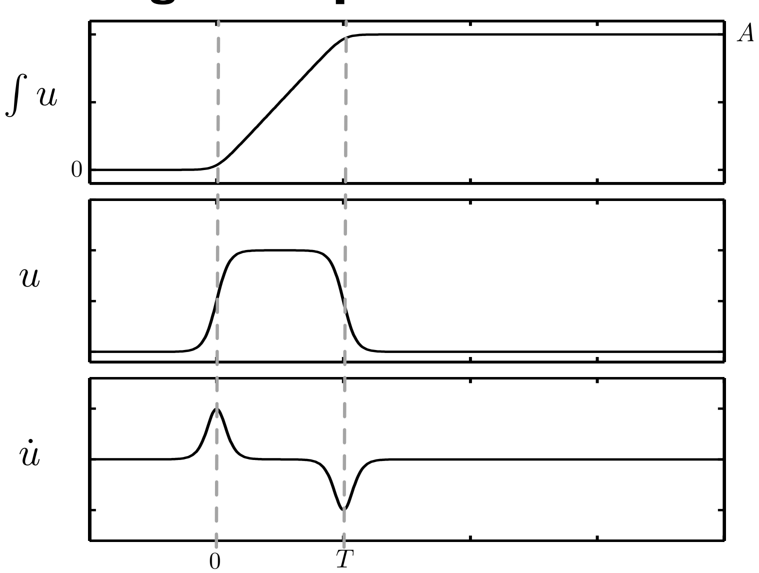

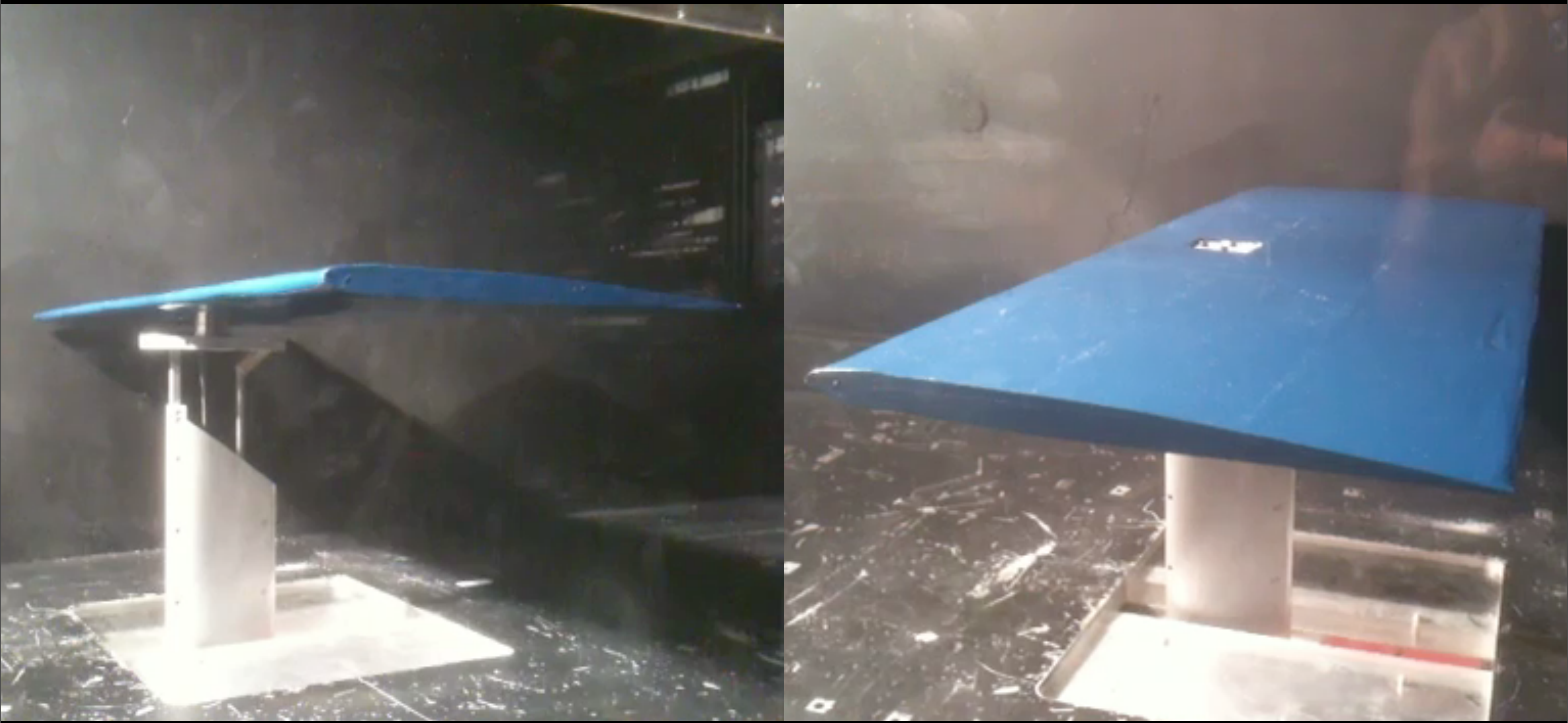

System ID maneuver

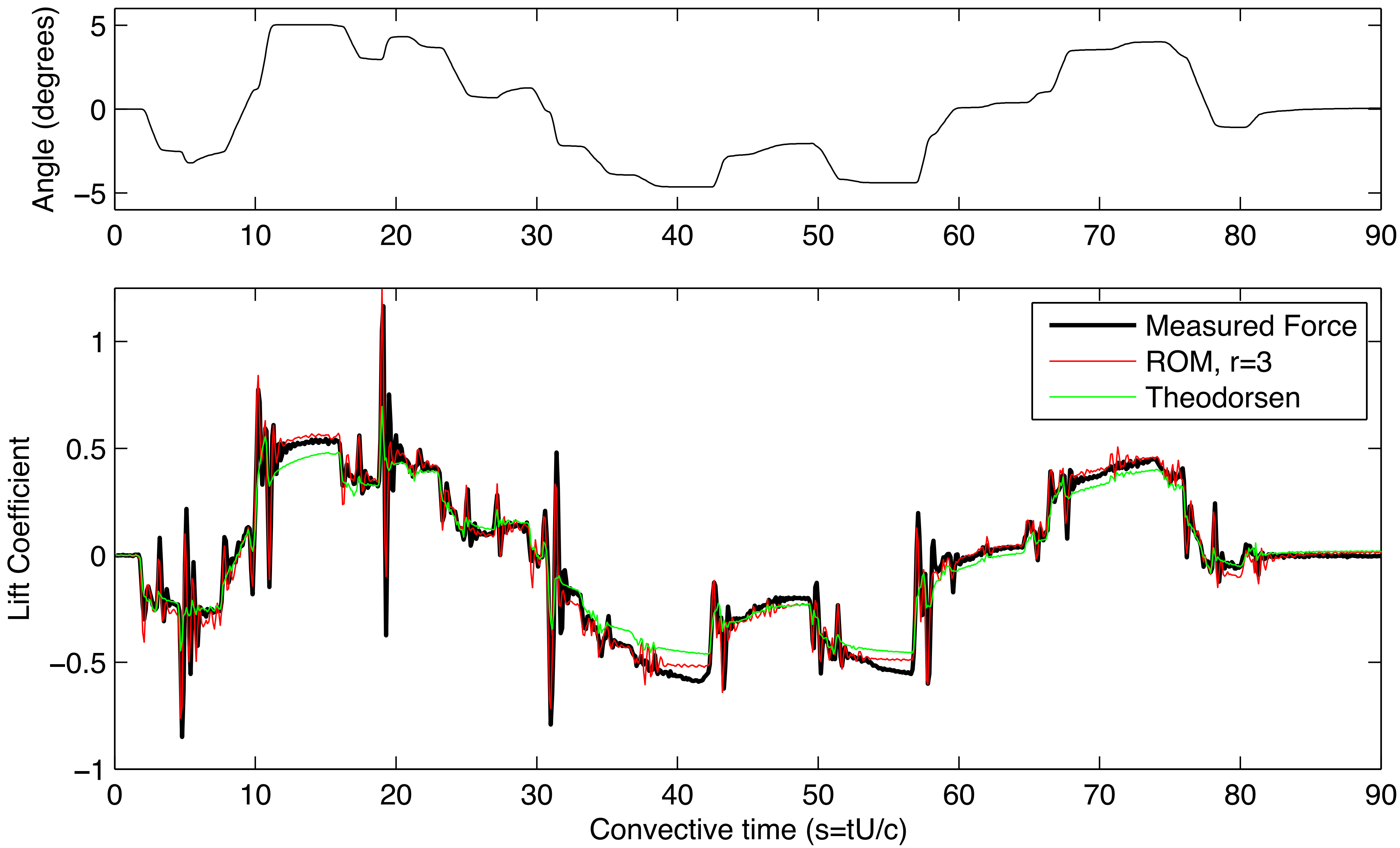

+/- 5 degree manuever, excites large range of frequencies

Reduced order model outperforms Theodorsen at low and high frequencies

AOA = 0 degrees

Three system ID maneuvers

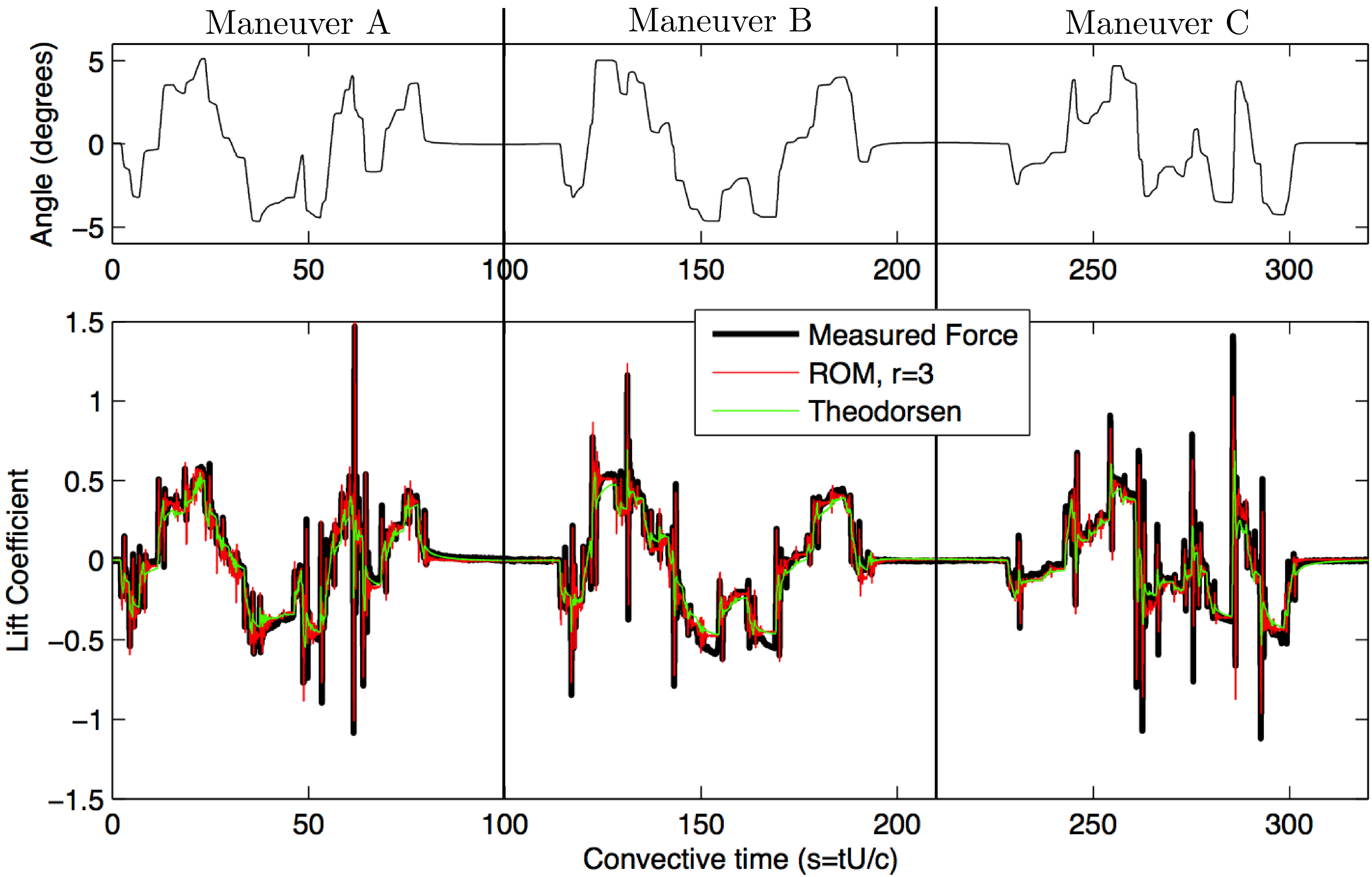

AOA = 0 degrees

We tried three system ID maneuvers: A, B and C.

System ID maneuver

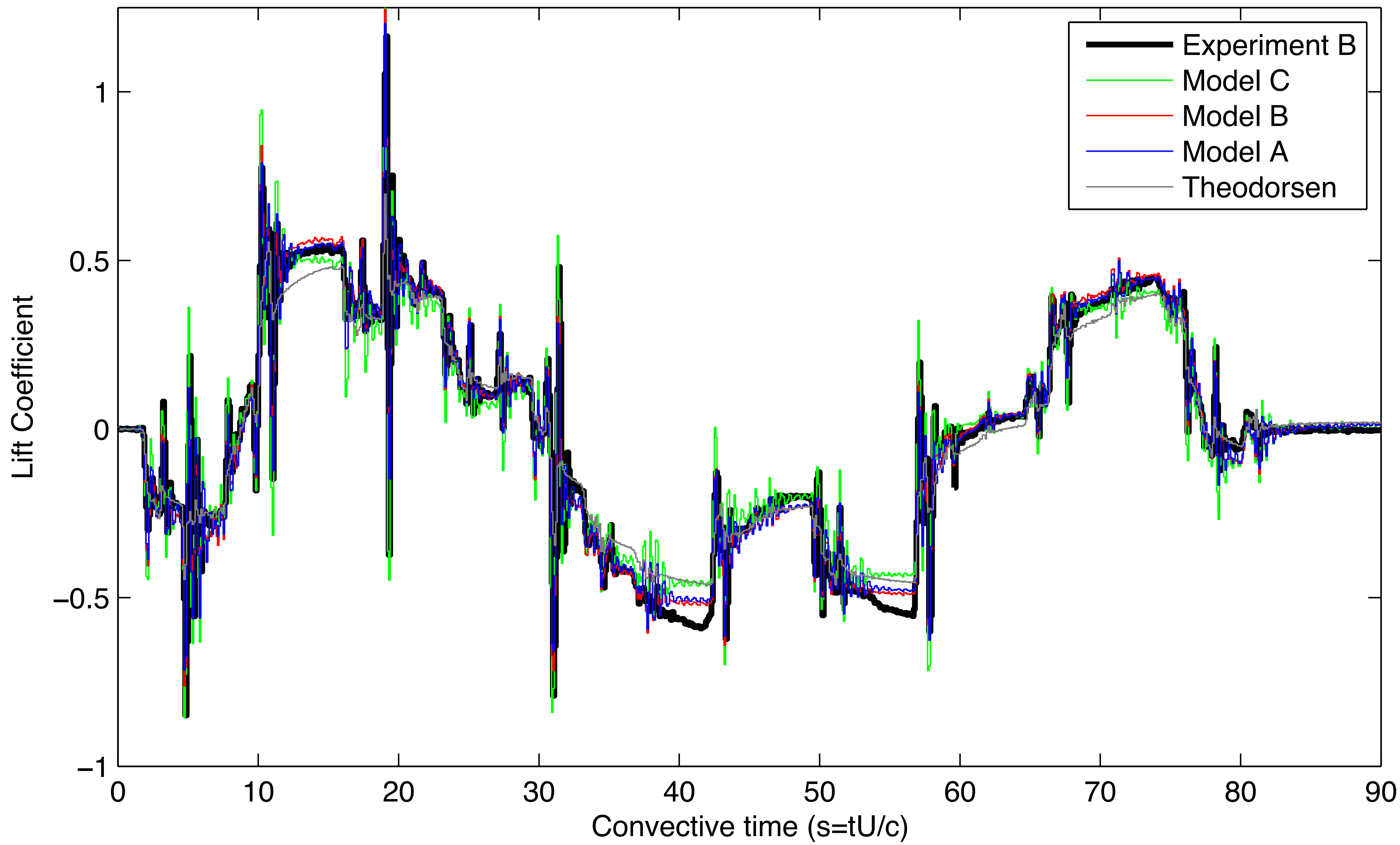

Bootstrap: It is important that models obtained from each ID maneuver accurately reproduce every other maneuver

AOA = 0 degrees

Bode plot and Markov parameters

Bode plot

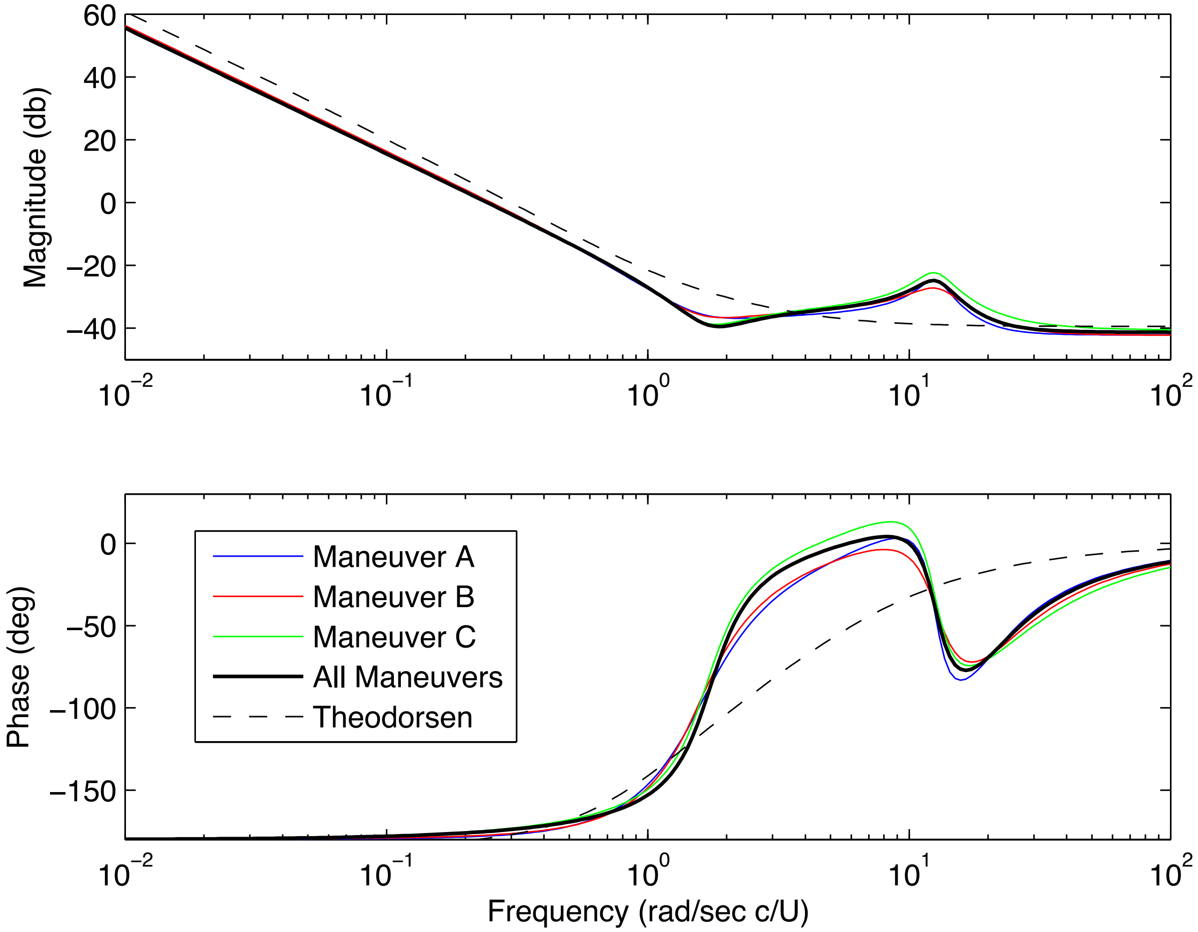

Markov Parameters

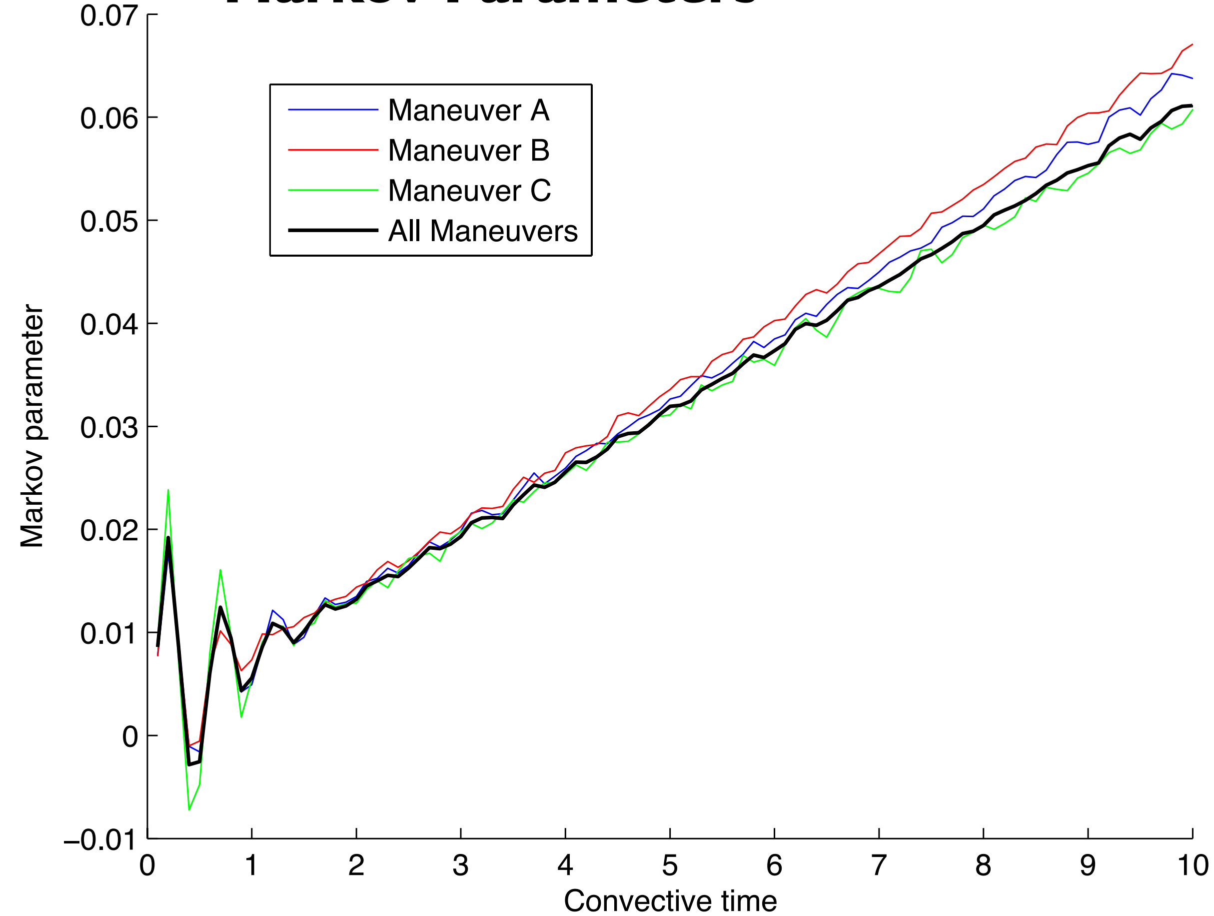

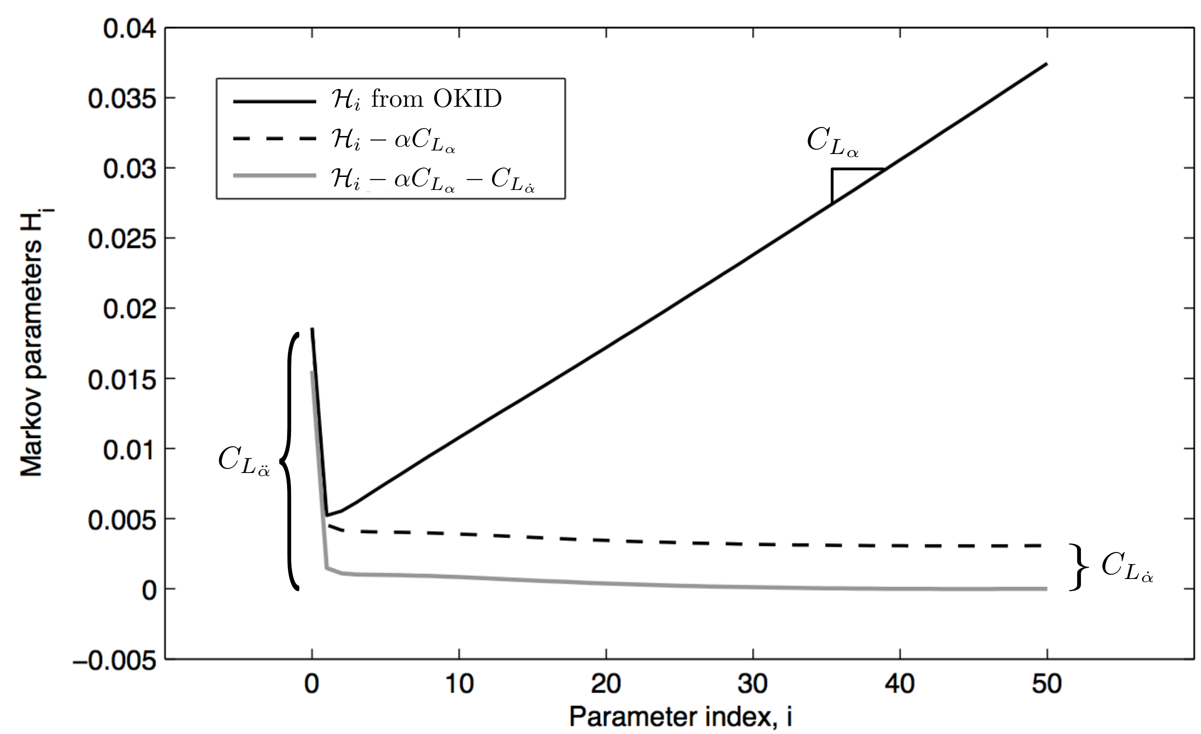

Combined maneuver effectively blends each of the three individual maneuvers

Added-mass is not exclusively in first Markov parameter, but is instead distributed in the first few, contributing to the added-mass "bump"

AOA = 0 degrees

System ID maneuver

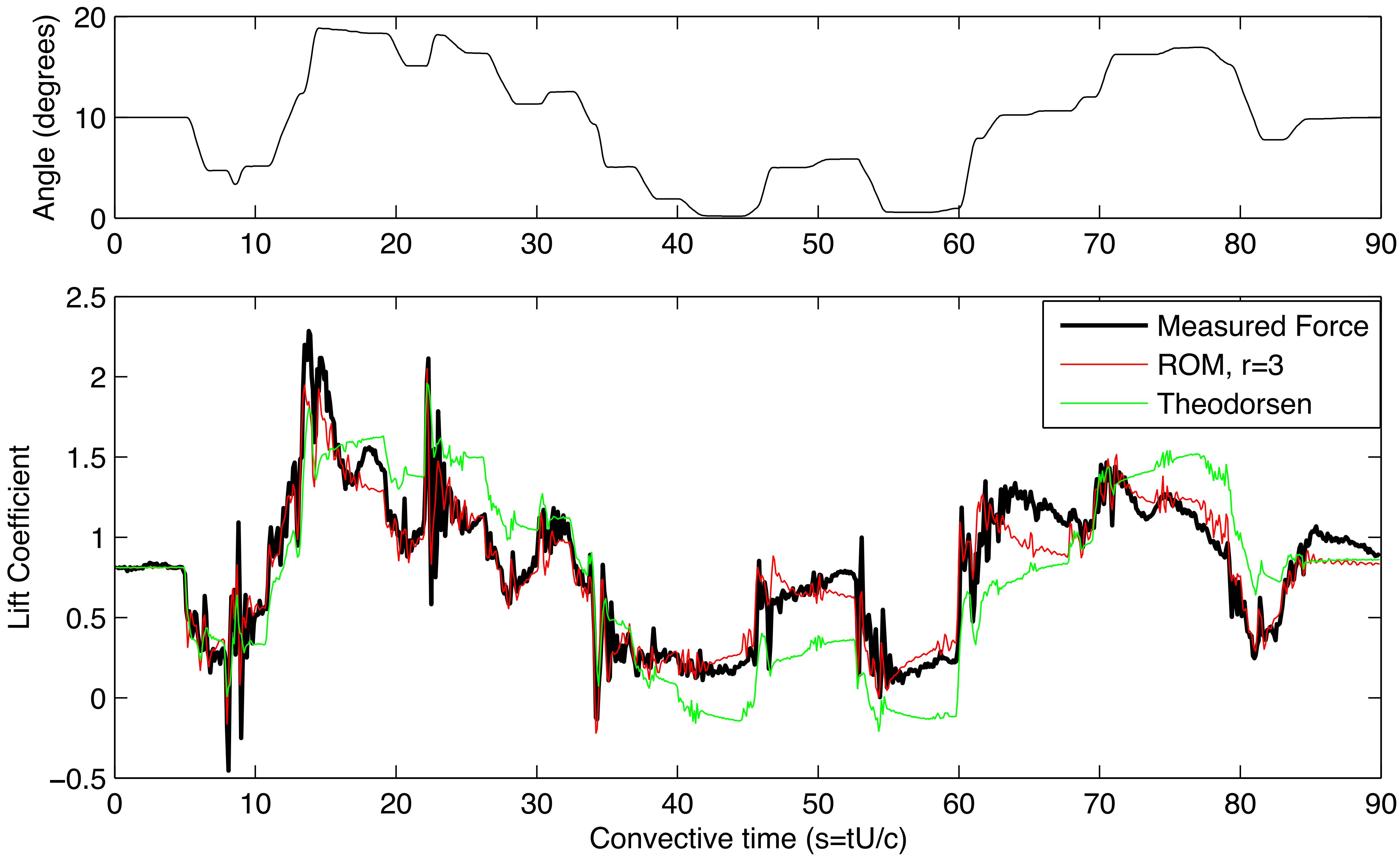

Theodorsen is significantly worse, due to large base angle of attack and flow separation effects.

+/- 10 degree manuever

AOA = 10 degrees

Bode plot and Markov parameters

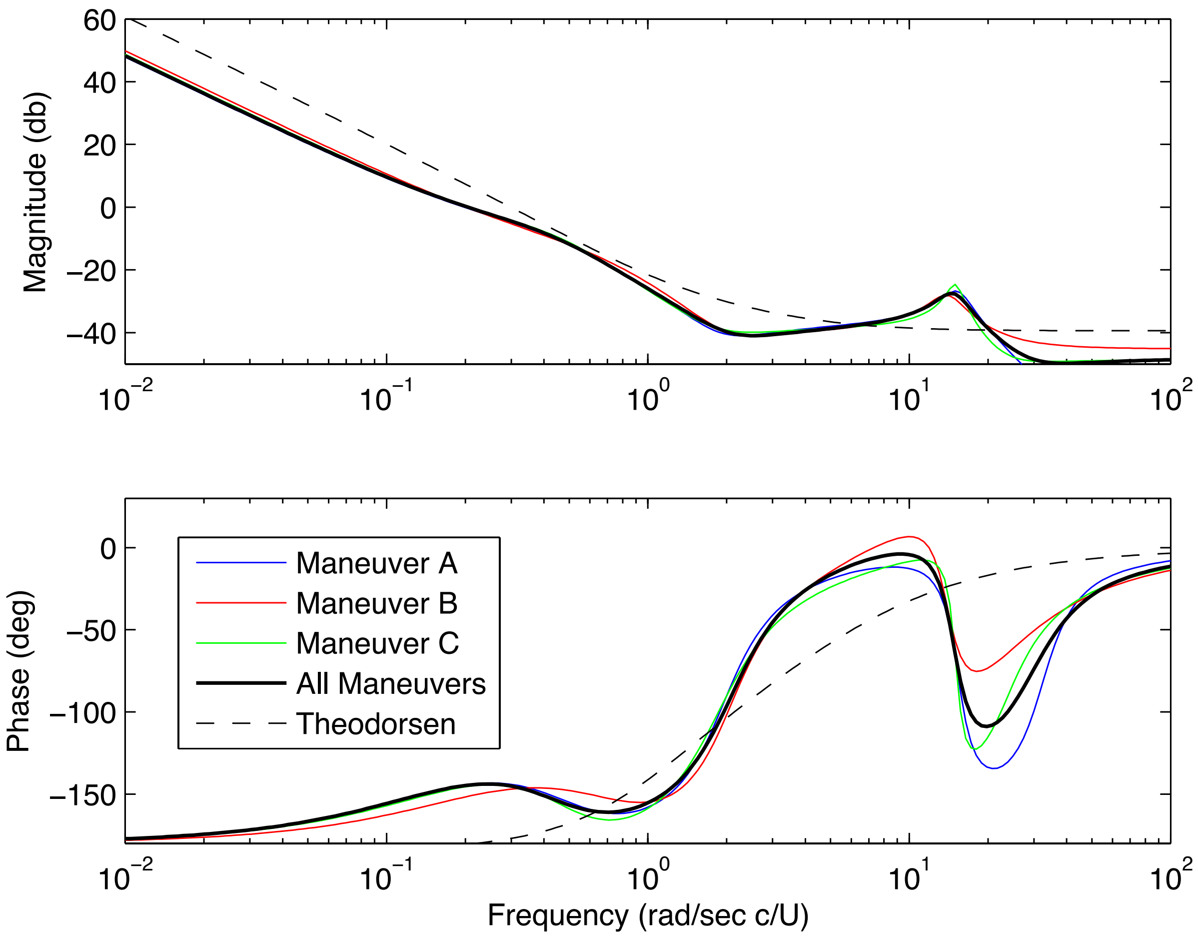

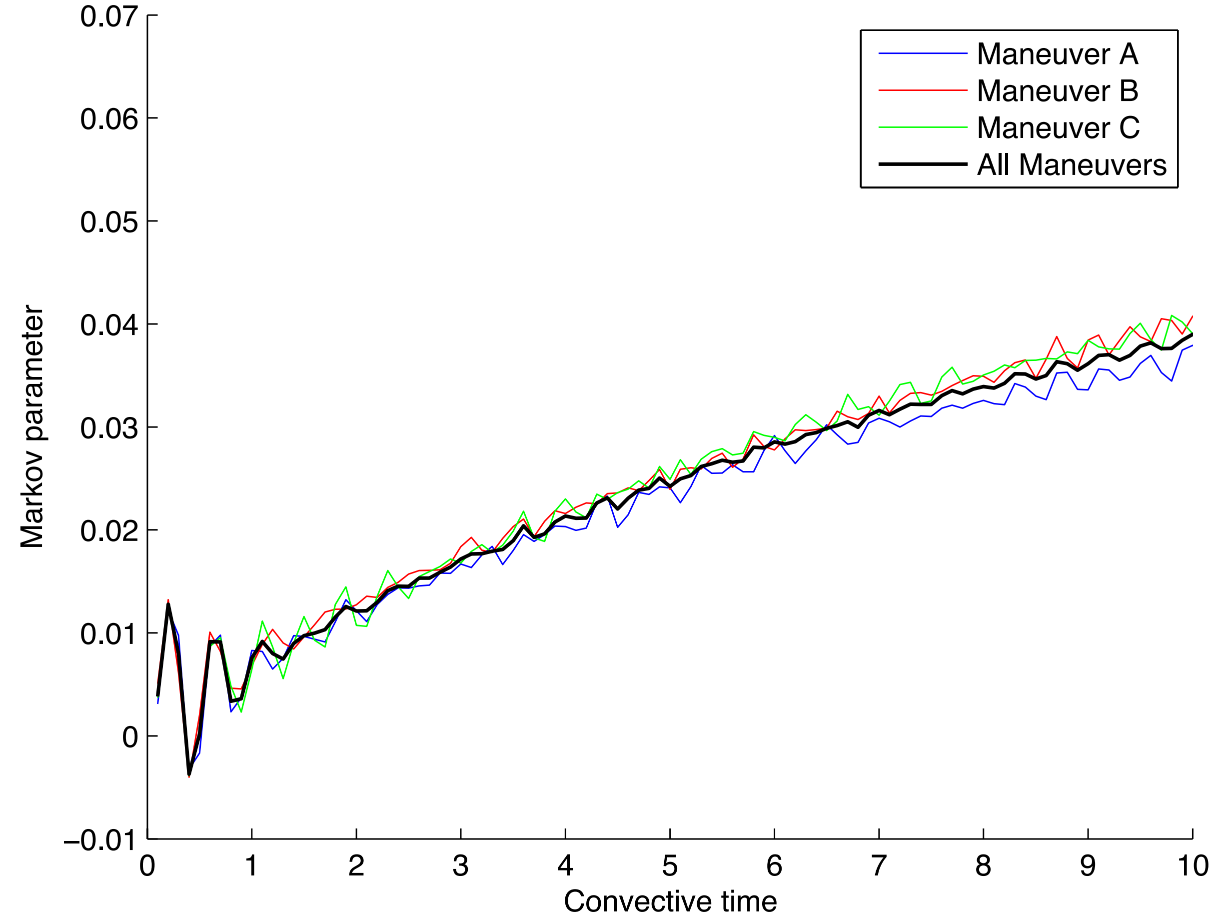

Flatter Markov parameters indicate smaller lift coefficient slope

Convergence to asymptote at lower frequency indicate longer transient decay to steady state (more separated flow)

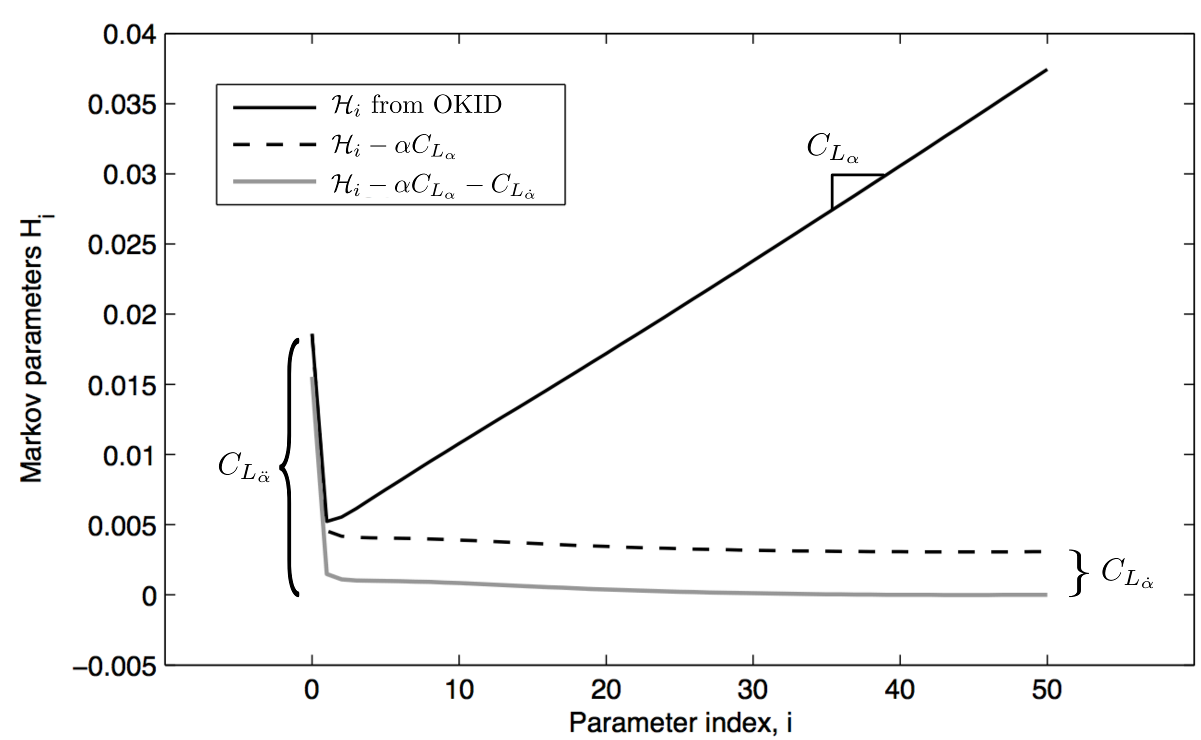

AOA = 10 degrees

AoA=00 vs. AoA=10

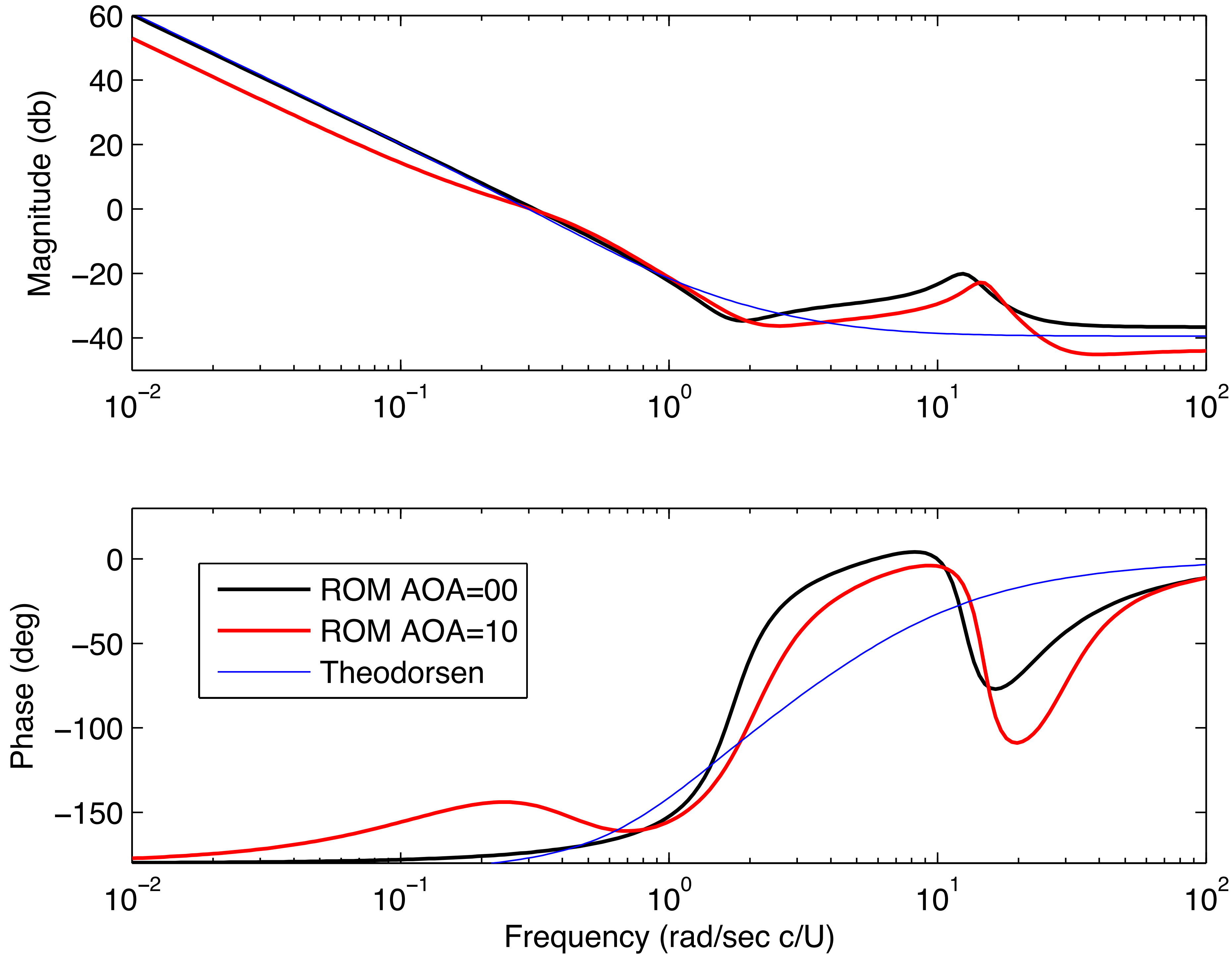

Trend is similar to DNS, where low frequency asymptote converges at lower frequency, for larger angle of attack.

Pure Plunge

AOA = 0 degrees

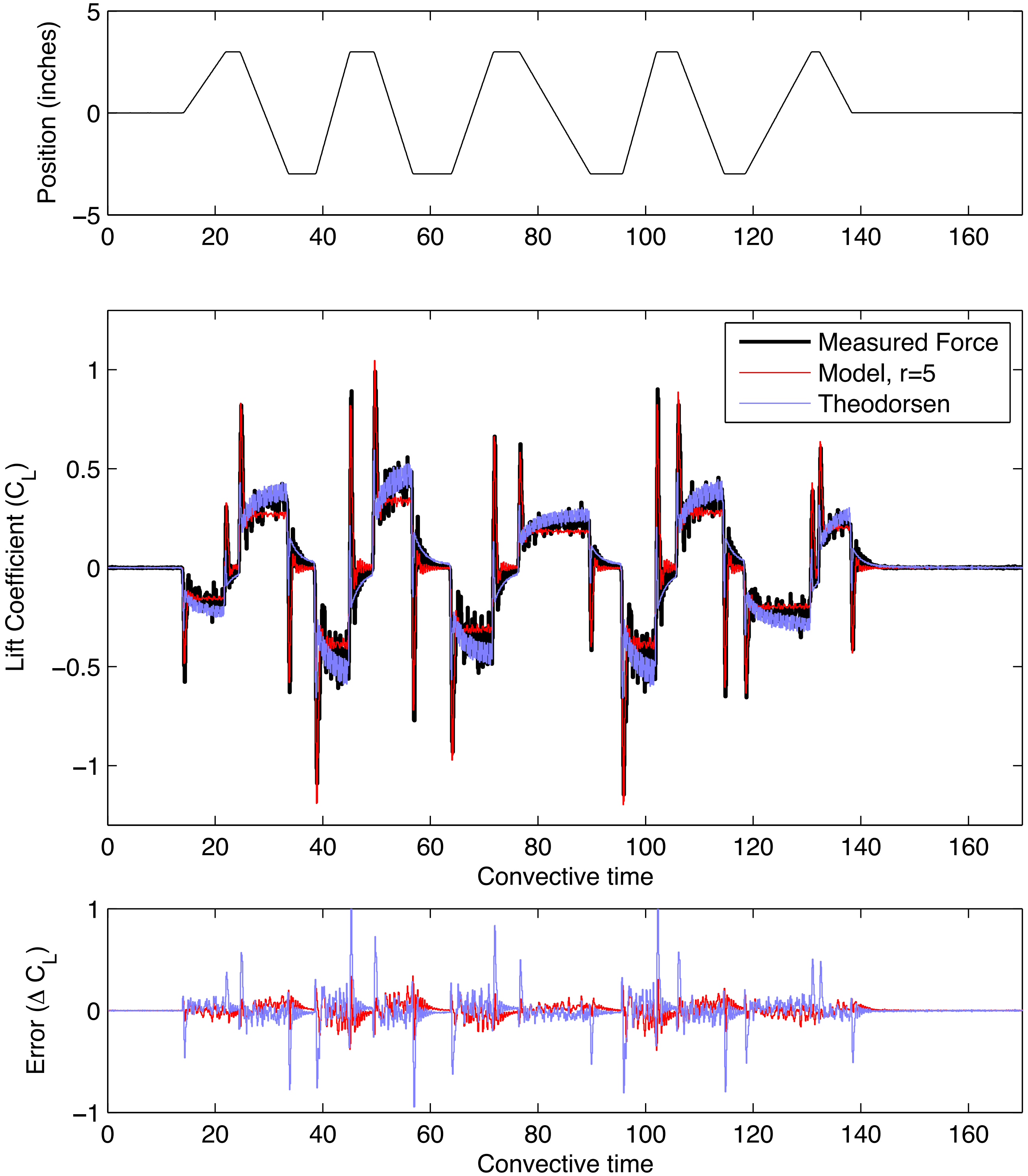

AOA = 10 degrees

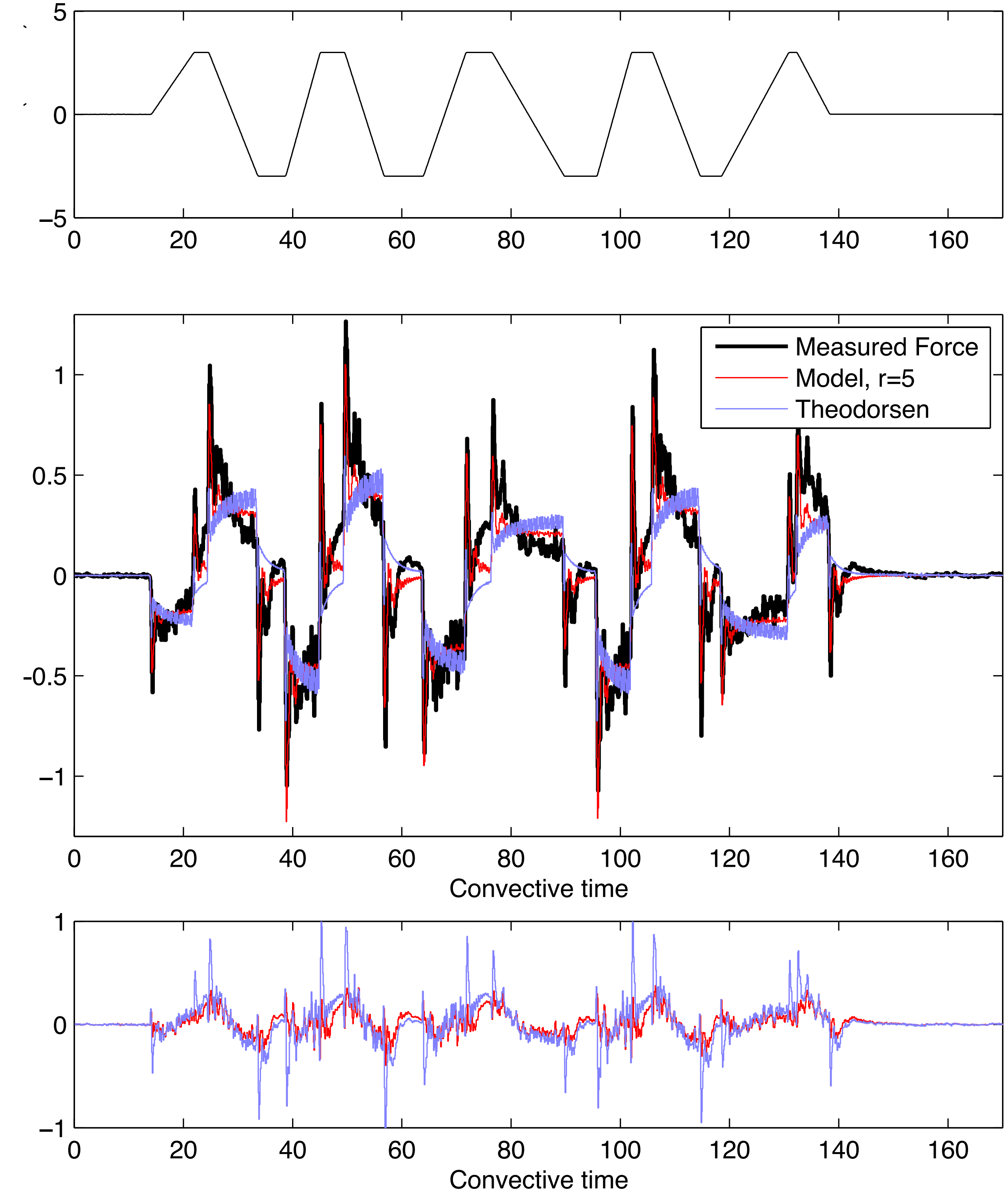

Nonlinear Unsteady Models

What we know

1. Hopf bifurcation at $\alpha = 28^\circ$
2. Linear models capture conjugate pair
3. Linear models based on overarching nonlinear model (Navier-Stokes)

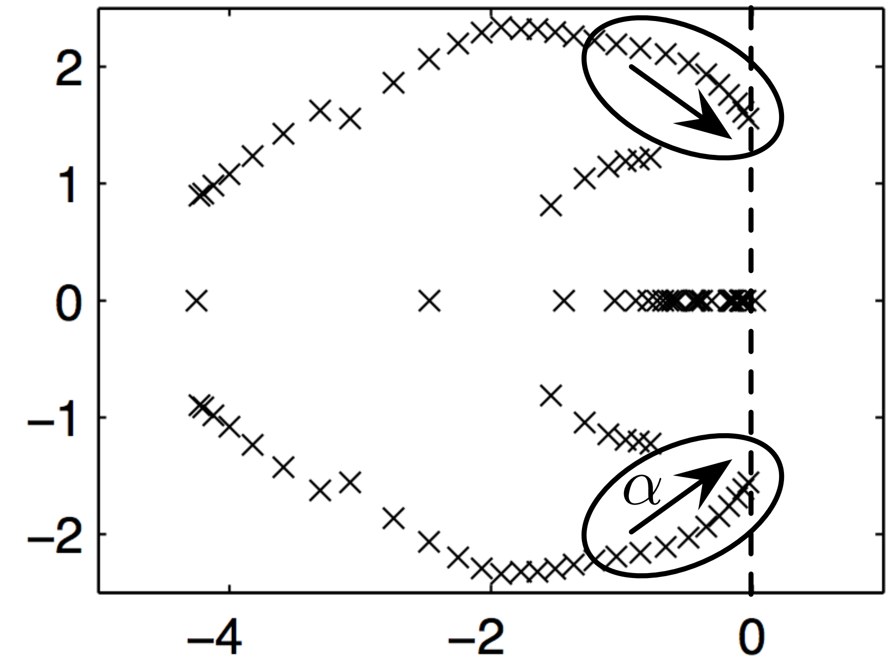

Is it possible to obtain nonlinear reduced order model?

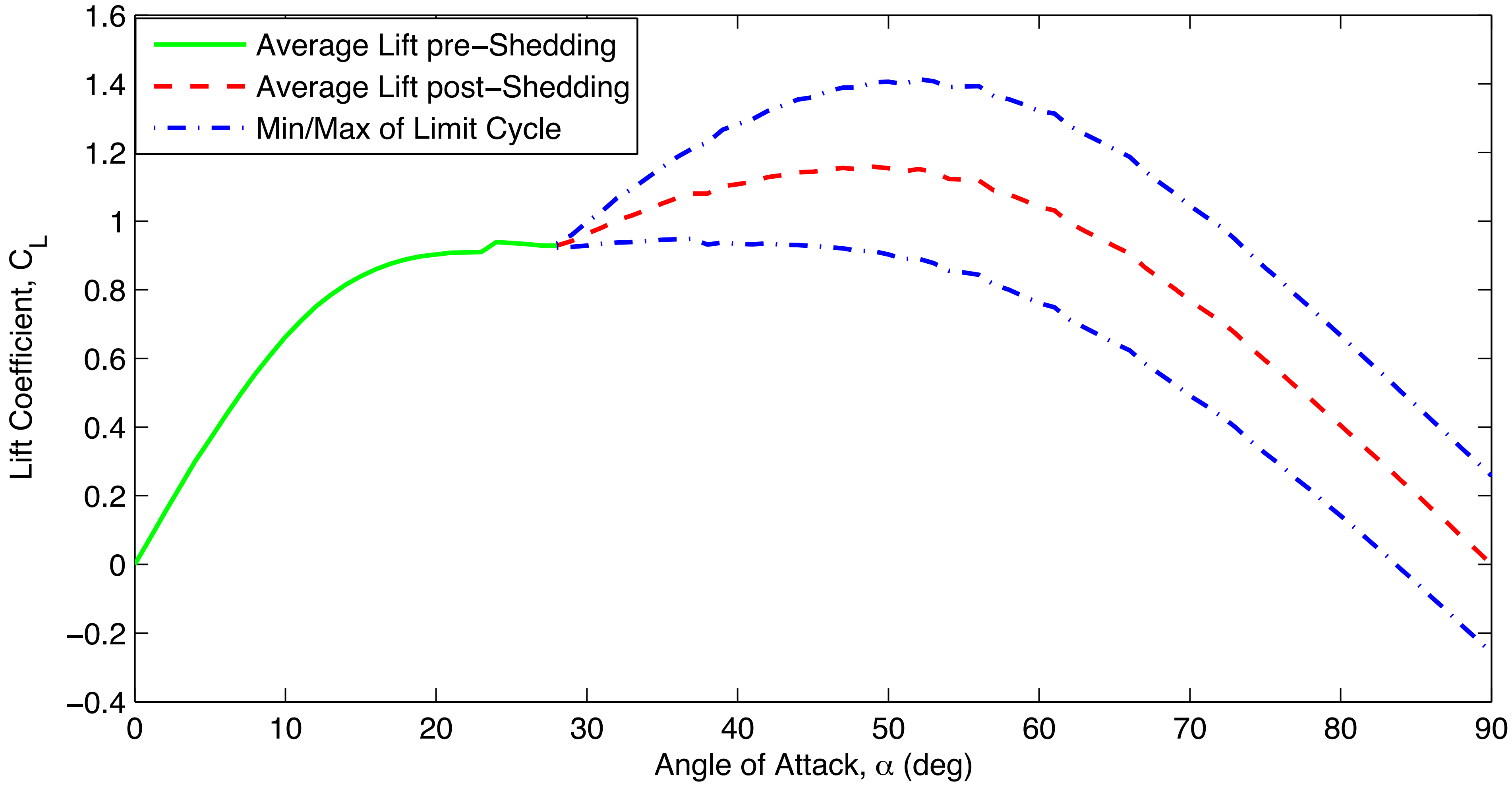

Linearize about Periodic Orbit

Impulse at each phase

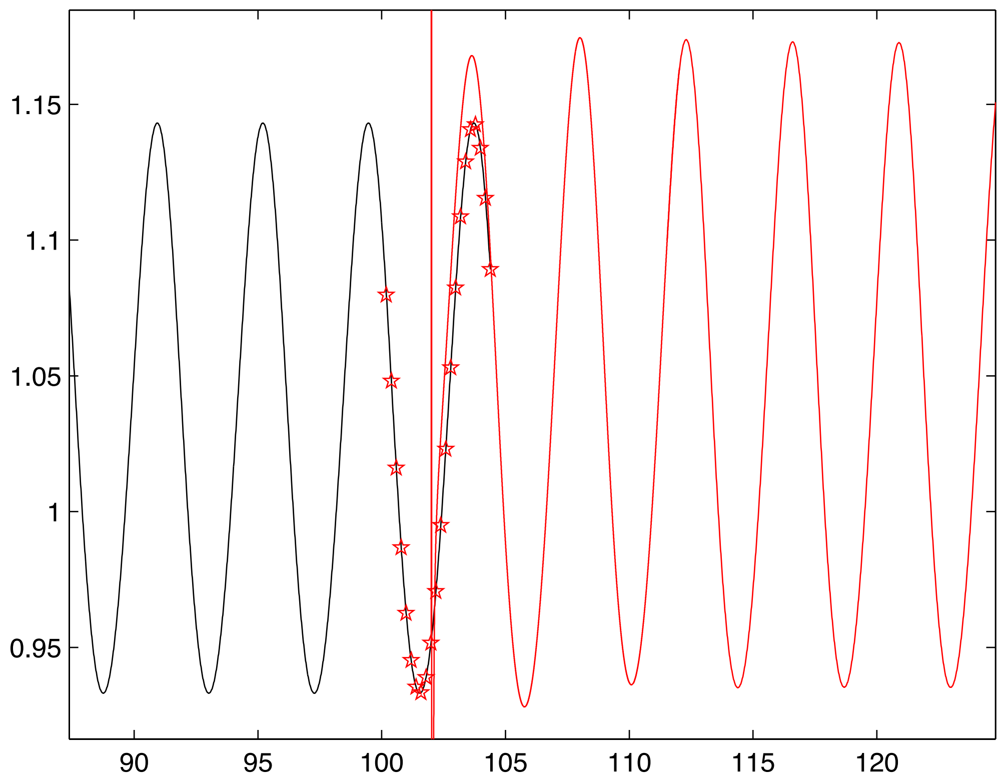

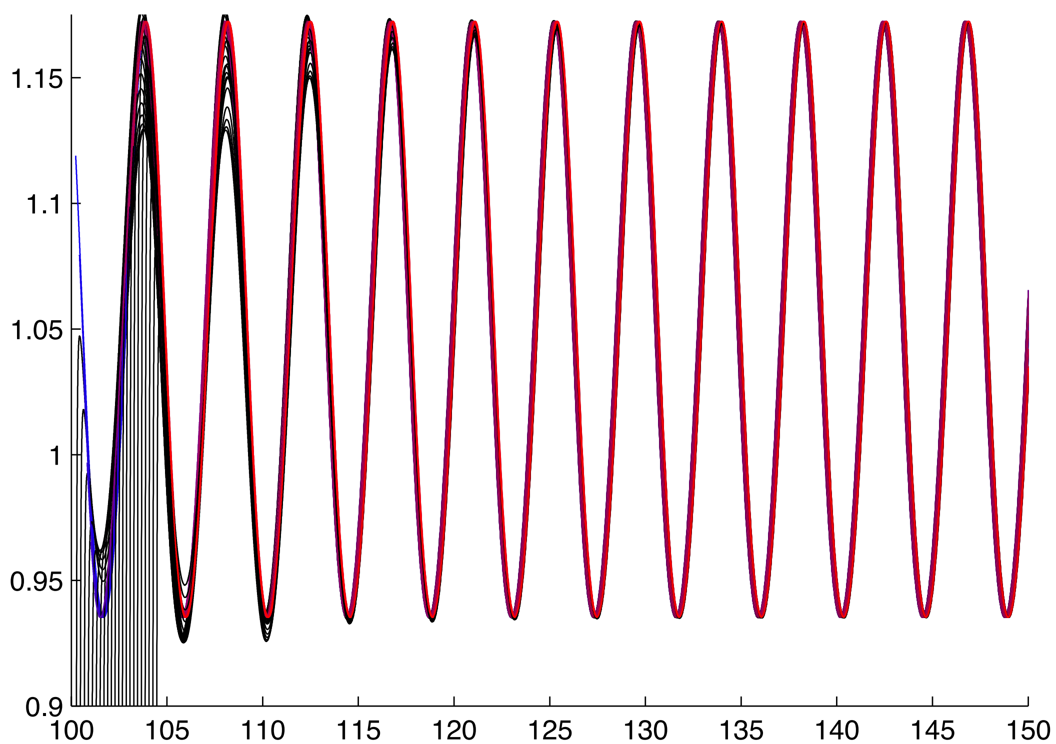

Modeling Approaches

1. Lifted/Periodic ERA
2. Nonlinear indicial response (convolution)
3. Other???

Transient dynamics

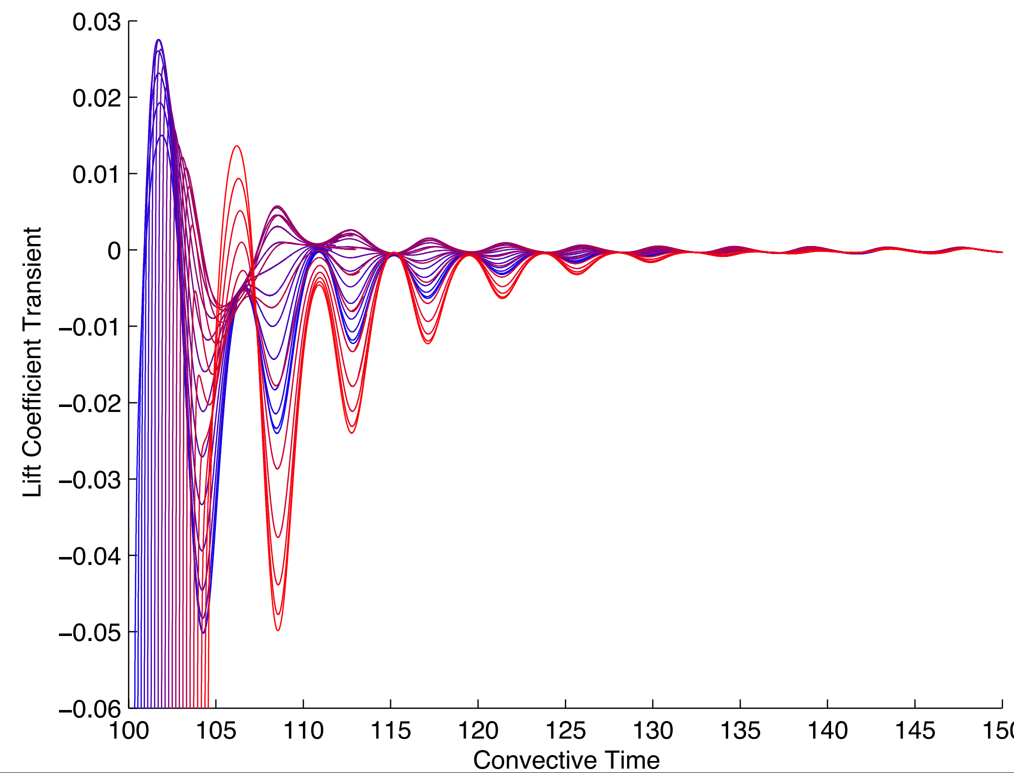

Conclusions

Accurate, efficient reduced order models

- **Models are linearization of full nonlinear model**
- **Constructed for specific geometry, Reynolds number**
- **Based on various input maneuvers**

Modeling techniques applied to two test problems

- **Simulated flat plate airfoil, Re=100**
- **Wind tunnel experiment, Re=65,000**
- **Pitch and plunge dynamics investigated**
- **Reduced order model outperforms Theodorsen's model for all cases, especially at large angle of attack**

Future Work:

- **Use pitch/plunge models for optimal control (maneuver, lift stabilization)**
- **Combine into nonlinear model with limit cycle dynamics**

Wagner, 1925.

Theodorsen, 1935.

Leishman, 2006.

OL, Altman, Eldredge, Garmann, and Lian, 2010

Brunton and Rowley, AIAA ASM 2009-2011

Juang and Pappa, 1985.

Ma, Ahuja, Rowley, 2010.

Juang, Phan, Horta, Longman, 1991.


QUESTIONS?